NONLINEAR FAULT DIAGNOSIS AND RECOVERY FOR SATELLITES USING PARAMETER ESTIMATION TECHNIQUES

Tao Jiang

A thesis
in
The Department
of
Electrical and Computer Engineering

Presented in Partial Fulfillment of the Requirements
For the Degree of Master of Applied Science
Concordia University
Montréal, Québec, Canada

September 2004

Your file Votre référence
ISBN: 0-612-94701-7
Our file Notre référence
ISBN: 0-612-94701-7

Abstract

Nonlinear Fault Diagnosis and Recovery for Satellites Using Parameter Estimation Techniques

Tao Jiang

Increasing demands on reliability for safety critical control systems require robustness and fault tolerance, capabilities that are subjected to unexpected anomalies and failures in actuators, sensors or subsystems. Specifically in time-critical systems such as spacecrafts and satellites, the autonomous fault detection, isolation and recovery (FDIR) requirements become of paramount importance and necessity.

This thesis focus is emphasized on the nonlinear fault diagnosis and recovery problems for both the satellite's orbital model and the satellite's attitude model through construction of residual generators that are based on least-squares parameter estimation techniques. By viewing system anomaly caused by faults and/or malfunctions as changes of certain parameters in the system, our goal is to detect, isolate and recover from the faults through estimating these parameters and adaptively redesigning the controllers. Given that the system with the triggered recovery procedure will be different from the system without it, two different fault detection and isolation subsystems are considered and applied to the different cases. The convergence properties of these two subsystems are shown analytically. Furthermore, the robustness properties of these residual generators are investigated, and subsequently, the corresponding decision logic and thresholds for the fault diagnosis are properly selected

and specified.

The possibility of extending the application of the proposed residual generators to a general class of nonlinear systems is also investigated and promising preliminary results in this research direction are also presented.

Acknowledgments

I am indebted to the members of my thesis examining committee for their time and suggestions during the thesis defense. Special thanks go to my supervisor Dr. K. Khorasani who was available for interesting and lively discussions whenever I walked into his office. Working with him is always a pleasure.

Many thanks to my friends and classmates during my stay at Concordia University. I specially express my gratitude to Yongjun Yu, Zhan Sun and Yanxia Zhang for their help.

Finally, I thank my family for their moral and financial support during my study in Montreal. This work is dedicated to them.

This research is supported in part by the Natural Science and Engineering Research Council of Canada (NSERC).

Contents

List of Figures ix

1 Introduction 1

1.1 Contributions of the Thesis 7

1.2 Outline of the Thesis 8

2 Problem Formulation 10

2.1 Preliminaries 10

2.2 Isolation of Concurrent Faults 16

2.3 Satellite Orbital Model 18

2.4 Satellite Attitude Model 24

2.5 Justification and Necessity for Development of Nonlinear FDIR . . . 37

3 FDIR Scheme for the Satellite Orbital Model 44

3.1 Sliding Mode Controller 44

3.2 Solvability of a Nonlinear FDIR Scheme and Coordinate Transformations 49

3.3 Application of the New Residual Generator 60

3.3.1 Fault detection before triggering the recovery process 60

3.3.2 Fault detection after triggering the recovery process 64
3.4 Impacts of Uncertainties and Disturbances on the Residual Generator 67
3.4.1 Uncertainties in the system parameters 68
3.4.2 Uncertainties in the system outputs 69
3.4.3 Impact of the Disturbance 72
3.5 Decision Logic and Recovery Subsystem 72
3.6 Simulation Results 73

4 FDIR Scheme for the Satellite Attitude Model 81

4.1 The Variable Structure Control 81
4.2 Development of the New Residual Generator 84
4.2.1 The fault detection and isolation before triggering the recovery procedure 85
4.2.2 The fault detection and isolation after triggering the recovery procedure 88
4.3 Impacts of Uncertainties and Disturbances on the Residual Generator 91
4.3.1 Parametric uncertainties 92
4.3.2 Uncertainties of outputs 93
4.3.3 Impacts of disturbances 95
4.4 Selection of the Threshold Logic 95
4.5 Simulation Results 97

5 Generalization of the FDIR Scheme to General Nonlinear Systems 105

6 Conclusions and Future Work **111**

6.1 Future Direction of Research 114

6.2 Contributions of the Thesis 116

List of Figures

2.1 Two–body model of dynamics 18

2.2 Elliptic orbit of a satellite 21

2.3 Rigid body in motion relative to an inertial reference frame 24

2.4 Rigid body with a body-fixed reference frame 27

2.5 Linear observer applied to the nonlinear system ($\hat{x}_1^0 = x_1^0$) 39

2.6 Linear observer applied to the nonlinear system ($\hat{x}_1^0 \neq x_1^0$) 40

2.7 Application of nonlinear observer to the faulty system ($\hat{x}^0 = x^0$) . . . 42

2.8 Application of nonlinear observer to the faulty system ($\hat{x}^0 \neq x^0$) . . . 42

3.1 Transfer orbit and phasing orbit 74

3.2 Apogee and perigee 76

3.3 The behavior of the FDIR on the satellite orbital model 78

3.4 (Continued)The behavior of the FDIR on the satellite orbital model 79

3.5 (Continued)The behavior of the FDIR on the satellite orbital model 80

4.1 Impacts of the disturbances on the attitude control subsystem of a satellite 100

4.2 (Continued)Impacts of the disturbances on the attitude control subsystem of a satellite 101

4.3 The behavior of the FDIR residual generator on the satellite attitude model subject to failures in actuators 1 and 3 102

4.4 (Continued)The behavior of the FDIR residual generator on the satellite attitude model subject to failures in actuators 1 and 3 103

4.5 (Continued)The behavior of the FDIR residual generator on the satellite attitude model subject to failures in actuators 1 and 3 104

Chapter 1

Introduction

With an increasing requirement for dynamic systems to be more secure and more reliable, fault tolerance in a control system is becoming more and more critical and important. In conventional and traditional approaches, the control systems for a spacecraft are implemented by manual activities on the ground. Navigation, maneuver, and fault diagnosis and recovery are primarily all ground operations and activities. The ground stations receive the necessary telemetry information for the health monitoring and status checks through communications with the spacecraft, which are then manually processed and analyzed and subsequently sent the appropriate command back to control subsystems of the spacecraft. Human operators on the ground station primarily supervise the whole process. Clearly, the most obvious disadvantage of this strategy emanates from the fact that the distance between the ground and the spacecraft could become exceedingly large. The long distance between the ground operators and the spacecraft could lead to significant delays in the communication between them. Given that a number of spacecraft activities are

time-critical, especially those that are dealing with fault diagnosis and recovery can therefore not afford the delay caused by the latencies in the communication. Consequently, equipped with the more advanced computers and computational resources that are installed on the today's spacecrafts, autonomous fault tolerant control system capabilities and requirements on the spacecrafts have been receiving a great deal of attention in the research community recently [19].

A fault tolerant control system needs to first detect and isolate the presence and location of the faults, and then recover from the identified faults by reconfiguring the control system architectures. The consideration and development of these three tasks is known as Fault Detection, Isolation and Recovery (FDIR) Problem. There are broadly speaking two main approaches for addressing the FDIR problem, namely history-based and model-based techniques [21, 22].

Compared with the history-based approaches to FDIR, which depend on knowledge processed from past experiences, model-based methods rely on interactions between various dynamical system components and variables. Over the past decades, a number of model-based methods for FDIR have been developed [12, 39]. In this thesis we focus our attention to only model-based techniques.

Among the common model-based techniques is the qualitative causal method [23]. In this method, the cause and effect reasoning about the model behavior is analyzed and investigated. Researchers have used fault-trees [23] to backwardly seek the possible original causes for observed anomalous system behaviors. The main disadvantage of this method is that one has to generate a large number of hypotheses in order to avoid poor resolution, which could result in ambiguous decisions. Furthermore, the

large number of potential hypotheses would naturally lead to a very high burden on the on-line computational resources.

Another very common and an important type of model-based technique is known as residual-based methods [12], where the FDIR process can be divided into three distinct stages. The first stage is to generate a signal (also called residual) that is sensitive to the occurrence of a given fault category. Considering and treating faults as inputs to the system, a specific residual must generate sufficient information so that one is able to discriminate and recognize the occurrence of a fault and separate this specific fault from other faults. The second stage is to use residuals to make appropriate decisions according to a pre-assigned logic corresponding to the location of the fault occurrence. Finally, the recovery task will estimate the severity of the fault and subsequently reconfigure the control system to condition the system into a manageable and desirable operational mode.

Parity space approach [24, 25, 26, 27] is among the residual-based techniques considered in the literature. Reference [12] has provided the main idea of parity space approach. This approach basically checks the consistency of the mathematical governing equations of the system through two types of redundancies: (i) direct redundancy, which makes use of relationships among redundant sensor outputs, or (ii) temporal redundancy, which counts on dynamic relationships between outputs and inputs. The parity space approach leads to a special type of an observer, called dead-beat observer.

Other than the parity space approach, many researchers simply use Luenberger observers or Kalman filters to monitor the system performance. In the absence of

uncertainties and disturbances, the errors between the state estimates and the actual values of the states diminish to zero, while the presence of faults will increase the errors on the contrary. For example, in [10, 11] Clark used this simple observer-based method, and checked the increment of the errors by threshold logic. In order to avoid the false alarm caused by uncertainties and disturbances, the threshold must be larger than zero, although this will decrease the sensibility to faults. Furthermore, enhanced capability of isolating faults can be realized by utilizing a bank of observers driven by the actual output vector that is making decisions based on multiple hypothesis testing. In this methodology, each observer is designed for a different fault hypothesis. The hypotheses are then examined with respect to likelihood functions.

Beard [1] and Jones [2] have done further work on the observer-based techniques. The Beard-Jones detection filter is a type of Luenberger observer too. However, the appealing feature of their approach is that by selecting an appropriate observer gain matrix that makes residuals caused by the actuator faults belong to the output modes, the residual caused by a given fault becomes independent with other faults. Note, however, that they only proved a sufficient condition for detecting faults by designing their special observer as a detection filter. Also, the sufficient condition is quite limited as the fault modes have to satisfy a strong mutual detectability condition. Massoumnia [3] re-stated Beard-Jones approach in a geometric sense and successfully extended this idea into a more general case, in which residuals resulted from actuator faults could belong to more than the output modes. More importantly, sufficient and necessary conditions of solvability of the residual generation for a linear time-invariant system was obtained.

Another residual-based method is the parameter estimation method. Frank [12] and Isermann [13] have presented the main idea behind this method. It makes use of the fact that faults of a dynamic system are reflected in the physical parameters of the system. It detects the faults through estimating the parameters of the mathematical model of the system. If the estimates of the parameters deviate from the nominal values, it may be declared that a fault has occurred.

The above stated model-based methods are all represented in the time domain. Aside from the time domain methods, frequency domain methods have also been investigated in the literature [14, 28]. Fong et al. [14] made use of a "finite time frequency response estimator" to realize fault detection. This finite time frequency response estimator is constructed using discrete Fourier transform, and the estimator will always have some deviations from its nominal response when faults occur. These deviations lead to a decision logic based on a statistical decision theory. The frequency domain methods have several advantages. Firstly, there is no need to know the order of the plant in advance; this method in principle can take higher order and dimensional systems where the time domain methods may not be able to address. Secondly, engineers are quite familiar with frequency response methods for analyzing and designing desired behavior of the plant. However, there are also certain disadvantages in the frequency domain. First, the resolution of fault detection is very low. That is, the delay between the occurrence of the fault and the detection of this fault may be very long. Also, in order to satisfy persistence of excitation conditions, the input signals that are allowed in this method could be rather limited.

Unfortunately, all the methods described above are for linear systems and the

practical models in the real world are always nonlinear. One may linearize these practical models and then apply the above linear FDIR methods to the original system. However, linearization does lead to significant modelling errors, which could easily lead one to a false alarm, and consequently reduce the possibility of utilizing these techniques for solving nonlinear FDIR.

Along these lines, Persis et al. [4] have extended Massoumnia's method to nonlinear systems. They showed that the problem of fault detection and isolation for nonlinear systems is solvable if and only if there is an unobservability distribution that leads to a quotient subsystem which is unaffected by all faults but one. The unobservability distribution considered in nonlinear systems is similar to the unobservability subspace that is well-known in linear systems. If such a distribution exists, one could possibly perform coordinate transformation in the states leading to new output that emphasizes and facilitates an observable subsystem upon which it is possible to design a residual generator unaffected by all faults but one. Once one performs the coordinate transformations, the problem of detecting and isolating faults reduces to that of designing a residual generator for only the observable subsystem. In this thesis, this methodology will be used and applied to the problem of FDIR for spacecrafts.

Boškovi et al. [5, 37, 38] used multiple models' method to solve the problem of detecting and isolating actuator faults for the spacecraft attitude control model. This method is based upon multiple hypotheses testing. It is based on setting up a bank of estimators that are driven by the actual outputs of the attitude control system. One of these estimators is constructed in the nominal mode, and each of

the remaining estimators is constructed according to a specific possible failure mode. Thus, by checking the errors between the estimators and the actual output, and identifying the estimator that is yielding the least error, one could claim that the mode under which this estimator is set up is the current mode. This approach is basically the extension of the linear multiple hypothesis testing method. However, the disadvantage of this approach is that it cannot detect and isolate the presence of simultaneous and concurrent faults.

1.1 Contributions of the Thesis

In this thesis, our objective is to solve a nonlinear fault diagnosis problem for the observable subsystem of a satellite through parameter estimation method. We consider the anomalous performance of the system caused by faults as manifested by the changes of certain parameters. These parameters will be estimated using the least-squares algorithm, where the estimators are viewed as residual generators. Furthermore, the corresponding threshold logic which leads to a specific value is determined. If the residual surpasses this value, one could claim the occurrence of a fault. Following the detection and isolation of the fault, the recovery subsystem will calculate the severity and level of the fault based on the residual generator and reconfigure the control system accordingly.

The contributions of this thesis are listed as follows.

- A sliding mode controller is designed for the satellite's orbital model.
- The nonlinear fault diagnosis and recovery problems for the satellite's orbital

model and the satellite's attitude control model are investigated using parameter estimation techniques.

- The robustness properties of the proposed residual generators for the satellite's orbital model and the satellite's attitude control model are investigated.

- The generalization of the proposed residual generators to a general class of nonlinear systems is investigated and promising preliminary results are presented.

1.2 Outline of the Thesis

The outline of this thesis is as follows. In Chapter 2, the method in [4] will briefly be reviewed. The satellite orbital model and the satellite attitude control model, and the necessity of implementing nonlinear FDIR techniques are presented as well. In Chapter 3, a sliding mode controller is designed for the satellite orbital model, and the proposed residual generator will be applied to this system. The robustness of the new residual generator is also investigated theoretically and through numerical simulations. In Chapter 4, based on the results obtained in [5], our new residual generator is applied which replaces their residual generator developed based on multiple models method. The simulation results for the satellite orbital model and the satellite attitude control model are shown in Chapters 3 and 4, respectively. Finally, the generalization of the proposed residual generator to a more general class of nonlinear systems is theoretically investigated and promising preliminary results are presented in Chapter 5. In Chapter 6, conclusions and directions for future research

are included.

Chapter 2

Problem Formulation

2.1 Preliminaries

In the following, the method presented in [4] is briefly reviewed, which gives us the necessary and sufficient conditions for solving the problem of detecting and isolating faults for nonlinear systems. The reader may refer to [4] for all the details and further information. The mathematical concepts and definitions may be found in [16]. The essential parts of the work in [4] are reviewed here. It is assumed that the nonlinear system can be described by the following model:

$$\begin{aligned} \dot{x} &= f(x) + g(x)u + l(x)m_1 + p(x)w \\ y &= h(x) \end{aligned} \tag{2.1}$$

with state x defined in a neighborhood X of the origin in R^n, inputs $u \in R^m$, $m_1 \in R$, $w \in R^d$ and output $y \in R^q$, in which $f(x)$, the m columns $g_1(x), ..., g_m(x)$ of $g(x)$,

$l(x)$, and d columns $p_1(x), ..., p_d(x)$ of $p(x)$ are smooth vector fields, $h(x)$ is a smooth mapping and $f(0) = 0$, $h(0) = 0$. The notations u, m_1, and w of the input of (2.1) denote the input channel for the control purposes, the fault signal, and the disturbance signal, respectively.

By ignoring the faults and disturbances momentarily, then (2.1) becomes

$$\dot{x} = g_0(x) + \sum_{i=1}^{m} g_i(x)u_i$$
$$y = h(x) \tag{2.2}$$

where $g_0(x) = f(x)$.

Definition 2.1 Let U be an open set in R^n. Then the set of *smooth functions with compact support* (in U) is the set of functions $f : R^n \rightarrow C$ which are smooth (i.e., $\partial^\alpha f : R^n \rightarrow C$ is a continuous function for all multi-indices α) and supp(f) is compact and contained in U [20].

Definition 2.2 Suppose U is an open set in R^n, and suppose $D(U)$ is the topological vector space of smooth functions with compact support. A *distribution* is a linear continuous functional on $D(U)$, i.e., a linear continuous mapping $D(U) \rightarrow C$ [20].

Definition 2.3 Let $T : V \rightarrow W$ be a linear transformation. The set of all vectors in V that T maps to 0 is called the *kernel* (or *nullspace*) of T, and is denoted $KerT$. When the transformations are given by means of matrices, the *kernel* of the matrix A is

$$KerA = \{x \in V \,|Ax = 0\}$$

Definition 2.4 Given a distribution Δ, the distribution that is the smallest involutive distribution containing Δ is called the *involutive closure* of Δ [16].

Corresponding to (2.2), a distribution Δ is called conditioned invariant if it conforms

$$[g_i, \Delta \cap Ker\{dh\}] \subset \Delta, \qquad i = 0, \ldots, m \tag{2.3}$$

Further, we let $P = span\{p_1(x), ...p_d(x)\}$, and propose a nondecreasing sequence of distributions as following:

$$\begin{aligned} S_0 &= \bar{P} \\ S_{k+1} &= \bar{S}_k + \sum_{i=0}^{m} [g_i, \bar{S}_k \cap Ker\{dh\}] \end{aligned} \tag{2.4}$$

where $\bar{S}$ denotes the involutive closure of S. Suppose there is an integer k^* such that

$$S_{k^*+1} = \bar{S}_k \tag{2.5}$$

and let $\sum_*^P = \bar{S}_{k^*}$. Thus, $\sum_*^P$ is involutive, contains P and is conditioned invariant.

Let Θ be a fixed codistribution and define the following nondecreasing sequence of codistributions

$$\begin{aligned} Q_0 &= \Theta \cap span\{dh\} \\ Q_{k+1} &= \Theta \cap \left(\sum_{i=0}^{m} L_{g_i} Q_k + span\{dh\} \right) \end{aligned} \tag{2.6}$$

Suppose all the codistributions of this sequence are nonsingular, so that there is

an integer $k^* \leq n-1$ such that $Q_k = Q_{k*}$ for $k > k^*$, and set $\Omega^* = Q_{k^*}$. Then, it is convenient to use the notation

$$\Omega^* = o.c.a.\,(\Theta)$$

where "*o.c.a.*" stands for "observability codistribution algorithm".

Based on the properties (as discussed in details in [4]) of the two sequences (2.4) and (2.6), if (2.6) is initialized at $\left(\sum_*^P\right)^\perp$, then *o.c.a.* $\left(\left(\sum_*^P\right)^\perp\right)$ is the largest observability codistribution which is locally spanned by the exact differentials and contained in $P^\perp$.

According to [4], the necessary condition for solving the nonlinear fundamental problem of residual generation (defined in [4]) is:

$$(span\,\{l\})^\perp + o.c.a.\left(\left(\sum_*^P\right)^\perp\right) = T^*X \tag{2.7}$$

Furthermore, if the condition (2.7) holds, then we could possibly perform coordinate transformations in the states leading to the new output that characterizes an observable subsystem upon which it is possible to design a residual generator unaffected by all faults but one.

Definition 2.5 Suppose there is an open subset U of R^n. The *differential* or *gradient* of a real-valued function $\lambda(x)$ on U, denoted $d\lambda$, is the $1 \times n$ row vector whose i-th element is the partial derivative of λ with respect to x_i [16]. Its value at a point x is

thus

$$d\lambda(x) = \left(\frac{\partial \lambda}{\partial x_1} \quad \frac{\partial \lambda}{\partial x_2} \quad \cdots \quad \frac{\partial \lambda}{\partial x_n} \right)$$

Definition 2.6 A function $f : X \rightarrow Y$ is called *surjection* if, for every $y \in Y$, there is an $x \in X$ such that $f(x) = y$.

Consider the nonlinear system dynamics that is governed by (2.2). Let Ω be an observability codistribution, and n_1 be the dimension of Ω. When Ω is calculated according to the sequences (2.4) and (2.6), (2.6) is initialized at $\left(\sum_*^P\right)^\perp$, and Ω can be spanned by the exact differentials.

Suppose that $span\{dh\}$ is nonsingular. Let $p - n_2$ denote the dimension of $\Omega \cap span\{dh\}$, and suppose there exists a surjection $\Psi_1 : R^p \rightarrow R^{p-n_2}$ such that

$$\Omega \cap span\{dh\} = span\{d(\Psi_1 \circ h)\} \tag{2.8}$$

Fix $x^\circ \in X$ and let $y^\circ = h(x^\circ)$. Then, there exists a selection matrix H_2 such that

$$\Psi(y) = \begin{pmatrix} y_1 \\ y_2 \end{pmatrix} = \begin{pmatrix} \Psi_1(y) \\ H_2 y \end{pmatrix} \tag{2.9}$$

Choose a neighborhood U° of x° and a function Φ_1: $U^\circ \rightarrow R^{n_1}$ such that

$$\Omega = span\{d\Phi_1\} \tag{2.10}$$

at any point of U°. Then, there exists a function $\Phi_3 : U^\circ \rightarrow R^{n-n_1-n_2}$ such that

$$\Phi(x) = \begin{pmatrix} x_1 \\ x_2 \\ x_3 \end{pmatrix} = \begin{pmatrix} \Phi_1(x) \\ H_2 h(x) \\ \Phi_3(x) \end{pmatrix} \tag{2.11}$$

is a local diffeomorphism at x° in X. By applying this diffeomorphism to system (2.1), then system (2.1) becomes equivalently:

$$\begin{aligned}
\dot{x}_1 &= f_1(x_1, x_2) + g_1(x_1, x_2)u + l_1(x_1, x_2)m_1, x_1 \in R^{n_1} \\
\dot{x}_2 &= f_2(x_1, x_2, x_3) + g_2(x_1, x_2, x_3)u + p_1(x_1, x_2, x_3)w, x_2 \in R^{n_2} \\
\dot{x}_3 &= f_3(x_1, x_2, x_3) + g_3(x_1, x_2, x_3)u + p_2(x_1, x_2, x_3)w, x_3 \in R^{n-n_1-n_2} \\
y_1 &= h_1(x_1), y_1 \in R^{p-n_2} \\
y_2 &= x_2, y_2 \in R^{n_2}
\end{aligned} \tag{2.12}$$

Following the state space coordinate transformation, the disturbances w can only affect x_1-subsystem through x_2. However, since we observe x_2 through y_2, one may view x_2 as an input to the x_1-subsystem. The problem of detecting and isolating faults in the original nonlinear system (2.1) reduces to that of designing a residual generator for the observable subsystem [4]. However, either designing an estimator for the states of the system or its parameters require that the states of the system be uniformly bounded. Thus, if the open-loop system is not guaranteed to be state bounded, one has to design a controller to make the system stable and state bounded.

More importantly, when actuator faults occur, it is clear that the existing controllers will not work and the states will diverge most likely. Therefore, it is imperative that as soon as one detects the faults, one initiates the trigger for the redundant actuators for compensating the presence of faults. The difficulty that one is faced with is that one cannot control the system from the time the faults occur to the time the faults are detected. Therefore, there is a necessary condition for designing a residual generator for the observable subsystem. Specifically, the system should contain no finite escape time.

Based on the above review of the fault diagnosis of nonlinear systems, the main contribution of this thesis is to design a desirable residual generator for the observable subsystem. Our approach is based on parameter estimation. The actuator faults are viewed and considered as changes of the parameters. A nonlinear estimator is designed to identify these parameters and the estimators are treated as the residual generators. The proposed new residual generators are applied to two different dynamical models namely, satellite orbital model and satellite attitude control model.

2.2 Isolation of Concurrent Faults

For the nonlinear system (2.1), there is only one possible fault m_1. In this section, we will discuss the case in which there are possibilities of multiple concurrent faults. The key idea of isolating concurrent faults is to design a residual generator for each possible fault, where this residual generator is unaffected by all the faults except one

fault. Consider the system

$$\dot{x} = f(x) + \sum_{i=1}^{m} g_i(x)u_i + \sum_{i=1}^{s} l_i(x)m_i + p(x)w$$

$$y = h(x) \tag{2.13}$$

where there are now s possible faults. For i=1,..., s, set

$$\tilde{p}_i = (l_1 \quad \cdots \quad l_{i-1} \quad l_{i+1} \quad \cdots \quad l_s \quad p)$$

$$\tilde{w}_i = col\,(m_1, \cdots, m_{i-1}, m_{i+1}, \cdots, m_s, w)$$

Then, system (2.13) can be rewritten as

$$\dot{x} = f(x) + \sum_{i=1}^{m} g_i(x)u_i + l_i(x)m_i + \tilde{p}_i(x)\tilde{w}_i$$

$$y = h(x) \tag{2.14}$$

Let $\tilde{P}_i = span\,\{\tilde{p}_i\}$, so that we can use nondecreasing sequence (2.4) and (2.6), where (2.4) is initialized at $\tilde{P}_i$ and (2.6) is initialized at $\left(\sum_*^{\tilde{P}_i}\right)^{\perp}$, to find the largest observability codistribution which is locally spanned by the exact differentials and contained in $\tilde{P}_i^{\perp}$. Further, if this observability codistribution satisfies (2.7), we may transform the coordinates to have an observable subsystem upon which it is possible to design a residual generator affected only by m_i. If one can design such a residual generator for each m_i (i=1,..., s), one in effect can isolate these concurrent faults.

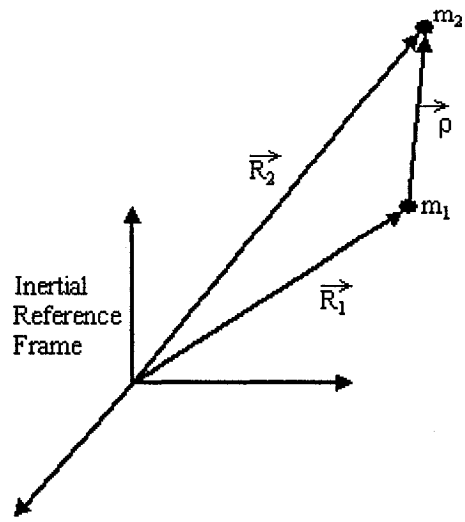

Figure 2.1: Two–body model of dynamics

2.3 Satellite Orbital Model

In reference [15], Wie discussed the satellite's orbital model in details. In this section, a brief overview of constructing a satellite's orbital model is presented. Consider two particles of masses m_1 and m_2 with position vectors $\vec{R}_1$ and $\vec{R}_2$, respectively, in an inertial reference frame, as shown in figure 2.1. According to Newton's second law and law of gravity, we have

$$m_1\ddot{\vec{R}}_1 = +\frac{Gm_1m_2}{\rho^3}\vec{\rho} \tag{2.15}$$

$$m_2\ddot{\vec{R}}_2 = -\frac{Gm_1m_2}{\rho^3}\vec{\rho} \tag{2.16}$$

where $G = 6.6695 \times 10^{-11} N \cdot m^2/kg^2$ is the universal gravitational constant.

Subtracting (2.15) times m_2 from (2.16) times m_1, we obtain

$$\ddot{\vec{\rho}} + \theta_1\frac{\vec{\rho}}{\rho^3} = 0 \tag{2.17}$$

where $\theta_1 = G(m_1 + m_2)$ is called the gravitational parameter of the two-body model, and $\rho = |\vec{\rho}|$. For the remainder of this discussion, it is assumed that m_1 stands for the earth and m_2 for the satellite, therefore $m_1 >> m_2$, and $\theta_1 \approx Gm_1$. Using basic knowledge of dynamics, it is well-known that: (1) the mechanical energy of the system, which is the sum of kinetic and potential energy, remains constant; and (2) the angular momentum of the system remains constant.

Taking the dot product of (2.17) with $\dot{\vec{\rho}}$ yields

$$\ddot{\vec{\rho}} \cdot \dot{\vec{\rho}} + \theta_1 \frac{\vec{\rho}}{\rho^3} \cdot \dot{\vec{\rho}} = 0$$

Therefore,

$$\frac{1}{2}\frac{d}{dt}\left(\dot{\vec{\rho}} \cdot \dot{\vec{\rho}}\right) + \theta_1 \frac{\rho\dot{\rho}}{\rho^3} = 0$$

This equation can be rewritten as

$$\frac{d}{dt}\left(\frac{v^2}{2} - \frac{\theta_1}{\rho}\right) = 0 \qquad \text{or} \qquad \frac{v^2}{2} - \frac{\theta_1}{\rho} = \text{const}$$

where $v = |\vec{v}| = \left|\dot{\vec{\rho}}\right| = \sqrt{\dot{\vec{\rho}} \cdot \dot{\vec{\rho}}}$. Thus, one obtains the energy equation

$$\varepsilon = \frac{v^2}{2} - \frac{\theta_1}{\rho} \tag{2.18}$$

where ε is called the total mechanical energy per unit mass or the specific mechanic energy, $v^2/2$ is the kinetic energy per unit mass, and $-\theta_1/\rho$ is the potential energy per unit mass.

The angular momentum per unit mass is given by:

$$\vec{h} = \vec{\rho} \times \dot{\vec{\rho}} = \vec{\rho} \times \vec{v} \tag{2.19}$$

From (2.17), we have

$$\ddot{\vec{\rho}} \times \vec{h} + \theta_1 \frac{\vec{\rho}}{\rho^3} \times \vec{h} = 0 \tag{2.20}$$

Since

$$\vec{\rho} \times \vec{h} = \vec{\rho} \times (\vec{\rho} \times \dot{\vec{\rho}}) = (\vec{\rho} \cdot \dot{\vec{\rho}})\vec{\rho} - (\vec{\rho} \cdot \vec{\rho})\dot{\vec{\rho}} \tag{2.21}$$

then we have

$$\frac{d}{dt}\left[\dot{\vec{\rho}} \times \vec{h} - (\theta_1/\rho)\vec{\rho}\right] = 0 \tag{2.22}$$

which implies

$$\dot{\vec{\rho}} \times \vec{h} - (\theta_1/\rho)\vec{\rho} = \theta_1 \vec{e} \tag{2.23}$$

where $\vec{e}$ is known as the eccentricity vector.

Taking the dot product of (2.23) with $\vec{\rho}$ gives

$$\vec{\rho} \cdot \dot{\vec{\rho}} \times \vec{h} - \vec{\rho} \cdot (\theta_1/\rho)\vec{\rho} = \vec{\rho} \cdot \theta_1 \vec{e} \tag{2.24}$$

Since $\vec{\rho} \cdot \dot{\vec{\rho}} \times \vec{h} = (\vec{\rho} \times \dot{\vec{\rho}}) \cdot \vec{h} = h^2$, (2.24) becomes

$$h^2 - \theta_1 \rho = \theta_1 \rho e \cos\phi \tag{2.25}$$

where ϕ is the angle between $\vec{\rho}$ and $\vec{e}$.

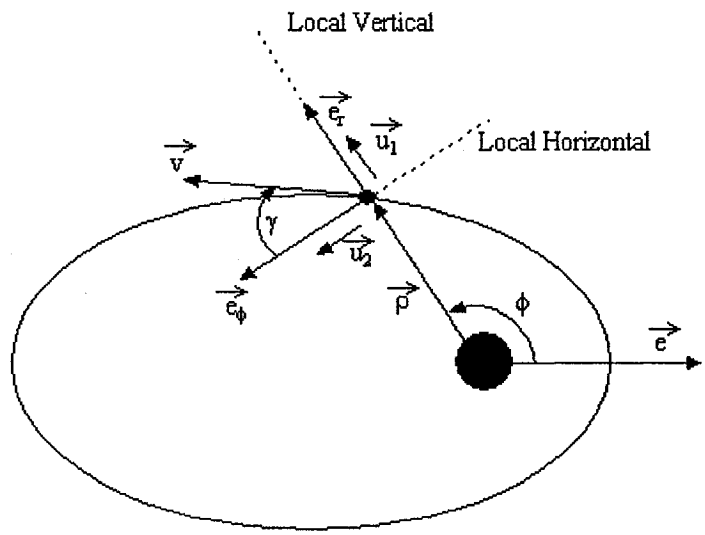

Figure 2.2: Elliptic orbit of a satellite

From (2.25), we have

$$\rho = \frac{p}{1 + e\cos\phi} \tag{2.26}$$

where

$$p = h^2/\theta_1 \tag{2.27}$$

The above analysis has actually been the proof of the Kepler's First Law. The orbit of the satellite around the earth is an ellipse, with the earth at one focus. Figure 2.2 illustrates this situation. Next, we will obtain and derive the satellite orbital model in polar coordinates.

From figure 2.2, it follows that $\vec{\rho} = \rho\vec{e}_r$, $\dot{\vec{e}}_r = \dot{\phi}\vec{e}_\phi$, and $\dot{\vec{e}}_\phi = -\dot{\phi}\vec{e}_r$. Therefore,

$$\dot{\vec{\rho}} = \dot{\rho}\vec{e}_r + r\dot{\vec{e}}_r = \dot{r}\vec{e}_r + r\dot{\phi}\vec{e}_\phi \tag{2.28}$$

$$\ddot{\vec{\rho}} = \ddot{\rho}\vec{e}_r + \dot{r}\dot{\phi}\vec{e}_\phi + r\ddot{\phi}\vec{e}_\phi - r\dot{\phi}^2\vec{e}_r + \dot{r}\dot{\phi}\vec{e}_\phi \tag{2.29}$$

From (2.17), we get

$$\ddot{\vec{\rho}} = -\theta_1 \frac{\vec{\rho}}{\rho^3} = \theta_1 \frac{\vec{e}_r}{\rho^2} \tag{2.30}$$

Combining equations (2.29) and (2.30), we have

$$\ddot{\rho} - \rho\dot{\phi}^2 = -\frac{\theta_1}{\rho^2} \tag{2.31}$$

$$\rho\ddot{\phi} + 2\dot{\rho}\dot{\phi} = 0 \tag{2.32}$$

Let $\dot{\rho} = v$ and $\dot{\phi} = \omega$, we obtain

$$\begin{cases} \dot{\rho} = v \\ \dot{v} = \rho\omega^2 - \frac{\theta_1}{\rho^2} \\ \dot{\phi} = \omega \\ \dot{\omega} = \frac{-2v\omega}{\rho} \end{cases} \tag{2.33}$$

Equation (2.33) is the satellite orbital model without external forces. Now, it is assumed that there are two external forces on the satellite as shown in figure 2.2 namely, $\vec{u}_1$ is along the direction of $\vec{e}_r$, and $\vec{u}_2$ is along the direction of $\vec{e}_\phi$. According to the Newton's second law, the satellite orbital model with external forces now becomes:

$$\begin{cases} \dot{\rho} = v \\ \dot{v} = \rho\omega^2 - \theta_1 \frac{1}{\rho^2} + \frac{1}{m_2} u_1 \\ \dot{\phi} = \omega \\ \dot{\omega} = -\frac{2v\omega}{\rho} + \frac{1}{m_2} \frac{u_2}{\rho} \end{cases} \tag{2.34}$$

where m_2 is the mass of the satellite, $u_1 = |\vec{u}_1|$, and $u_2 = |\vec{u}_2|$.

In the real world, it is practically impossible to avoid disturbances and in general there are possible faults that are affecting the satellite model. In this thesis, it is assumed that there is a disturbance in the input channel u_1 and a possible fault in the input channel u_2. Thus, the satellite orbital model can be written as:

$$\begin{cases} \dot{\rho} = v \\ \dot{v} = \rho\omega^2 - \theta_1 \frac{1}{\rho^2} + \theta_2 u_1 + w \\ \dot{\phi} = \omega \\ \dot{\omega} = -\frac{2v\omega}{\rho} + \theta_2 \frac{u_2}{\rho} + \theta_2 \frac{m}{\rho} + \theta_2 \frac{u_{2r}}{\rho} \end{cases}$$
$$\begin{cases} \nu_1 = \rho \\ \nu_2 = \phi \\ \nu_3 = \omega \end{cases} \tag{2.35}$$

in which (ρ, ϕ) denotes the position of the satellite in polar coordinates on the plane, v is the radial velocity, ω is the angular velocity and u_1, u_2 are the radial and tangential thrust, respectively, m is the fault signal and w represents the disturbance signal. The signal u_{2r} is a redundant input which is used for recovering the faulty system. The variable θ_2 is set equal to $1/m_2$, and θ_1 and θ_2 are supposed to be known parameters. The variables ν_1, ν_2 and ν_3 are output signals and are assumed to be available for measurement.

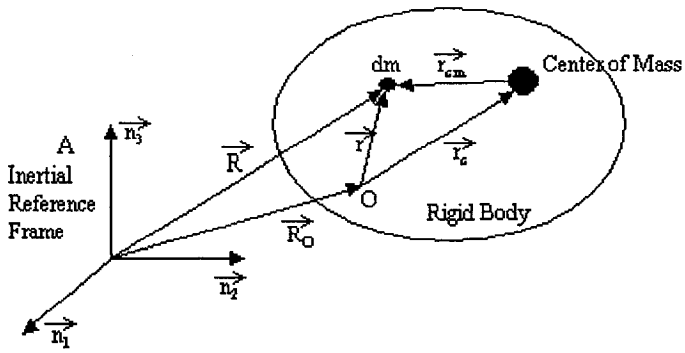

Figure 2.3: Rigid body in motion relative to an inertial reference frame

Furthermore, it is assumed that

$$m = -ku_2 \tag{2.36}$$

where k is a positive constant, $0 \leq k \leq 1$. When $k = 1$, it represents a total fault case.

2.4 Satellite Attitude Model

For all practical purposes, one can consider the satellite as a rigid body and study the satellite's attitude model by starting with the dynamic characteristic of a rigid body. In reference [15], Wie presented the satellite's attitude model in detail. Those results are summarized briefly in this section.

Consider a rigid body in motion with respect to an inertial reference frame A as shown in figure 2.3. The rotational equation of the rigid body's motion about an

arbitrary point O is written as:

$$\int \vec{r} \times \ddot{\vec{R}} dm = \vec{M}_O \tag{2.37}$$

where $\vec{r}$ represents the position vector of a infinitesimal mass element dm with respect to point O, $\ddot{\vec{R}}$ represents the position vector of dm with respect to the origin of the inertial reference frame A, and $\vec{M}_O$ is the total external moment on point O.

As shown in figure 2.3, $\vec{r}_c$ represents the position vector of the mass center with respect to point O, and $\vec{r}_{cm}$ represents the position vector of dm with respect to the mass center. Then we obtain

$$\int \vec{r} dm = m\vec{r}_c \tag{2.38}$$

$$\int \vec{r}_{cm} dm = 0 \tag{2.39}$$

where m represents the mass of the rigid body. Since $\vec{R} = \vec{R}_O + \vec{r}$, equation (2.37) becomes

$$\vec{h}_O + m\vec{r}_c \times \ddot{\vec{R}}_O = \vec{M}_O \tag{2.40}$$

where $\vec{h}_O$ is the relative angular momentum about point O, and

$$\vec{h}_O = \int \vec{r} \times \dot{\vec{r}} dm \tag{2.41}$$

Similar to the relative angular momentum about point O, the absolute angular

momentum about point O is defined as

$$\vec{H}_O = \int \vec{r} \times \dot{\vec{R}} dm \tag{2.42}$$

Combining equations (2.37) and (2.42), we have

$$\dot{\vec{H}}_O + m\dot{\vec{R}}_O \times \dot{\vec{r}}_c = \vec{M}_O \tag{2.43}$$

If the reference point O is either inertially fixed or at the center of mass of the rigid body, then

$$\dot{\vec{H}}_O = \vec{M}_O \quad \text{or} \quad \dot{\vec{h}}_O = \vec{M}_O \tag{2.44}$$

Next, we will introduce the inertial matrix of a rigid body. Consider a rigid body with a fixed-body reference frame B, where its origin is at the center of mass of the rigid body as shown in figure 2.4. In this figure, $\vec{R}_c$ is the position vector of the center of mass with respect to the origin of the inertial reference frame A, $\vec{\Omega}$ represents the angular velocity vector of the rigid body in the frame A, and $\vec{H}$ is the angular momentum vector of the rigid body about its mass center

$$\vec{H} = \int \vec{R}_{cm} \times \dot{\vec{R}} dm = \int \vec{R}_{cm} \times \dot{\vec{R}}_{cm} dm = \int \vec{R}_{cm} \times \left(\vec{\Omega} \times \vec{R}_{cm}\right) dm \tag{2.45}$$

since $\vec{R} = \vec{R}_c + \vec{R}_{cm}$, $\int \vec{R}_{cm} dm = 0$, and

$$\dot{\vec{R}}_{cm} = \left\{ \frac{d\vec{R}_{cm}}{dt} \right\}_A = \left\{ \frac{d\vec{R}_{cm}}{dt} \right\}_B + \vec{\Omega} \times \vec{R}_{cm} \tag{2.46}$$

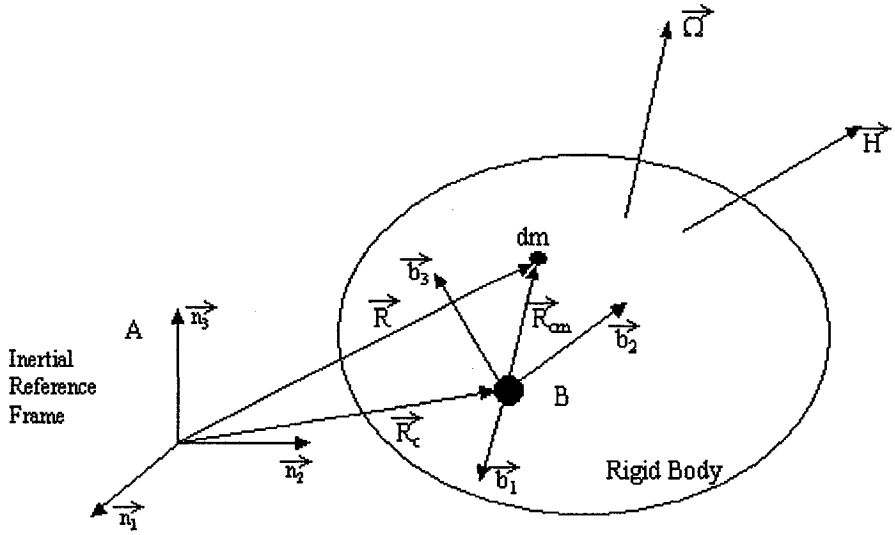

Figure 2.4: Rigid body with a body-fixed reference frame

and, $\left\{d\vec{R}_{cm}/dt\right\}_B = 0$ for a rigid body.

It is assumed that $\vec{R}_{cm}$ and $\vec{\Omega}$ are expressed according to

$$\vec{R}_{cm} = R_{cm1}\vec{b}_1 + R_{cm2}\vec{b}_2 + R_{cm3}\vec{b}_3 \tag{2.47}$$

$$\vec{\Omega} = \Omega_1\vec{b}_1 + \Omega_2\vec{b}_2 + \Omega_3\vec{b}_3 \tag{2.48}$$

where $\left\{\vec{b}_1, \vec{b}_2, \vec{b}_3\right\}$ represents a set of three orthogonal unit vectors, known as basis vectors of the frame B. The angular momentum vector of the rigid body about the center of mass can then be rewritten as

$$\begin{aligned}\vec{H} = &\left(J_{11}\Omega_1 + J_{12}\Omega_2 + J_{13}\Omega_3\right)\vec{b}_1 + \left(J_{21}\Omega_1 + J_{22}\Omega_2 + J_{23}\Omega_3\right)\vec{b}_2 \\ &+ \left(J_{31}\Omega_1 + J_{32}\Omega_2 + J_{33}\Omega_3\right)\vec{b}_3\end{aligned} \tag{2.49}$$

where J_{11}, J_{22} and J_{33} are the moments of inertia

$$J_{11} = \int (R_{cm2}^2 + R_{cm3}^2) dm \tag{2.50}$$

$$J_{22} = \int (R_{cm1}^2 + R_{cm3}^2) dm \tag{2.51}$$

$$J_{33} = \int (R_{cm1}^2 + R_{cm2}^2) dm \tag{2.52}$$

and J_{ij} $(i \neq j)$ are the products of inertia

$$J_{12} = J_{21} = -\int R_{cm1} R_{cm2} dm \tag{2.53}$$

$$J_{13} = J_{31} = -\int R_{cm1} R_{cm3} dm \tag{2.54}$$

$$J_{23} = J_{32} = -\int R_{cm2} R_{cm3} dm \tag{2.55}$$

Let the angular momentum vector be expressed as

$$\vec{H} = H_1 \vec{b}_1 + H_2 \vec{b}_2 + H_3 \vec{b}_3 \tag{2.56}$$

where

$$H_1 = J_{11}\Omega_1 + J_{12}\Omega_2 + J_{13}\Omega_3 \tag{2.57}$$

$$H_2 = J_{21}\Omega_1 + J_{22}\Omega_2 + J_{23}\Omega_3 \tag{2.58}$$

$$H_3 = J_{31}\Omega_1 + J_{32}\Omega_2 + J_{33}\Omega_3 \tag{2.59}$$

Consequently, we obtain

$$H = J\Omega \tag{2.60}$$

where $H = \begin{bmatrix} H_1 \\ H_2 \\ H_3 \end{bmatrix}$, $J = \begin{bmatrix} J_{11} & J_{12} & J_{13} \\ J_{21} & J_{22} & J_{23} \\ J_{31} & J_{32} & J_{33} \end{bmatrix}$, and $\Omega = \begin{bmatrix} \Omega_1 \\ \Omega_2 \\ \Omega_3 \end{bmatrix}$.

Here, J is called the inertia matrix of a rigid body about a fixed body reference frame B with its origin at the center of mass. Note that the inertia matrix of a rigid body is symmetric, that is $J = J^T$. Since $\vec{H}$ is the angular momentum vector of the rigid body about its center of mass, and we consider the reference point in (2.44) as the center of mass, equation (2.44) becomes

$$\dot{\vec{H}} = \vec{M} \tag{2.61}$$

where $\vec{M}$ represents the external moment acting on the rigid body about its center of mass, and we have

$$\dot{\vec{H}} = \left\{ \frac{d\vec{H}}{dt} \right\}_A = \left\{ \frac{d\vec{H}}{dt} \right\}_B + \vec{\Omega} \times \vec{H} \tag{2.62}$$

Therefore, combining (2.61) and (2.62), we have

$$\vec{M} = \left\{ \frac{d\vec{H}}{dt} \right\}_B + \vec{\Omega} \times \vec{H} \tag{2.63}$$

Let $\vec{M}$, $\vec{H}$, and $\vec{\Omega}$ be expressed by

$$\vec{M} = M_1\vec{b}_1 + M_2\vec{b}_2 + M_3\vec{b}_3$$

$$\vec{H} = H_1\vec{b}_1 + H_2\vec{b}_2 + H_3\vec{b}_3$$

$$\vec{\Omega} = \Omega_1\vec{b}_1 + \Omega_2\vec{b}_2 + \Omega_3\vec{b}_3$$

Substituting these into (2.63), we obtain

$$\begin{bmatrix} M_1 \\ M_2 \\ M_3 \end{bmatrix} = \begin{bmatrix} \dot{H}_1 \\ \dot{H}_2 \\ \dot{H}_3 \end{bmatrix} + \begin{bmatrix} 0 & -\Omega_3 & \Omega_2 \\ \Omega_3 & 0 & -\Omega_1 \\ -\Omega_2 & \Omega_1 & 0 \end{bmatrix} \begin{bmatrix} H_1 \\ H_2 \\ H_3 \end{bmatrix} \tag{2.64}$$

Combining (2.60) and (2.64), we have

$$\begin{aligned} \begin{bmatrix} M_1 \\ M_2 \\ M_3 \end{bmatrix} &= \begin{bmatrix} J_{11} & J_{12} & J_{13} \\ J_{21} & J_{22} & J_{23} \\ J_{31} & J_{32} & J_{33} \end{bmatrix} \begin{bmatrix} \dot{\Omega}_1 \\ \dot{\Omega}_2 \\ \dot{\Omega}_3 \end{bmatrix} \\ &+ \begin{bmatrix} 0 & -\Omega_3 & \Omega_2 \\ \Omega_3 & 0 & -\Omega_1 \\ -\Omega_2 & \Omega_1 & 0 \end{bmatrix} \begin{bmatrix} J_{11} & J_{12} & J_{13} \\ J_{21} & J_{22} & J_{23} \\ J_{31} & J_{32} & J_{33} \end{bmatrix} \begin{bmatrix} \Omega_1 \\ \Omega_2 \\ \Omega_3 \end{bmatrix} \end{aligned} \tag{2.65}$$

Therefore,

$$J\dot{\Omega} = -\Omega^{\times} J\Omega + M \tag{2.66}$$

where $\Omega^{\times} = \begin{bmatrix} 0 & -\Omega_3 & \Omega_2 \\ \Omega_3 & 0 & -\Omega_1 \\ -\Omega_2 & \Omega_1 & 0 \end{bmatrix}$, and $M = \begin{bmatrix} M_1 \\ M_2 \\ M_3 \end{bmatrix}$.

Equation (2.66) is the well-known Euler's rotation equation of motion for a rigid body such as a satellite. Normally, in control systems, one considers M as the input signal and use the symbol u to denote this, therefore we rewrite (2.66) as

$$J\dot{\Omega} = -\Omega^{\times} J\Omega + u \tag{2.67}$$

In the following, we will introduce the Euler parameters or the quaternions [15, 29, 30, 31, 32]. Suppose the unit vectors $\vec{a}_i$ and $\vec{b}_i$ $(i = 1, 2, 3)$ are fixed to the reference frame A and B. It is assumed that the rigid body rotates about a fixed axis, called Euler axis or eigenaxis. This axis is represented by a unit vector $\vec{e}$ as:

$$\begin{aligned} \vec{e} &= e_1\vec{a}_1 + e_2\vec{a}_2 + e_3\vec{a}_3 \\ &= e_1\vec{b}_1 + e_2\vec{b}_2 + e_3\vec{b}_3 \end{aligned} \tag{2.68}$$

where

$$e_1^2 + e_2^2 + e_3^2 = 1 \tag{2.69}$$

The Euler parameters or quaternions are now defined as following:

$$\varepsilon_1 = e_1 \sin(\theta/2) \tag{2.70}$$

$$\varepsilon_2 = e_2 \sin(\theta/2) \tag{2.71}$$

$$\varepsilon_3 = e_3 \sin(\theta/2) \tag{2.72}$$

$$\varepsilon_0 = \cos(\theta/2) \tag{2.73}$$

where θ is the rotation angle about the Euler axis, and we let $\varepsilon = \begin{bmatrix} \varepsilon_1 & \varepsilon_2 & \varepsilon_3 \end{bmatrix}^T$.

Due to (2.69), we obtain

$$\varepsilon^T\varepsilon + \varepsilon_0^2 = \varepsilon_1^2 + \varepsilon_2^2 + \varepsilon_3^2 + \varepsilon_0^2 = 1 \tag{2.74}$$

We now define the direction cosine matrix $C = C^{B/A}$ such that

$$\begin{bmatrix} \vec{b}_1 \\ \vec{b}_2 \\ \vec{b}_3 \end{bmatrix} = C \begin{bmatrix} \vec{a}_1 \\ \vec{a}_2 \\ \vec{a}_3 \end{bmatrix} \tag{2.75}$$

which can be rewritten as

$$\begin{bmatrix} \vec{a}_1 \\ \vec{a}_2 \\ \vec{a}_3 \end{bmatrix} = C^{-1} \begin{bmatrix} \vec{b}_1 \\ \vec{b}_2 \\ \vec{b}_3 \end{bmatrix} = C^T \begin{bmatrix} \vec{b}_1 \\ \vec{b}_2 \\ \vec{b}_3 \end{bmatrix} \tag{2.76}$$

Referring to the results presented in [15], we know that

$$C = \begin{bmatrix} 1-2\left(\varepsilon_2^2+\varepsilon_3^2\right) & 2\left(\varepsilon_1\varepsilon_2+\varepsilon_3\varepsilon_0\right) & 2\left(\varepsilon_1\varepsilon_3+\varepsilon_2\varepsilon_0\right) \\ 2\left(\varepsilon_2\varepsilon_1-\varepsilon_3\varepsilon_0\right) & 1-2\left(\varepsilon_1^2+\varepsilon_3^2\right) & 2\left(\varepsilon_2\varepsilon_3+\varepsilon_1\varepsilon_0\right) \\ 2\left(\varepsilon_3\varepsilon_1+\varepsilon_2\varepsilon_0\right) & 2\left(\varepsilon_3\varepsilon_2-\varepsilon_1\varepsilon_0\right) & 1-2\left(\varepsilon_1^2+\varepsilon_2^2\right) \end{bmatrix} \tag{2.77}$$

Taking the time derivative of (2.76) with respect to the reference frame A, we obtain

$$\begin{aligned} \begin{bmatrix} 0 \\ 0 \\ 0 \end{bmatrix} &= \dot{C}^T \begin{bmatrix} \vec{b}_1 \\ \vec{b}_2 \\ \vec{b}_3 \end{bmatrix} + C^T \begin{bmatrix} \dot{\vec{b}}_1 \\ \dot{\vec{b}}_2 \\ \dot{\vec{b}}_3 \end{bmatrix} \\ &= \dot{C}^T \begin{bmatrix} \vec{b}_1 \\ \vec{b}_2 \\ \vec{b}_3 \end{bmatrix} + C^T \begin{bmatrix} \vec{\Omega} \times \vec{b}_1 \\ \vec{\Omega} \times \vec{b}_2 \\ \vec{\Omega} \times \vec{b}_3 \end{bmatrix} \\ &= \dot{C}^T \begin{bmatrix} \vec{b}_1 \\ \vec{b}_2 \\ \vec{b}_3 \end{bmatrix} - C^T \begin{bmatrix} 0 & -\Omega_3 & \Omega_2 \\ \Omega_3 & 0 & -\Omega_1 \\ -\Omega_2 & \Omega_1 & 0 \end{bmatrix} \begin{bmatrix} \vec{b}_1 \\ \vec{b}_2 \\ \vec{b}_3 \end{bmatrix} \end{aligned} \tag{2.78}$$

where

$$\dot{C} = \begin{bmatrix} \dot{C}_{11} & \dot{C}_{12} & \dot{C}_{13} \\ \dot{C}_{21} & \dot{C}_{22} & \dot{C}_{23} \\ \dot{C}_{31} & \dot{C}_{32} & \dot{C}_{33} \end{bmatrix} \tag{2.79}$$

Thus, we have

$$\left[\dot{C}^T - C^T\Omega^\times\right]\begin{bmatrix}\vec{b}_1\\ \vec{b}_2\\ \vec{b}_3\end{bmatrix} = \begin{bmatrix}0\\ 0\\ 0\end{bmatrix} \tag{2.80}$$

therefore,

$$\dot{C}^T - C^T\Omega^\times = 0 \tag{2.81}$$

Since $(\Omega^\times)^T = -\Omega^\times$, we have

$$\dot{C} + \Omega^\times C = 0 \tag{2.82}$$

From (2.82), we obtain

$$\Omega_1 = \dot{C}_{21}C_{31} + \dot{C}_{22}C_{32} + \dot{C}_{23}C_{33} \tag{2.83}$$

$$\Omega_2 = \dot{C}_{31}C_{11} + \dot{C}_{32}C_{12} + \dot{C}_{33}C_{13} \tag{2.84}$$

$$\Omega_3 = \dot{C}_{11}C_{21} + \dot{C}_{12}C_{22} + \dot{C}_{13}C_{23} \tag{2.85}$$

Substituting C_{ij} and $\dot{C}_{ij}$ from (2.77) and (2.82) into (2.83)–(2.85), we obtain

$$\Omega_1 = 2\left(\dot{\varepsilon}_1\varepsilon_0 + \dot{\varepsilon}_2\varepsilon_3 - \dot{\varepsilon}_3\varepsilon_2 - \dot{\varepsilon}_0\varepsilon_1\right) \tag{2.86}$$

$$\Omega_2 = 2\left(\dot{\varepsilon}_2\varepsilon_0 + \dot{\varepsilon}_3\varepsilon_1 - \dot{\varepsilon}_1\varepsilon_3 - \dot{\varepsilon}_0\varepsilon_2\right) \tag{2.87}$$

$$\Omega_3 = 2\left(\dot{\varepsilon}_3\varepsilon_4 + \dot{\varepsilon}_1\varepsilon_2 - \dot{\varepsilon}_2\varepsilon_1 - \dot{\varepsilon}_0\varepsilon_3\right) \tag{2.88}$$

Differentiating (2.74), we have

$$0 = 2\left(\dot{\varepsilon}_1\varepsilon_1 + \dot{\varepsilon}_2\varepsilon_2 - \dot{\varepsilon}_3\varepsilon_3 - \dot{\varepsilon}_0\varepsilon_0\right) \tag{2.89}$$

These four equations can be rewritten in a compact matrix form as

$$\begin{bmatrix} \Omega_1 \\ \Omega_2 \\ \Omega_3 \\ 0 \end{bmatrix} = 2 \begin{bmatrix} \varepsilon_0 & \varepsilon_3 & -\varepsilon_2 & -\varepsilon_1 \\ -\varepsilon_3 & \varepsilon_0 & \varepsilon_1 & \varepsilon_2 \\ \varepsilon_2 & -\varepsilon_1 & \varepsilon_0 & -\varepsilon_3 \\ \varepsilon_1 & \varepsilon_2 & \varepsilon_3 & \varepsilon_0 \end{bmatrix} \begin{bmatrix} \dot{\varepsilon}_1 \\ \dot{\varepsilon}_2 \\ \dot{\varepsilon}_3 \\ \dot{\varepsilon}_0 \end{bmatrix} \tag{2.90}$$

Since the 4×4 matrix in the above equation is orthonormal, we can obtain the differential equations for the Euler parameters as:

$$\begin{bmatrix} \dot{\varepsilon}_1 \\ \dot{\varepsilon}_2 \\ \dot{\varepsilon}_3 \\ \dot{\varepsilon}_0 \end{bmatrix} = \frac{1}{2} \begin{bmatrix} \varepsilon_0 & -\varepsilon_3 & \varepsilon_2 & \varepsilon_1 \\ \varepsilon_3 & \varepsilon_0 & -\varepsilon_1 & \varepsilon_2 \\ -\varepsilon_2 & \varepsilon_1 & \varepsilon_0 & \varepsilon_3 \\ -\varepsilon_1 & -\varepsilon_2 & -\varepsilon_3 & \varepsilon_0 \end{bmatrix} \begin{bmatrix} \Omega_1 \\ \Omega_2 \\ \Omega_3 \\ 0 \end{bmatrix} \tag{2.91}$$

Based on the already developed kinematic equations for the satellite which is considered to be a rigid body through the equations (2.67) and (2.91), thrusters that provide external torques about three mutually perpendicular axes that define a body-fixed frame B is now introduced to these equations. The equations of motion can

therefore be expressed as following:

$$J\dot{\Omega} = -\Omega^{\times} J\Omega + u + m + u_r + w \tag{2.92}$$

$$\dot{\varepsilon} = \frac{1}{2}(\varepsilon^{\times} + \varepsilon_0 \mathrm{I})\Omega \tag{2.93}$$

$$\dot{\varepsilon}_0 = -\frac{1}{2}\varepsilon^T \Omega \tag{2.94}$$

where $\Omega \in R^3$ represents the inertial angular velocity of the satellite with respect to an inertial frame A, $J = J^T$ represents the positive definite inertia matrix of the satellite, $\varepsilon \in R^3$ and $\varepsilon_0 \in R$ represent the quaternions representing the orientation of B with respect to the inertial frame A and $\varepsilon^T\varepsilon + \varepsilon_0^2 = 1$, and I represents a 3×3 identity matrix, $u = [\ u_1 \quad u_2 \quad u_3\ ]^T$ is the vector of actual control torques generated by the actuator thrusters. All the control torque channels may have faults which are represented by m_1, m_2, and m_3, respectively, and $m = [\ m_1 \quad m_2 \quad m_3\ ]^T$ is the vector of these possible faulty torques. In addition, we assume that

$$m_i = -k_i u_i, \quad i = 1, 2, 3 \tag{2.95}$$

where k_i is a positive constant and $0 \leq k_i \leq 1$. The parameter $k_i = 1$ represents a total fault in the control channel i. Let us denote $k = \begin{bmatrix} k_1 & k_2 & k_3 \end{bmatrix}^T$, $u_r = [\ u_{r1} \quad u_{r2} \quad u_{r3}\ ]^T$ denote the vector of actual redundant control torques, where it is assumed that the redundant control torques are fault free, and $w = [\ w_1 \quad w_2 \quad w_3\ ]^T$ represents the vector of disturbances. Furthermore, it is assumed that the total

control authority is limited, that is $-u_{mi} \leq u_i \leq u_{mi}$, $(i = 1, 2, 3)$, and we let

$$u_m = \begin{bmatrix} u_{m1} & u_{m2} & u_{m3} \end{bmatrix}^T$$

In addition, it is assumed that we can measure the inertial angular velocity and quaternions directly.

2.5 Justification and Necessity for Development of Nonlinear FDIR

As mentioned in Chapter 1, a number of FDIR methods have been developed in the literature for linear systems, but all real-life systems are practically nonlinear. In order to practically implement the linear FDIR techniques developed in the literature, most of the researchers advocate linearizing the nonlinear systems firstly, and then design the FDIR system based on the linearized system and apply it to the original nonlinear system. However, there are two obvious disadvantages with this strategy. First, linearization which is an approximation procedure will result in modelling errors, which may lead to false alarms for the FDIR algorithms. Second, linearization may hinder solvability conditions for the fault detection schemes. In this section, we will use an example to illustrate these two problems.

Consider a nonlinear system modelled by

$$\begin{cases} \dot{x}_1 = -x_1 - x_2^2 + 1 + u + m \\ \dot{x}_2 = x_1^2 - x_2 \end{cases} \tag{2.96}$$

$$\begin{cases} y_1 = x_1 \\ y_2 = x_2 \end{cases} \tag{2.97}$$

where x_i $(i = 1, 2)$ are the states, y_i $(i = 1, 2)$ are the outputs, u is an input, and m represents the input fault.

By linearizing the nonlinear system at $x = \begin{bmatrix} 0 & 0.1 \end{bmatrix}^T$, we obtain the linearized system

$$\begin{cases} \dot{x}_1 = -x_1 - 0.2x_2 + 1 + u + m \\ \dot{x}_2 = -x_2 \end{cases} \tag{2.98}$$

For the above linearized system, one can simply use an observer for the state x_1 to detect the input fault according to

$$\dot{\hat{x}}_1 = -\hat{x}_1 - 0.2y_2 + 1 + u - (y_1 - \hat{x}_1) \tag{2.99}$$

$$e = y_1 - \hat{x}_1 \tag{2.100}$$

Now, consider the linear observer (2.99) and (2.100) as the residual generator for the original nonlinear system. If the state estimate error e deviates from zero, one may claim the occurrence of a fault. The behavior of this residual generator is simulated in figures 2.5 and 2.6 with the input signal chosen as $u = 0.6\cos t - 1$. In

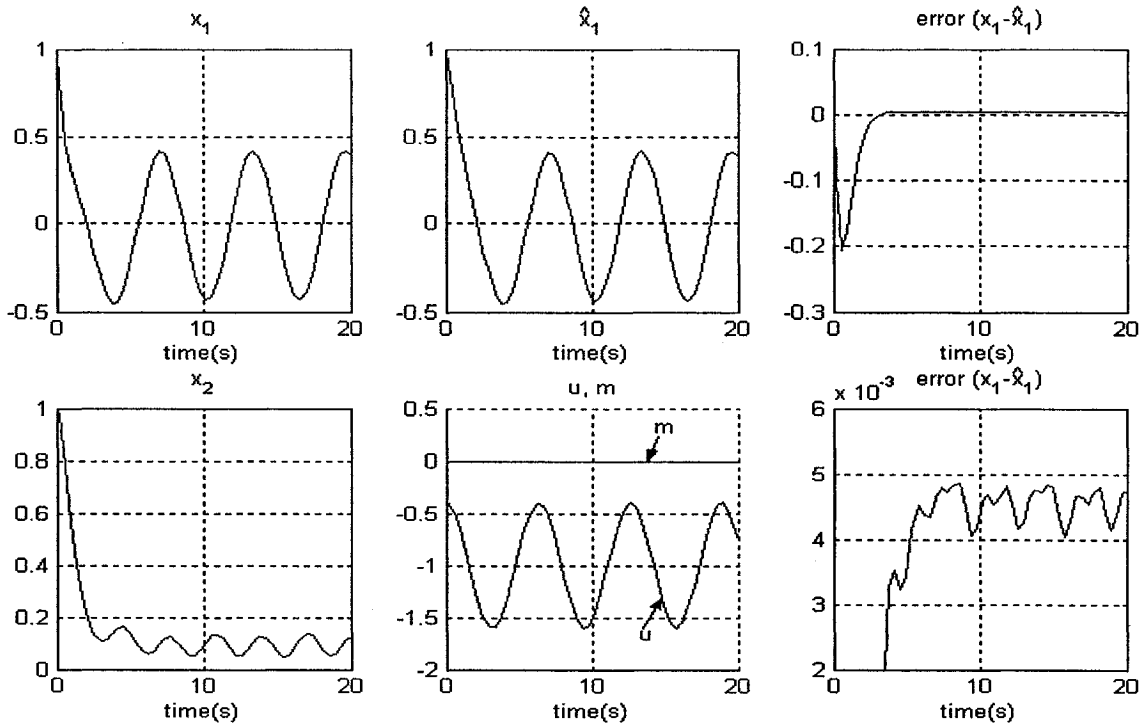

Figure 2.5: Linear observer applied to the nonlinear system ($\hat{x}_1^0 = x_1^0$)

the simulation results of figure 2.5, the initial values of the states are $x^0 = \begin{bmatrix} 1 & 1 \end{bmatrix}^T$ and the initial value of the observer is $\hat{x}_1^0 = 1$ with presence of no fault in the system. The only difference between the results in figure 2.6 and the ones in figure 2.5 is that the initial value of the observer is $\hat{x}_1^0 = 0$ in figure 2.6. Clearly, from these figures, one can easily observe that even when there is no fault, the error e is not zero which may lead one to conclude a false alarm.

Clearly, there are some remedies to this "false alarm" problem for linear FDIR schemes. For example, the nonlinear model can be linearized at several operating points in the domain of feasible motion of the system, and consequently multiple linear models are scheduled and estimated. However, the challenge still remains in reducing the number of linearized models to as few as possible to cover the whole

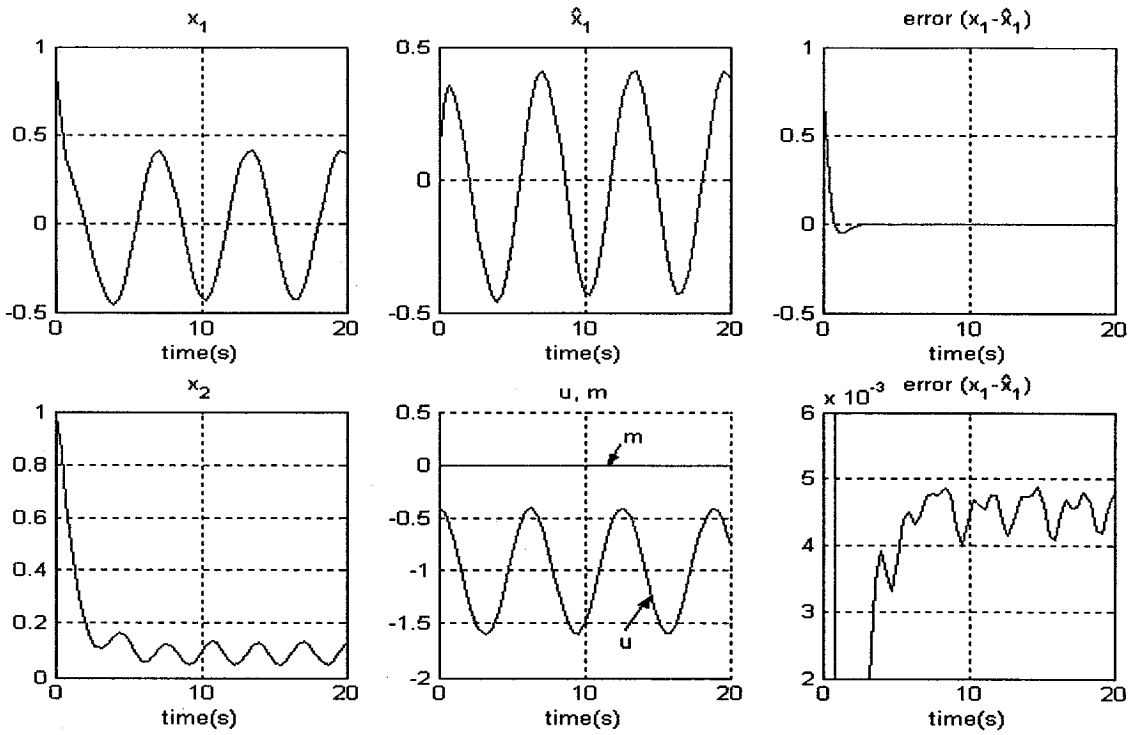

Figure 2.6: Linear observer applied to the nonlinear system ($\hat{x}_1^0 \neq x_1^0$)

motion dynamics. Otherwise, the structure of the FDIR system is going to be very large and complex.

Another disadvantage of applying linear FDIR methods to nonlinear systems is that linear techniques may hinder the possibility of solving the FDIR problem. We will use system (2.96) to illustrate this problem with the only difference from the above example being that we only have one output, namely

$$y_2 = x_2 \tag{2.101}$$

We continue to linearize the original system at the equilibrium point $x = \begin{bmatrix} 0 & 0.1 \end{bmatrix}^T$ to obtain the linearized system (2.98). Using the only output as (2.101), one cannot design a linear observer for the state x_1. Furthermore, from equation (2.98), it is

simple to note that the fault m cannot affect the state x_2 through x_1. That is, we cannot design a desirable linear residual generator when we have only one output y_2 (state x_1 is unobservable).

However, by inspecting the original nonlinear system (2.96), it is clear that the fault m does indeed affect x_2 through x_1, so it should be possible to design a residual generator for the nonlinear system with only one output (2.101). In the following, we will design a nonlinear observer for the original system as a candidate residual generator to determine whether it can detect the fault as given by

$$\begin{cases} \dot{\hat{x}}_1 = -\hat{x}_1 - \hat{x}_2^2 + 1 + u + 4\,(y_2 - \hat{x}_2) \\ \dot{\hat{x}}_2 = \hat{x}_1^2 - \hat{x}_2 + 2\,(y_2 - \hat{x}_2) \end{cases} \tag{2.102}$$

$$e = y_2 - \hat{x}_2 \tag{2.103}$$

Figures 2.7 and 2.8 show the behavior of this nonlinear observer. In figure 2.7, the initial values of the states are selected as $x_0 = \begin{bmatrix} 1 & 1 \end{bmatrix}^T$ and the initial values of the observed states are $\hat{x}_0 = \begin{bmatrix} 1 & 1 \end{bmatrix}^T$. The system is subjected to a total loss of actuator and fault ($m = -u$) occurring at the time $t = 10s$. One can observe from the figure that from the time $t = 10s$ the residual error e deviates from zero indicating the presence of a fault. In figure 2.8, the initial values of the observed states are $\hat{x}_0 = \begin{bmatrix} 0 & 0 \end{bmatrix}^T$. One can observe that after the transients have settled down, the residual error becomes zero which, however, deviates from zero from the time $t = 10s$ when the fault occurs.

Using this example, we can conclude that the nonlinear observer we proposed may

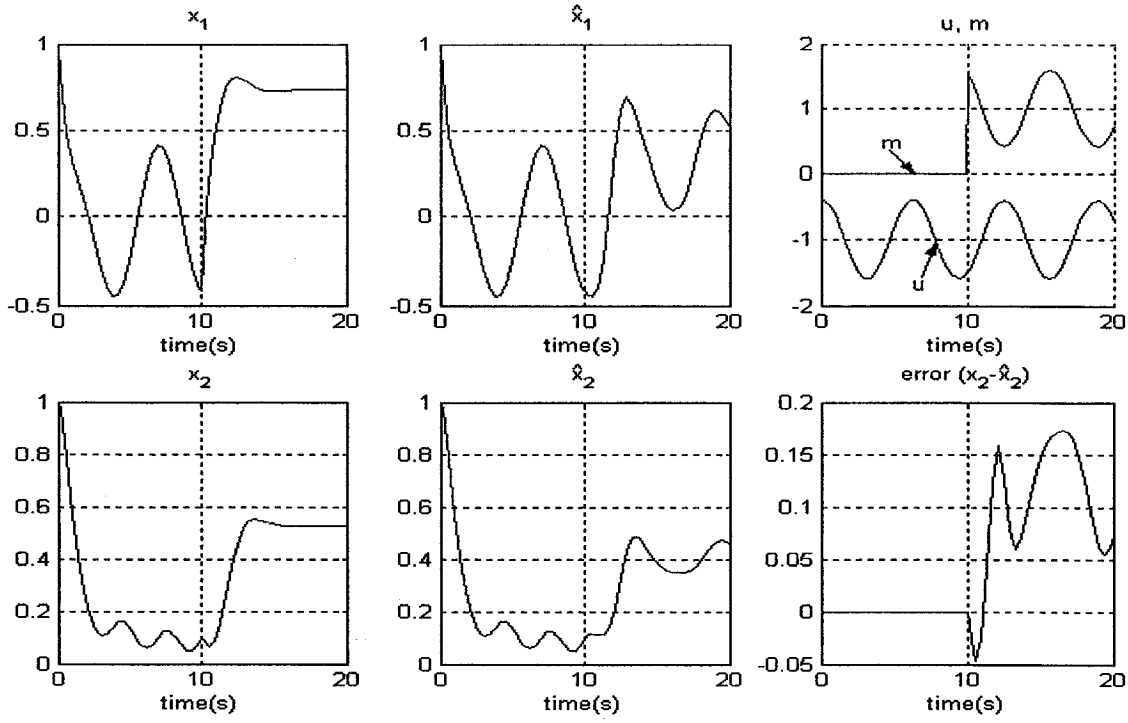

Figure 2.7: Application of nonlinear observer to the faulty system ($\hat{x}^0 = x^0$)

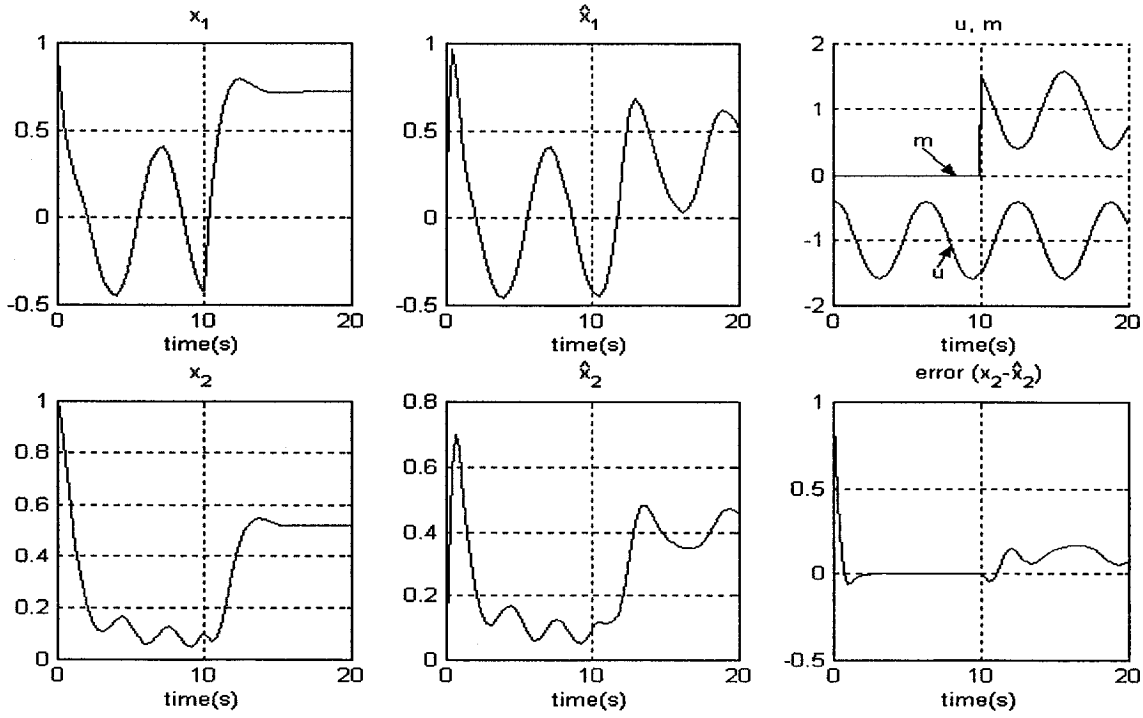

Figure 2.8: Application of nonlinear observer to the faulty system ($\hat{x}^0 \neq x^0$)

be considered as an effective residual generator whereas the linearization procedure hinders this possibility. The linearization procedure may also increase the presence of "false alarm", and reduce the possiblity of solving the FDIR problem. Consequently, nonlinear FDIR methods have recently received a great deal of attention in the literature.

Chapter 3

FDIR Scheme for the Satellite Orbital Model

3.1 Sliding Mode Controller

In this section, we introduce and develop sliding mode controllers [18, 33] for the satellite orbital model. In the sliding mode control, trajectories are forced to reach a sliding manifold in finite time, followed by a *sliding phase* during which the trajectories are confined to the manifold and the dynamical system is represented by the reduced-order model. Our control goal is to force the open-loop system (2.35) track certain desirable reference trajectories, namely we assume that ρ is required to track r_1 and ϕ to track r_2, with the derivative of r_1 and r_2, that is $\dot{r}_1$ and $\dot{r}_2$, respectively, is also given.

Note that the parameter θ_2 and the state ρ are always greater than zero, since ρ is the distance from the satellite to the earth's core and θ_2 is the reciprocal of the

satellite's mass. The detailed information about this model is given in section 2.3.

At first, we assume that all the states of the system are available for measurement. Subsequently, the full-state feedback controller is augmented with an observer for the state υ, which in reality is not available for measurement.

We set the vector $R = \begin{bmatrix} r_1 & \dot{r}_1 & r_2 & \dot{r}_2 \end{bmatrix}^T$, and the tracking error vector as

$$\begin{pmatrix} e_1 \\ e_2 \\ e_3 \\ e_4 \end{pmatrix} = \begin{pmatrix} \rho - r_1 \\ \upsilon - \dot{r}_1 \\ \phi - r_2 \\ \omega - \dot{r}_2 \end{pmatrix} \tag{3.1}$$

Therefore, we obtain

$$\begin{pmatrix} \dot{e}_1 \\ \dot{e}_2 \\ \dot{e}_3 \\ \dot{e}_4 \end{pmatrix} = \begin{pmatrix} \dot{\rho} - \dot{r}_1 \\ \dot{\upsilon} - \ddot{r}_1 \\ \dot{\phi} - \dot{r}_2 \\ \dot{\omega} - \ddot{r}_2 \end{pmatrix} = \begin{pmatrix} \upsilon - \dot{r}_1 \\ \rho\omega^2 - \theta_1 \frac{1}{\rho^2} + \theta_2 u_1 - \ddot{r}_1 \\ \omega - \dot{r}_2 \\ -\frac{2\upsilon\omega}{\rho} + \theta_2 \frac{u_2}{\rho} - \ddot{r}_2 \end{pmatrix}$$

That is,

$$\begin{pmatrix} \dot{e}_1 \\ \dot{e}_2 \\ \dot{e}_3 \\ \dot{e}_4 \end{pmatrix} = \begin{pmatrix} e_2 \\ \rho\omega^2 - \theta_1 \frac{1}{\rho^2} + \theta_2 u_1 - \ddot{r}_1 \\ e_4 \\ -\frac{2\upsilon\omega}{\rho} + \theta_2 \frac{u_2}{\rho} - \ddot{r}_2 \end{pmatrix}$$

By selecting the sliding surfaces according to $\begin{cases} s_1 = a_1 e_1 + e_2 \\ s_2 = a_2 e_3 + e_4 \end{cases}$ where $a_1 > 0$, $a_2 > 0$, we obtain

$$\dot{s}_1 = a_1 \dot{e}_1 + \dot{e}_2 = a_1(v - \dot{r}_1) + \rho\omega^2 - \theta_1 \frac{1}{\rho^2} + \theta_2 u_1 - \ddot{r}_1 \tag{3.2}$$

$$\dot{s}_2 = a_2 \dot{e}_3 + \dot{e}_4 = a_2(\omega - \dot{r}_2) - \frac{2v\omega}{\rho} + \theta_2 \frac{u_2}{\rho} - \ddot{r}_2 \tag{3.3}$$

Assume that

$$\left| \frac{a_1(v - \dot{r}_1) + \rho\omega^2 - \theta_1 \frac{1}{\rho^2} - \ddot{r}_1}{\theta_2} \right| \leq \hat{k}_1 \tag{3.4}$$

$$\left| \frac{a_2(\omega - \dot{r}_2) - \frac{2v\omega}{\rho} - \ddot{r}_2}{\theta_2/\rho} \right| \leq \hat{k}_2 \tag{3.5}$$

where the parameters $\hat{k}_1$ and $\hat{k}_2$ represent the saturation of inputs u_1 and u_2, that is, $|u_1| \leq \hat{k}_1$ and $|u_2| \leq \hat{k}_2$. Given the references r_1 and r_2, we cannot guarantee that equations (3.4) and (3.5) always hold. Consequently, we cannot always design an effective sliding mode controller given r_1, r_2, $\hat{k}_1$ and $\hat{k}_1$.

Consequently, we propose the control inputs according to

$$\begin{aligned} u_1 &= -k_1 sgn(s_1), \qquad k_1 > \hat{k}_1 \\ u_2 &= -k_2 sgn(s_2), \qquad k_2 > \hat{k}_2 \end{aligned} \tag{3.6}$$

Using $\begin{cases} V_1 = (1/2)s_1^2 \\ V_2 = (1/2)s_2^2 \end{cases}$ as Lyapunov-like function candidates [18], we have

$$\begin{aligned}
\dot{V}_1 = s_1\dot{s}_1 &= s_1\left(a_1(v-\dot{r}_1)+\rho\omega^2-\theta_1\frac{1}{\rho^2}+\theta_2 u_1-\ddot{r}_1\right)\\
&= s_1\left(a_1(v-\dot{r}_1)+\rho\omega^2-\theta_1\frac{1}{\rho^2}-\ddot{r}_1\right)+s_1\theta_2 u_1\\
&\leq s_1\theta_2\hat{k}_1+s_1\theta_2 u_1 < s_1\theta_2 k_1+s_1\theta_2(-k_1 sgn(s_1))\\
&\leq |s_1|\theta_2 k_1-|s_1|\theta_2 k_1 = 0
\end{aligned}$$

and,

$$\begin{aligned}
\dot{V}_2 = s_2\dot{s}_2 &= s_2\left(a_2(\omega-\dot{r}_2)-\frac{2v\omega}{\rho}+\theta_2\frac{u_2}{\rho}-\ddot{r}_2\right)\\
&= s_2\left(a_2(\omega-\dot{r}_2)-\frac{2v\omega}{\rho}-\ddot{r}_2\right)+s_2\theta_2\frac{u_2}{\rho}\\
&\leq \frac{s_2\theta_2\hat{k}_2}{\rho}+\frac{s_2\theta_2 u_2}{\rho}\\
&< \frac{s_2\theta_2 k_2}{\rho}+\frac{s_2\theta_2(-k_2 sgn(s_2))}{\rho}\\
&\leq \frac{|s_2|\theta_2 k_2}{\rho}-\frac{|s_2|\theta_2 k_2}{\rho}=0
\end{aligned}$$

Since $\dot{V}_1 < 0$ and $\dot{V}_2 < 0$, the motion of the system will reach the sliding surfaces s_1 and s_2 in finite time. Consequently, on the sliding surfaces, the motion of the system is governed by $\dot{e}_1 = -a_1 e_1$ and $\dot{e}_3 = -a_2 e_3$. As a_1 and a_2 are positive, $e(t)$ tends to zero as t tends to infinity.

The above observation leads one to conclude that (3.6) is a desirable controller.

We are in a position to design a nonlinear estimator for the state v which is not available for measurement as follows

$$\begin{pmatrix} \dot{\hat{\rho}} \\ \dot{\hat{v}} \end{pmatrix} = \begin{pmatrix} \hat{v} + G(\nu_1 - \hat{\rho}) \\ \hat{\rho}\nu_3^2 - \theta_1 \frac{1}{\hat{\rho}^2} + \theta_2 u_1 + G^2(\nu_1 - \hat{\rho}) \end{pmatrix}$$

where $\hat{v}$ is the estimate of v and G is a positive constant gain of the estimator.

Therefore equation (3.1) is rewritten as

$$\begin{pmatrix} e_1 \\ e_2 \\ e_3 \\ e_4 \end{pmatrix} = \begin{pmatrix} \rho - r_1 \\ \hat{v} - \dot{r}_1 \\ \phi - r_2 \\ \omega - \dot{r}_2 \end{pmatrix} \tag{3.7}$$

One of the main problems of sliding mode controller is the undesirable high frequency chattering behavior of the system. In order to reduce the chattering effects [5], we instead choose the following as the controller

$$\begin{aligned} u_1 &= -k_1 \frac{s_1}{|s_1| + \delta} \\ u_2 &= -k_2 \frac{s_2}{|s_2| + \delta} \end{aligned} \tag{3.8}$$

where δ is a small positive constant. When s_i $(i = 1, 2)$ is a small value, $\frac{s_i}{|s_i|+\delta}$ will also be small. Consequently, the high frequency chattering can be reduced.

The above proposed sliding mode controller for the satellite orbital model will be used in the simulations in section 3.6 as designing a residual generator requires that the states of the system be uniformly bounded.

3.2 Solvability of a Nonlinear FDIR Scheme and Coordinate Transformations

Persis et al. [4] have already applied their geometric nonlinear control approach to a satellite orbital model. In this section, we will review this application in some detail. The objective is to check the solvability conditions for a nonlinear FDIR scheme as applied to the satellite orbital model and obtain the coordinate transformations that highlight the construction of observable subsystem, upon which the residual generator is designed. In the following, a detailed and step by step procedure toward this goal is provided.

The First Step: Finding $\sum_*^P$

In this step, we will use algorithm (2.4) to calculate the minimal conditioned invariant distribution containing span$\{p\}$, that is $\sum_*^P$. For the system (2.35), the disturbance vector field is given by

$$p = \begin{bmatrix} 0 & 1 & 0 & 0 \end{bmatrix}^T \tag{3.9}$$

Let

$$P = span\,\{p\} \tag{3.10}$$

According to the non-decreasing sequence (2.4), we obtain

$$S_0 = \bar{P} = P \tag{3.11}$$

where $\bar{P}$ denotes the involutive closure of P. Let h denote the smooth output mapping for the system (2.35), that is, we have

$$h = \begin{bmatrix} \rho & \phi & \omega \end{bmatrix}^T \tag{3.12}$$

Therefore,

$$dh = \begin{bmatrix} 1 & 0 & 0 & 0 \\ 0 & 0 & 1 & 0 \\ 0 & 0 & 0 & 1 \end{bmatrix} \tag{3.13}$$

so that

$$Ker\{dh\} = \begin{bmatrix} 0 & 1 & 0 & 0 \end{bmatrix}^T \tag{3.14}$$

Combining (3.11) and (3.14), we obtain

$$\bar{S}_0 \cap Ker\{dh\} = S_0 \cap Ker\{dh\} = \begin{bmatrix} 0 & 1 & 0 & 0 \end{bmatrix}^T \tag{3.15}$$

For the system (2.35), let us denote

$$g_0 = \begin{bmatrix} v \\ \rho\omega^2 - \theta_1/\rho \\ \omega \\ -2v\omega/\rho \end{bmatrix}, g_1 = \begin{bmatrix} 0 \\ \theta_2 \\ 0 \\ \theta_2/\rho \end{bmatrix}$$

Therefore,

$$\begin{aligned}
&\left[g_0, \bar{S}_0 \cap Ker\left\{dh\right\}\right] = -\partial g_0 \cdot \bar{S}_0 \cap Ker\left\{dh\right\} \\
&= -\begin{bmatrix} 0 & 1 & 0 & 0 \\ \omega^2 + \frac{2\theta_1}{\rho^3} & 0 & 0 & 2\rho\omega \\ 0 & 0 & 0 & 1 \\ \frac{2v\omega}{\rho^2} & -\frac{2\omega}{\rho} & 0 & -\frac{2v}{\rho} \end{bmatrix} \begin{bmatrix} 0 \\ 1 \\ 0 \\ 0 \end{bmatrix} = -\begin{bmatrix} 1 & 0 & 0 & -2\omega/\rho \end{bmatrix}^T
\end{aligned}$$

and

$$\begin{aligned}
&\left[g_1, \bar{S}_0 \cap Ker\left\{dh\right\}\right] = -\partial g_1 \cdot \bar{S}_0 \cap Ker\left\{dh\right\} \\
&= -\begin{bmatrix} 0 & 0 & 0 & 0 \\ 0 & 0 & 0 & 0 \\ 0 & 0 & 0 & 0 \\ -\theta_2/\rho & 0 & 0 & 0 \end{bmatrix} \begin{bmatrix} 0 \\ 1 \\ 0 \\ 0 \end{bmatrix} = 0
\end{aligned}$$

Consequently,

$$S_1 = span\left\{\begin{bmatrix} 0 & 1 & 0 & 0 \end{bmatrix}^T, \begin{bmatrix} 1 & 0 & 0 & -\frac{2\omega}{\rho} \end{bmatrix}^T\right\} \tag{3.16}$$

Let us denote $f_1 = \begin{bmatrix} 0 & 1 & 0 & 0 \end{bmatrix}^T$ and $f_2 = \begin{bmatrix} 1 & 0 & 0 & -\frac{2\omega}{\rho} \end{bmatrix}^T$. We now compute

$$[f_1, f_2] = \partial f_2 \cdot f_1 - \partial f_1 \cdot f_2$$

$$= \begin{bmatrix} 0 & 0 & 0 & 0 \\ 0 & 0 & 0 & 0 \\ 0 & 0 & 0 & 0 \\ -2\omega/\rho^2 & 0 & 0 & -2/\rho \end{bmatrix} \begin{bmatrix} 0 \\ 1 \\ 0 \\ 0 \end{bmatrix} = 0$$

It now follows that, $rank \begin{pmatrix} f_1 & f_2 \end{pmatrix} = rank \begin{pmatrix} f_1 & f_2 & [f_1, f_2] \end{pmatrix}$. Thus, $\bar{S}_1 = S_1$ according to the results in [16]. We now have

$$\bar{S}_1 \cap Ker\{dh\} = \begin{bmatrix} 0 & 1 & 0 & 0 \end{bmatrix}^T \tag{3.17}$$

Since $S_2 = \bar{S}_1 + \sum_{i=0}^{1} [g_i, \bar{S}_1 \cap Ker\{dh\}]$, we obtain

$$S_2 = \bar{S}_1$$

Consequently,

$$\sum\nolimits_*^P = \bar{S}_1 = span\left\{ \begin{bmatrix} 0 & 1 & 0 & 0 \end{bmatrix}^T, \begin{bmatrix} 1 & 0 & 0 & -\frac{2\omega}{\rho} \end{bmatrix}^T \right\} \tag{3.18}$$

and $\sum_*^P \cap Ker\{dh\}$ is a smooth distribution when $\rho \neq 0$, so $\left(\sum_*^P\right)^\perp$ is the maximal conditioned invariant codistribution which is locally spanned by the exact differentials.

The Second Step: Finding $\left(\sum_*^P\right)^\perp$

Utilizing the procedure that is described in [16] (section 1.4 on Fobenius Theorem), we now calculate $\left(\sum_*^P\right)^\perp$. Let

$$f_1 = \begin{bmatrix} 0 \\ 1 \\ 0 \\ 0 \end{bmatrix}, \quad f_2 = \begin{bmatrix} 1 \\ 0 \\ 0 \\ -2\omega/\rho \end{bmatrix}, \quad f_3 = \begin{bmatrix} 0 \\ 0 \\ 0 \\ 1 \end{bmatrix}, \quad f_4 = \begin{bmatrix} 0 \\ 0 \\ 1 \\ 0 \end{bmatrix}$$

Next, we will calculate the flows for the vector fields f_i $(i = 1, 2, 3, 4)$.

(i) The flow for f_1 is calculated as:

$$\begin{matrix} \dot{\rho} = 0 \\ \dot{v} = 1 \\ \dot{\phi} = 0 \\ \dot{\omega} = 0 \end{matrix} \Rightarrow \begin{cases} \rho(t) = \rho^0 \\ v(t) = t + v^0 \\ \phi(t) = \phi^0 \\ \omega(t) = \omega^0 \end{cases} \Rightarrow \Phi_{z_1}^{f_1} = \begin{bmatrix} \rho \\ z_1 + v \\ \phi \\ \omega \end{bmatrix}$$

(ii) The flow for f_2 is calculated as:

$$\begin{matrix} \dot{\rho} = 1 \\ \dot{v} = 0 \\ \dot{\phi} = 0 \\ \dot{\omega} = -\frac{2\omega}{\rho} \end{matrix} \Rightarrow \begin{cases} \rho(t) = t + \rho^0 \\ v(t) = v^0 \\ \phi(t) = \phi^0 \\ \omega(t) = \frac{\omega^0 (\rho^0)^2}{(t+\rho^0)^2} \end{cases} \Rightarrow \Phi_{z_2}^{f_2} = \begin{bmatrix} z_2 + \rho \\ v \\ \phi \\ \frac{\omega \rho^2}{(z_2+\rho)^2} \end{bmatrix}$$

(iii) The flow for f_3 is calculated as:

$$\begin{matrix} \dot{\rho} = 0 \\ \dot{\upsilon} = 0 \\ \dot{\phi} = 0 \\ \dot{\omega} = 1 \end{matrix} \Rightarrow \begin{cases} \rho(t) = \rho^0 \\ \upsilon(t) = \upsilon^0 \\ \phi(t) = \phi^0 \\ \omega(t) = t + \omega^0 \end{cases} \Rightarrow \Phi_{z_3}^{f_3} = \begin{bmatrix} \rho \\ \upsilon \\ \phi \\ z_3 + \omega \end{bmatrix}$$

(iv) The flow for f_4 is calculated as:

$$\begin{matrix} \dot{\rho} = 0 \\ \dot{\upsilon} = 0 \\ \dot{\phi} = 1 \\ \dot{\omega} = 0 \end{matrix} \Rightarrow \begin{cases} \rho(t) = \rho^0 \\ \upsilon(t) = \upsilon^0 \\ \phi(t) = t + \phi^0 \\ \omega(t) = \omega^0 \end{cases} \Rightarrow \Phi_{z_4}^{f_4} = \begin{bmatrix} \rho \\ \upsilon \\ z_4 + \phi \\ \omega \end{bmatrix}$$

Let $\begin{bmatrix} \rho^0 & \upsilon^0 & \phi^0 & \omega^0 \end{bmatrix}^T = \begin{bmatrix} 1 & 0 & 0 & 0 \end{bmatrix}^T$, then we obtain

$$\begin{bmatrix} \rho \\ \upsilon \\ \phi \\ \omega \end{bmatrix} = \Psi(z_1, z_2, z_3, z_4) = \Phi_{z_1}^{f_1} \circ \Phi_{z_2}^{f_2} \circ \Phi_{z_3}^{f_3} \circ \Phi_{z_4}^{f_4} \begin{bmatrix} \rho^0 \\ \upsilon^0 \\ \phi^0 \\ \omega^0 \end{bmatrix} = \begin{bmatrix} z_2 + 1 \\ z_1 \\ z_4 \\ \frac{z_3}{(z_2+1)^2} \end{bmatrix}$$

$$\begin{bmatrix} z_1 \\ z_2 \\ z_3 \\ z_4 \end{bmatrix} = \Psi^{-1}(x_1, x_2, x_3, x_4) = \begin{bmatrix} \upsilon \\ \rho - 1 \\ \omega\rho^2 \\ \phi \end{bmatrix}$$

Therefore,

$$\left(\sum\nolimits_*^P\right)^\perp = span\left\{dz_3, dz_4\right\} = span\left\{d\phi, d\left(\rho^2\omega\right)\right\} \tag{3.19}$$

The Third Step: Finding *o.c.a.* $\left(\left(\sum_*^P\right)^\perp\right)$

At this stage we will calculate the maximal observability codistribution that is locally spanned by exact differentials and contained in $P^\perp$ via the algorithm (2.6).

From (3.13), we obtain

$$span\left\{dh\right\} = span\left\{\begin{pmatrix} 1 & 0 & 0 & 0 \end{pmatrix}, \begin{pmatrix} 0 & 0 & 1 & 0 \end{pmatrix}, \begin{pmatrix} 0 & 0 & 0 & 1 \end{pmatrix}\right\} \tag{3.20}$$

$$\begin{aligned} \left(\sum\nolimits_*^P\right)^\perp &= span\left\{d\phi, d\left(\rho^2\omega\right)\right\} \\ &= span\left\{\begin{pmatrix} 0 & 0 & 1 & 0 \end{pmatrix}, \begin{pmatrix} 2\rho\omega & 0 & 0 & \rho^2 \end{pmatrix}\right\} \end{aligned} \tag{3.21}$$

Obviously, $span\left\{dh\right\} \supset \left(\sum_*^P\right)^\perp$, and

$$Q_0 = \left(\sum\nolimits_*^P\right)^\perp \cap span\left\{dh\right\} = \left(\sum\nolimits_*^P\right)^\perp$$

Since $\sum_{i=0}^{1} L_{gi}Q_0 + span\{dh\} \supset span\{dh\} \supset \left(\sum_*^P\right)^\perp$, then

$$\left(\sum_*^P\right)^\perp \cap \left(\sum_{i=0}^{1} L_{gi}Q_0 + span\{dh\}\right) = \left(\sum_*^P\right)^\perp$$

Therefore,

$$o.c.a\left(\left(\sum_*^P\right)^\perp\right) = \left(\sum_*^P\right)^\perp \tag{3.22}$$

For system (2.35), $l = \begin{bmatrix} 0 & 0 & 0 & 1 \end{bmatrix}^T$, hence we get

$$span\{l\} = span\left\{\begin{bmatrix} 0 & 0 & 0 & 1 \end{bmatrix}\right\} \tag{3.23}$$

Combining (3.21), (3.22) and (3.23), one can observe that the condition (2.7) is satisfied. Therefore, coordinate transformations in the states exist that lead to the new output characterizing an observable subsystem upon which it is possible to design a residual generator unaffected by the disturbance w but the fault m.

The Fourth Step: Finding the Coordinate Transformations

We have

$$\begin{aligned}\Omega = \left(\sum_*^P\right)^\perp &= span\left\{d\phi, d\left(\rho^2\omega\right)\right\} \\ &= span\left\{\begin{pmatrix} 0 & 0 & 1 & 0 \end{pmatrix}, \begin{pmatrix} 2\rho\omega & 0 & 0 & \rho^2 \end{pmatrix}\right\}\end{aligned}$$

Consequently, the dimension of Ω is $n_1 = 2$. With p as the dimension of h, we get

$p = 3$. Note that

$$\Omega \cap span\{dh\} = \Omega$$

and

$$p - n_2 = 2 \Rightarrow n_2 = 1$$

Therefore, there exists a surjection $\Psi_1 : R^p \rightarrow R^{p-n_2}$ such that

$$\Omega \cap span\{dh\} = span\{d(\Psi_1 \circ h)\}$$

Our goal is to find $span\{d(\Psi_1 \circ h)\} = \Omega = span\{d\phi, d(\rho^2\omega)\}$, therefore, we can set $\Psi_1 = (\nu_2, \nu_1^2\nu_3)$. Then, there exists a selection matrix H_2 (a matrix in which any row has all 0 entries but one, which is equal to 1). We let:

$$H_2 = \begin{bmatrix} 0 & 0 & 0 \\ 0 & 0 & 0 \\ 1 & 0 & 0 \end{bmatrix}, \text{ then } H_2 v = \begin{bmatrix} 0 & 0 & 0 \\ 0 & 0 & 0 \\ 1 & 0 & 0 \end{bmatrix} \begin{bmatrix} \nu_1 \\ \nu_2 \\ \nu_3 \end{bmatrix} = \nu_1$$

$$\Psi(y) = \begin{bmatrix} y_1 \\ \\ y_2 \end{bmatrix} = \begin{bmatrix} y_{11} \\ y_{12} \\ y_2 \end{bmatrix} = \begin{bmatrix} \nu_2 \\ \nu_1^2\nu_3 \\ \nu_1 \end{bmatrix} = \begin{bmatrix} \phi \\ \rho^2\omega \\ \rho \end{bmatrix} \text{ is a local diffeomorphism at } y^0$$

in R^p. Choose a neighborhood U^0 of x^0 and a function $\Phi_1 : U^0 \rightarrow R^{n_1}$ such that

$$\Omega = span\{d\Phi_1\}$$

Obviously, here, $\Phi_1 = (\phi, \rho^2\omega)$.

At any point of U^0, there exists a function $\Phi_3 : U^0 \to R^{n-n_1-n_2}$ such that

$$\Phi(x) = \begin{bmatrix} x_1 \\ x_2 \\ x_3 \end{bmatrix} = \begin{pmatrix} \Phi_1 \\ H_2 h \\ \Phi_3 \end{pmatrix}, \text{ where we now set } \Phi_3 = v, \text{ hence we have}$$

$$\Phi(x) = \begin{bmatrix} x_{11} \\ x_{12} \\ x_2 \\ x_3 \end{bmatrix} = \begin{bmatrix} \phi \\ \rho^2\omega \\ \rho \\ v \end{bmatrix}, \text{ thus we obtain}$$

$$\begin{cases} \dot{x}_{11} = \dot{\phi} = \omega = \frac{x_{12}}{x_2^2} \\ \dot{x}_{12} = 2\rho\omega\dot{\rho} + \rho^2\dot{\omega} = \theta_2\rho u_2 + \theta_2\rho m = \theta_2 x_2 u_2 + \theta_2 x_2 m \\ \dot{x}_2 = \dot{\rho} = v = x_3 \\ \dot{x}_3 = \dot{v} = \rho\omega^2 - \theta_1\frac{1}{\rho^2} + \theta_2 u_1 + w = \frac{x_2 x_{12}^2}{x_2^4} - \frac{\theta_1}{x_2^2} + \theta_2 u_1 + w \end{cases}$$

Therefore, we obtain the coordinate transformation in the state space that is:

$$x_1 = \begin{pmatrix} \phi \\ \rho^2\omega \end{pmatrix}, \quad x_2 = \rho, \text{ and } x_3 = v$$

and, the coordinate changes for the output space is given by:

$$y_1 = \begin{pmatrix} \nu_2 \\ \\ \nu_1^2 \nu_3 \end{pmatrix} \text{ and } y_2 = \nu_1.$$

Consequently, in the new coordinates, the system (2.35) becomes

$$\begin{cases} \begin{cases} \dot{x}_{11} = \frac{x_{12}}{x_2^2} \\ \dot{x}_{12} = \theta_2 x_2 u_2 + \theta_2 x_2 m + \theta_2 x_2 u_{2r} \\ \dot{x}_2 = x_3 \\ \dot{x}_3 = \frac{x_2 x_{12}^2}{x_2^4} - \frac{\theta_1}{x_2^2} + \theta_2 u_1 + w \end{cases} \\ \begin{cases} y_{11} = x_{11} \\ y_{12} = x_{12} \\ y_2 = x_2 \end{cases} \end{cases} \tag{3.24}$$

We now designate the x_1-subsystem as characterized by

$$\begin{cases} \begin{cases} \dot{x}_{11} = \frac{x_{12}}{y_2^2} \\ \dot{x}_{12} = \theta_2 y_2 u_2 + \theta_2 y_2 m + \theta_2 y_2 u_{2r} \end{cases} \\ \begin{cases} y_{11} = x_{11} \\ y_{12} = x_{12} \end{cases} \end{cases} \tag{3.25}$$

We could consider the above subsystem as a system with inputs u_2, m, u_{2r} and y_2. Because the state x_{11} will not affect x_{12}, we could focus on the subsystem (3.26) to detect the fault m, namely

$$\dot{y}_{12} = \theta_2 y_2 u_2 + \theta_2 y_2 m + \theta_2 y_2 u_{2r} \tag{3.26}$$

3.3 Application of the New Residual Generator

Given the assumption $m = -ku_2$ as in (2.36), the equation (3.26) becomes

$$\dot{y}_{12} = \theta_2 y_2(1-k)u_2 + \theta_2 y_2 u_{2r} \tag{3.27}$$

By identifying k according to the measurable signals y_{12} and y_2 and the known inputs u_2, u_{2r}, one can determine if there is a fault occurring in the system and if so what is the severity of the fault. In this section, we will use a least-squares algorithm to estimate k. The reader could refer to [7] for detailed information about parameter estimation. We will apply two different residual generators to the system, one with the redundant input actuator and the other one without the redundant input actuator.

3.3.1 Fault detection before triggering the recovery process

Once a fault is detected and isolated, we will trigger the recovery subsystem and use the redundant actuator u_{2r} to compensate for the fault m. Thus, before triggering the recovery subsystem, the redundant input u_{2r} is set to zero. Equation (3.27) becomes simply

$$\dot{y}_{12} = \theta_2 y_2(1-k)u_2 \tag{3.28}$$

Let us define the variable U as

$$U = \theta_2 y_2 u_2 \tag{3.29}$$

and $K = 1 - k$, then (3.28) may be rewritten as

$$\dot{y}_{12} = KU \tag{3.30}$$

We now propose a candidate system of equations for estimating k as follows

$$\bar{U} = \frac{1}{s+a}U \tag{3.31}$$

$$\bar{y}_{12} = \frac{1}{s+a}y_{12} \tag{3.32}$$

$$\hat{y}_{12} = \hat{K}\bar{U} + a\bar{y}_{12} \tag{3.33}$$

$$\varepsilon = \frac{y_{12} - \hat{y}_{12}}{n^2} \tag{3.34}$$

$$\dot{P} = \beta P - \frac{1}{n^2}P^2\bar{U}^2 \tag{3.35}$$

$$\dot{\hat{K}} = P\varepsilon\bar{U} \tag{3.36}$$

$$\hat{k} = 1 - \hat{K} \tag{3.37}$$

where a is a positive constant, $n > 0$ is the normalizing signal set according to $n^2 = 1 + \bar{U}^2$, $\beta \geq 0$ is the forgetting factor, $\hat{K}$ is the estimate of K, and $\hat{k}$ is the estimate of k accordingly.

In the next lemma, we will prove the convergence of $\hat{k}$.

Lemma 1 Under the coordinate transformation $x_1 = \begin{pmatrix} \phi & \rho^2\omega \end{pmatrix}^T$, $x_2 = \rho$, $x_3 = \upsilon$ and $y_1 = \begin{pmatrix} \nu_2 & \nu_1^2\nu_3 \end{pmatrix}^T$, $y_2 = \nu_1$ to the satellite orbital model (2.35) and the system

of equations (3.31)-(3.37), the estimate of the parameter k, that is $\hat{k}$ converges to k.

Towards this end consider the dynamical system

$$z = \frac{s}{s+a} y_{12} + \frac{a}{s+a} y_{12} \tag{3.38}$$

where $a > 0$. Let $\begin{cases} z_1 = \frac{s}{s+a} y_{12} \\ z_2 = \frac{a}{s+a} y_{12} \end{cases}$,

that is $\begin{cases} \dot{z}_1 = -a z_1 + \dot{y}_{12} \\ \dot{z}_2 = -a z_2 + a y_{12} \end{cases}$.

Here, we consider z_1 and z_2 as two states, and $\dot{y}_{12}$ and y_{12} are two inputs, respectively.

We now propose a Lyapunov function candidate

$$V = (z - y_{12})^2 = (z_1 + z_2 - y_{12})^2$$

where at $z = y_{12}$, $V = 0$, and $V > 0$, $\forall z \neq y_{12}$. The time derivative of V along the trajectories of the $\dot{z}_1$ and $\dot{z}_2$ are given by

$$\begin{aligned} \dot{V} &= 2(z_1 + z_2 - y_{12})(\dot{z}_1 + \dot{z}_2 - \dot{y}_{12}) \\ &= 2(z_1 + z_2 - y_{12})(-a z_1 - a z_2 + a y_{12}) \\ &= -2a(z_1 + z_2 - y_{12})^2 \\ &= -2a(z - y_{12})^2 < 0, \qquad \forall z \in R - \{y_{12}\} \end{aligned}$$

According to Barbashin-Krasovskii theorem [18], it then follows that $\lim_{t\to\infty} z = y_{12}$. Since

$$\frac{s}{s+a}y_{12} + \frac{a}{s+a}y_{12} = \frac{K}{s+a}U + \frac{a}{s+a}y_{12} = K\bar{U} + a\bar{y}_{12}$$

then $\left(K\bar{U} + a\bar{y}_{12}\right)$ tends to y_{12} as $t \to \infty$. Therefore, $\varepsilon = \frac{y_{12}-\hat{y}_{12}}{n^2}$ tends to $\frac{(K-\hat{K})\bar{U}}{n^2}$ as $t \to \infty$. Consequently, after the transients for z converging to y_{12}, we obtain

$$\varepsilon = \frac{(K-\hat{K})\bar{U}}{n^2}$$

We now consider a Lyapunov function:

$$W = \frac{\left(\hat{K}-K\right)^2}{2}$$

where at $\hat{K} = K$, $W = 0$ and $W > 0$, $\forall \hat{K} \neq K$. After the transients for z converging to y_{12}, the time derivative of W along the trajectories of $\dot{\hat{K}}$ becomes

$$\begin{aligned}\dot{W} &= \left(\hat{K}-K\right)\dot{\hat{K}} \\ &= \left(\hat{K}-K\right)P\varepsilon\bar{U} = -\frac{\left(\hat{K}-K\right)^2 P\bar{U}^2}{n^2}\end{aligned}$$

Considering equation (3.35), we can calculate the solution of P according to [7],

$$P(t) = \left[e^{-\beta t}P^{-1}(0) + \int_0^t e^{-\beta(t-\tau)}\frac{\bar{U}^2}{n^2}d\tau\right]^{-1}$$

where $P(t) > 0$ when $P(0) > 0$. It now follows that $-\frac{\left(\hat{K}-K\right)^2 P\bar{U}^2}{n^2} < 0, \forall \hat{K} \in R - \{K\}$,

and $\dot{W}$ will be less than zero after the transients for z converging to y_{12}. Therefore, $\hat{K}$ tends to K, according to Barbashin-Krasovskii theorem, and $\hat{k}$ tends to k as $t \rightarrow \infty$

From the above proof, one can observe that the controller will affect the estimate's rate of convergence, but will not affect the stability of the fault detection estimate.

3.3.2 Fault detection after triggering the recovery process

After triggering the recovery process, u_{2r} will be set to $\hat{k}u_2$, which will attempt to compensate the failure. Hence equation (3.27) becomes

$$\dot{y}_{12} = \theta_2 y_2(u_2 + \hat{k}u_2) - k\theta_2 y_2 u_2 \tag{3.39}$$

We now propose a candidate estimator for k, which is different from the one utilized before triggering the recovery process, and is governed according to the following equations (3.40)-(3.47):

$$U = \theta_2 y_2(u_2 + \hat{k}u_2) \tag{3.40}$$

$$\bar{U} = \frac{1}{s+a}U \tag{3.41}$$

$$\bar{y}_{12} = \frac{1}{s+a}y_{12} \tag{3.42}$$

$$\hat{y}_{12} = \hat{K}\bar{U} + a\bar{y}_{12} \tag{3.43}$$

$$\varepsilon = \frac{y_{12} - \hat{y}_{12}}{n^2} \tag{3.44}$$

$$\dot{P} = \beta P - \frac{1}{n^2}P^2\bar{U}^2 \tag{3.45}$$

$$\dot{\hat{K}} = P\varepsilon\bar{U} \tag{3.46}$$

$$\hat{k} = \frac{1-\hat{K}}{\hat{K}} \tag{3.47}$$

Lemma 2 Under the condition of Lemma 1 following the detection of the fault, the estimate of the fault after triggering the recovery process according to (3.40)-(3.47) will converge asymptotically, that $\lim_{t\to\infty} \hat{k} = k$.

According to the proof in Lemma 1 and equation (3.38), z tends to y_{12}, as $t \to \infty$, and $z = y_{12}$ after the transients for z converging to y_{12}. And by combining (3.39) and (3.40), we have

$$\dot{y}_{12} = \left(1 - \frac{k}{1+\hat{k}}\right) U$$

and, from equation (3.47) we have

$$\hat{K} = 1 - \frac{\hat{k}}{1+\hat{k}} \tag{3.48}$$

Thus,

$$\frac{s}{s+a} y_{12} + \frac{a}{s+a} y_{12} = \frac{\left(1 - \frac{k}{1+\hat{k}}\right)}{s+a} U + \frac{a}{s+a} y_{12} = \left(1 - \frac{k}{1+\hat{k}}\right) \bar{U} + a\bar{y}_{12}$$

and

$$\left(1 - \frac{k}{1+\hat{k}}\right) \bar{U} + a\bar{y}_{12} \to y_{12}$$

Therefore,

$$\varepsilon = \frac{y_{12} - \hat{y}_{12}}{n^2} = \frac{\left(1 - \frac{k}{1+\hat{k}} - \hat{K}\right) \bar{U}}{n^2}$$

hence

$$\dot{\hat{K}} = P\varepsilon\bar{U} = P\frac{\hat{k}-k}{1+\hat{k}}\frac{\bar{U}^2}{n^2} \tag{3.49}$$

From (3.48), we now have

$$\dot{\hat{K}} = -\frac{\dot{\hat{k}}}{\left(1+\hat{k}\right)^2} \tag{3.50}$$

Combining (3.49) and (3.50), we obtain

$$\dot{\hat{k}} = \frac{-P(\hat{k}-k)(1+\hat{k})\bar{U}^2}{n^2}$$

By proposing a Lyapunov function candidate

$$V = \frac{1}{2}\left(\hat{k}-k\right)^2$$

and taking its time derivative along the trajectories of $\dot{\hat{k}}$ we get

$$\dot{V} = \left(\hat{k}-k\right)\dot{\hat{k}} = \frac{-P\left(1+\hat{k}\right)\bar{U}^2\left(\hat{k}-k\right)^2}{n^2}$$

Given that when the system is in the recovery mode, $\hat{k}$ is larger than a threshold (this will be discussed later), which is larger than zero, then $(1+\hat{k})$ must be larger than zero. Also, $P(t) > 0$ when $P(0) > 0$. Thus, $\frac{-P\left(1+\hat{k}\right)\bar{U}^2\left(\hat{k}-k\right)^2}{n^2} < 0$, $\forall\hat{k} \in R - \{k\}$, and $\dot{V}$ will be less than zero after the transients for z converging to y_{12}. Therefore, according to Barbashin-Krasovskii theorem, $\hat{k} = k$ is a stable equilibrium point, and $\hat{k}$ tends to k as $t \to \infty$.

Remark

From the proofs of the two lemmas, we can observe that $\hat{k}$ tends to k in both cases with different algorithms. Therefore, we will consider $\hat{k}$ as our residual generator. More importantly, since we can estimate the value of k, we will calculate the severity of the fault, and then trigger the recovery process and initiate the redundant actuator thruster to compensate for the fault. In addition, even after invoking the redundant thruster, we could still estimate the k successfully. Furthermore, one can observe that once the controller of the system ensures the states remain bounded, it will not change the convergence properties of the residual generator although it will affect the performance of the residual generator.

3.4 Impacts of Uncertainties and Disturbances on the Residual Generator

The crux of the residual generator we introduced above is to estimate k as a parameter. The assumption of this design is that other parameters are precisely known and the measurement of outputs is perfect with no uncertainty. Uncertainties existing in parameters and outputs and disturbances might impact the estimate of k. In this section, we will investigate the impact of uncertainties and disturbances on the residual generator. The significance of this study is that it will help us to select the detection threshold for avoiding "false alarm".

Uncertainties will affect the residual generator through two ways: (i) they may

affect the construction of the coordinate transformations and (ii) they appear in the observable subsystem that was used to estimate k. Since we focus on system (3.27) to estimate k, we are concerned with the construction of the state x_{12}. According to the state coordinate transformations we have:

$$\dot{x}_{12} = 2\rho\omega\dot{\rho} + \rho^2\dot{\omega} \tag{3.51}$$

Any uncertainties in (3.51) and in the state representation of $\dot{\rho}$ and $\dot{\omega}$ in (2.35) might affect the residual generator. Furthermore, in the discussion below, we only consider the case in which $u_{2r} = 0$.

3.4.1 Uncertainties in the system parameters

In system (2.35), there are two parameters θ_1 and θ_2. The parameter θ_1 will not affect the residual generator because it does not appear in (3.51) and the state representation of $\dot{\rho}$ and $\dot{\omega}$. However, θ_2 will affect the residual generator through $\dot{\omega}$. Assume that the actual $\theta_{2r} = \delta_1\theta_2$, then we have

$$\dot{y}_{12} = \dot{x}_{12} = \delta_1\theta_2 x_2 u_2 + \delta_1\theta_2 x_2 m = \delta_1\theta_2 x_2 K u_2 = \delta_1 KU \tag{3.52}$$

According to Lemma 1, after the transients for z converging to y_{12} we have

$$\frac{s}{s+a}y_{12} + \frac{a}{s+a}y_{12} = y_{12}$$

and as well

$$\delta_1 K\bar{U} + a\bar{y}_{12} = y_{12}$$

and

$$\varepsilon = \frac{y_{12} - \hat{y}_{12}}{n^2} = \frac{(\delta_1 K - \hat{K})\bar{U}}{n^2}$$

Assuming that $\dot{\tilde{K}} = \dot{\hat{K}} - \dot{K}$, then

$$\begin{aligned}\dot{\tilde{K}} &= \dot{\hat{K}} - \dot{K} = P\varepsilon\bar{U} \\ &= P\frac{(\delta_1 K - \hat{K})\bar{U}^2}{n^2} = \frac{-P\tilde{K}\bar{U}^2 - P(1-\delta_1)K\bar{U}^2}{n^2}\end{aligned}$$

Thus, $\tilde{K} \to (\delta_1 - 1)K$, and accordingly,

$$\hat{k} \to 1 - \delta_1(1-k) \quad as \quad t \to \infty \tag{3.53}$$

From the above analysis, one can observe that the uncertainty of the parameter u_2 affects the estimation of k. The equation (3.53) indicates that even when there is no fault ($k = 0$), the estimate of k will not be zero due to the uncertainty of the parameter u_2.

3.4.2 Uncertainties in the system outputs

There are three outputs in the satellite orbital model, namely ν_1, ν_2 and ν_3 that are used to measure the states ρ, ϕ and ω, respectively. Due to the errors of sensor measurements of these states, the outputs obtained might be the corrupted versions

of the actual states. Since ϕ does not appear in (3.51) and the state representation of $\dot{\rho}$ and $\dot{\omega}$, the uncertainty of ϕ will not affect the residual generator.

Uncertainty of ρ

Assume that the actual output ρ is given by $\rho_r = \delta_2 \rho$. Since $\dot{\rho}_r = \upsilon$, then $\delta_2 \dot{\rho} = \upsilon$, thus

$$\begin{aligned}\dot{x}_{12} &= 2\rho\omega\dot{\rho} + \rho^2\dot{\omega} \\ &= \frac{2\rho\omega\upsilon}{\delta_2} + \rho^2(-\frac{2\upsilon\omega}{\delta_2\rho} + \theta_2\frac{u_2+m}{\delta_2\rho}) \\ &= \frac{1}{\delta_2}\rho\theta_2 K u_2\end{aligned}$$

According to Lemma 1, after the transients for z converging to y_{12} we have

$$\frac{s}{s+a}y_{12} + \frac{a}{s+a}y_{12} = y_{12}$$

and also we get

$$\begin{aligned}\varepsilon = \frac{y_{12} - \hat{y}_{12}}{n^2} &= \frac{(K\bar{U})/\delta_2 + a\bar{y}_{12} - (\hat{K}\bar{U} + a\bar{y}_{12})}{n^2} \\ &= \frac{(K/\delta_2 - \hat{K})\bar{U}}{n^2}\end{aligned}$$

Assuming that $\tilde{\dot{K}} = \dot{\hat{K}} - \dot{K}$, then

$$\begin{aligned}\tilde{\dot{K}} = \dot{\hat{K}} - \dot{K} &= P\varepsilon\bar{U} \\ &= \frac{P(K/\delta_2 - \hat{K})\bar{U}^2}{n^2} = \frac{-P\tilde{K}\bar{U}^2 - P(1-1/\delta_2)K\bar{U}^2}{n^2}\end{aligned}$$

Thus, $\tilde{K} \rightarrow (\frac{1}{\delta_2} - 1)K$, and accordingly,

$$\hat{k} \rightarrow 1 - \frac{1}{\delta_2}(1-k) \quad as \quad t \rightarrow \infty \tag{3.54}$$

Uncertainty of ω

Assume that the actual ω is given by $\omega_r = \delta_3 \omega$ Since

$$\dot{\omega}_r = -\frac{2\omega_r v}{\rho} + \theta_2 \frac{u_2 + m}{\rho}$$

then

$$\dot{\omega} = -\frac{2\omega v}{\rho} + \theta_2 \frac{u_2 + m}{\delta_3 \rho}$$

and

$$\begin{aligned} \dot{x}_{12} &= 2\rho\omega\dot{\rho} + \rho^2\dot{\omega} \\ &= 2\rho\omega v + \rho^2 \left(-\frac{2\omega v}{\rho} + \theta_2 \frac{u_2 + m}{\delta_3 \rho} \right) \\ &= \frac{1}{\delta_3}\theta_2 \rho K u_2 \end{aligned}$$

Based on the analysis of the uncertainty of ρ, we can easily observe that

$$\hat{k} \rightarrow 1 - \frac{1}{\delta_3}(1-k) \quad as \quad t \rightarrow \infty \tag{3.55}$$

Remark

From the above analysis of uncertainties in the system outputs, one can observe

that the uncertainties of sensor measurement of the states ρ and ω will affect the residual generator since they appear in the observable subsystem (3.51). Furthermore, even when there is no fault, the estimate of k will not be zero according to (3.54) and (3.55), that should be considered when the threshold is designed.

3.4.3 Impact of the Disturbance

In the original model of the system (2.35), there is only a disturbance signal w. The objective of the coordinate transformations is to find an observable subsystem upon which we can design a residual generator unaffected by this disturbance w. Observe from system (3.24) that after coordinates transformations, w may affect x_1-subsystem only through x_2. However, since we measure the state x_2, we can view x_2 as an input for the x_1-subsystem. Thus, the residual generator based on x_1-subsystem with the input x_2 will not be affected by the disturbance w.

3.5 Decision Logic and Recovery Subsystem

When considering the estimate of k as the residual generator, it would take some transient time for $\hat{k}$ to converge to k. That implies that during the transient period, $\hat{k}$ could be very different from k and one cannot determine if there is a fault in the system based on the residual generator. Thus, in our simulations, we estimate the time $\hat{k}$ needs to converge to k. Only after this period and $\hat{k}$ surpassing the threshold, one could claim that a fault has occurred.

Another important problem is that of selecting a suitable threshold for the residual

generator in order to avoid producing false alarms that may be caused by uncertainties and disturbances. As we have discussed in Chapter 2, the range of k is $0 \leq k \leq 1$ and k will deviate from zero which is caused by the occurrence of a fault. If there are no uncertainties and the measurement of outputs are noise free, $\hat{k}$ will then converge to k without an error and one can claim the occurrence of a fault as soon as $\hat{k} \neq 0$. However, as we have discussed in the above sections, the uncertainties may affect the residual generator. In order to reduce the call for false alarms, one has to properly set a threshold.

We have investigated that the presence of only three uncertainties that are affecting the residual generator according to results in section 3.4. It is assumed that we know the size of δ_1, δ_2 and δ_3. Consequently, we calculate the biggest positive errors that caused by these uncertainties when no fault exists according to (3.53), (3.54) and (3.55). Therefore, we may consider the sum of these positive errors as a measure for our threshold.

Once the residual $\hat{k}$ exceeds this threshold, the recovery process will be initiated. That is, the redundant input u_{2r} will be set to $\hat{k}u_2$ instead of zero for compensating the fault. Consequently, the residual generator is the one introduced in section 3.3.2.

3.6 Simulation Results

At certain points in time one has to change the satellite's orbit. For example, after the launch of a geosynchronous orbital satellite by a rocket, the satellite has to go through several different orbits until it arrives at the final geosynchronous

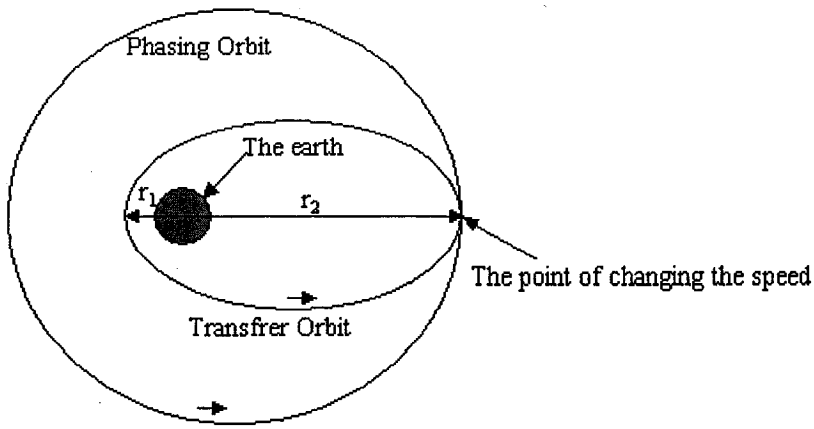

Figure 3.1: Transfer orbit and phasing orbit

orbit. The Geostationary Operational Environment Satellite (GOES) [34] is such a geosynchronous orbital satellite. The GOES undergoes six orbits changes after the separation from Atlas 1, namely transfer orbit, phasing orbit, trim–1 orbit, trim–2 orbit, post–AAM trim orbit, post-trim orbit and geosynchronous orbit. Here, the transfer orbit is the orbit the satellite undergoes after separation. Phasing orbit is the one the satellite enters after the first apogee maneuver firing.

One would change the velocity vector of the satellite in magnitude or direction by thrusters in order to change the orbit. Since the propulsion system operates for changing orbit for only a very short time period compared to the orbital period, we consider the orbit maneuver as an impulsive change in the velocity while the position remains fixed. By referring to the orbits of the GOES, we will simulate the process of changing a geosynchronous satellite's orbit from transfer orbit to phasing orbit. Figure 3.1 illustrates this case. The simulation of the motion of the satellite is as follows: starting at the apogee on the transfer orbit, the satellite will go around the earth for one cycle, and when it arrives the apogee again, it will speed up to enter

the phasing orbit, the simulation ends when it arrives the apogee for the third time. The ellipses of phasing orbit and transfer orbit are tangent at the apogee of these two orbits. In the simulation provided in this section, we assume:

1. The satellite's mass is 500kg;
2. In the transfer orbit phase, the perigee is 6544.5 km and apogee is 48789 km;
3. In the phasing orbit phase, the perigee is 23408 km and apogee is 48789 km;
4. The range of u_1 is $-200N \leq u_1 \leq 200N$;
5. The range of u_2 is $-400N \leq u_2 \leq 400N$;
6. The size of δ_1, δ_2 and δ_3 are $1 - 10^{-3} \leq \delta_i \leq 1 + 10^{-3}$, $i = 1, 2, 3$, respectively.

In the simulation, the sliding mode controller developed in section 3.1 is applied to ensure the states to be bounded. We will use two force-free systems (2.33) to represent the transfer orbit and phasing orbit respectively, and consider them as the references for the control system design. We have to know the initial conditions, which are at apogee, of the force-free systems. Since the distance of the apogee is 48789 km, the radial velocity at the apogee is zero, and the angle ϕ of the satellite in polar coordinates at apogee is zero too, therefore one has to calculate the angular velocities at apogee on the transfer orbit and phasing orbit.

In figure 3.2, r_1 represents the distance of perigee, r_2 represents the distance of apogee, v is the velocity of the satellite at apogee, and ω is the angular velocity accordingly. We have shown that the orbit of the satellite around the earth is an ellipse

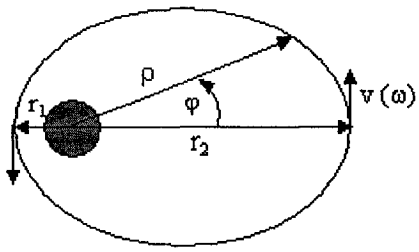

Figure 3.2: Apogee and perigee

as governed by equation (2.26). In the ellipse, e in (2.26) is known as eccentricity. Also, according to the property of ellipse, eccentricity can be written as

$$e = \frac{r_2 - r_1}{r_2 + r_1} \tag{3.56}$$

And we assume

$$a = \frac{1}{2}(r_2 + r_1) \tag{3.57}$$

At apogee,

$$h = r_2 \cdot v \tag{3.58}$$

where $h = \left|\vec{h}\right|$, and $\vec{h}$ is the angular momentum per unit mass.

According to (2.25), we obtain

$$(r_2 \cdot v)^2 - \theta_1 r_2 = \theta_1 r_2 \frac{r_2 - r_1}{r_2 + r_1} \tag{3.59}$$

Therefore, from (3.59), we have

$$v = \sqrt{(2\theta_1/r_2) - (\theta_1/a)} \tag{3.60}$$

$$\omega = \frac{\sqrt{(2\theta_1/r_2) - (\theta_1/a)}}{r_2} \tag{3.61}$$

Consequently we can calculate the angular velocities at apogee on the transfer orbit and phasing orbit from equations (3.57) and (3.61).

Figures 3.3, 3.4 and 3.5 illustrate the effects of the FDIR system we introduced above. According to the assumption of the sizes of δ_1, δ_2 and δ_3, and (3.53), (3.54) and (3.55), the threshold in this case is set to 3×10^{-3}. In the simulation results shown, we let the input u_2 be completely faulty at time 30000 second.

From figure 3.4(f), figure 3.5(a) and figure 3.5(b), one can observe the effects of the estimate of k. Due to some of the uncertainties, $\hat{k}$ is not zero before the occurrence of the fault exactly. In figure 3.5(a), after the fault occurs, $\hat{k}$ exceeds the threshold, 3×10^{-3}, very quickly, and in figure 3.5(b), it takes around only four seconds for $\hat{k}$ to identify the complete fault in the actuator/thruster.

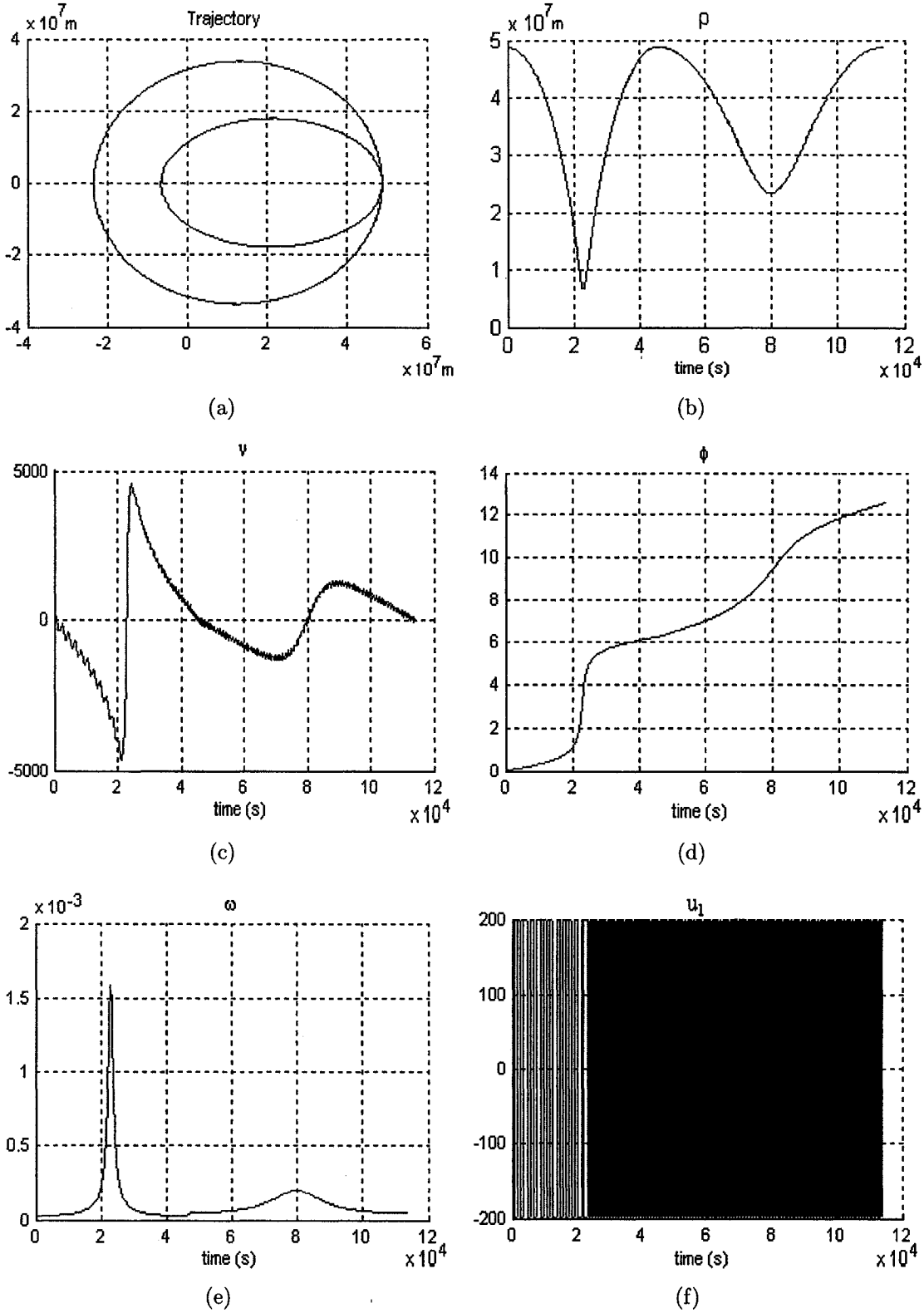

Figure 3.3: The behavior of the FDIR on the satellite orbital model

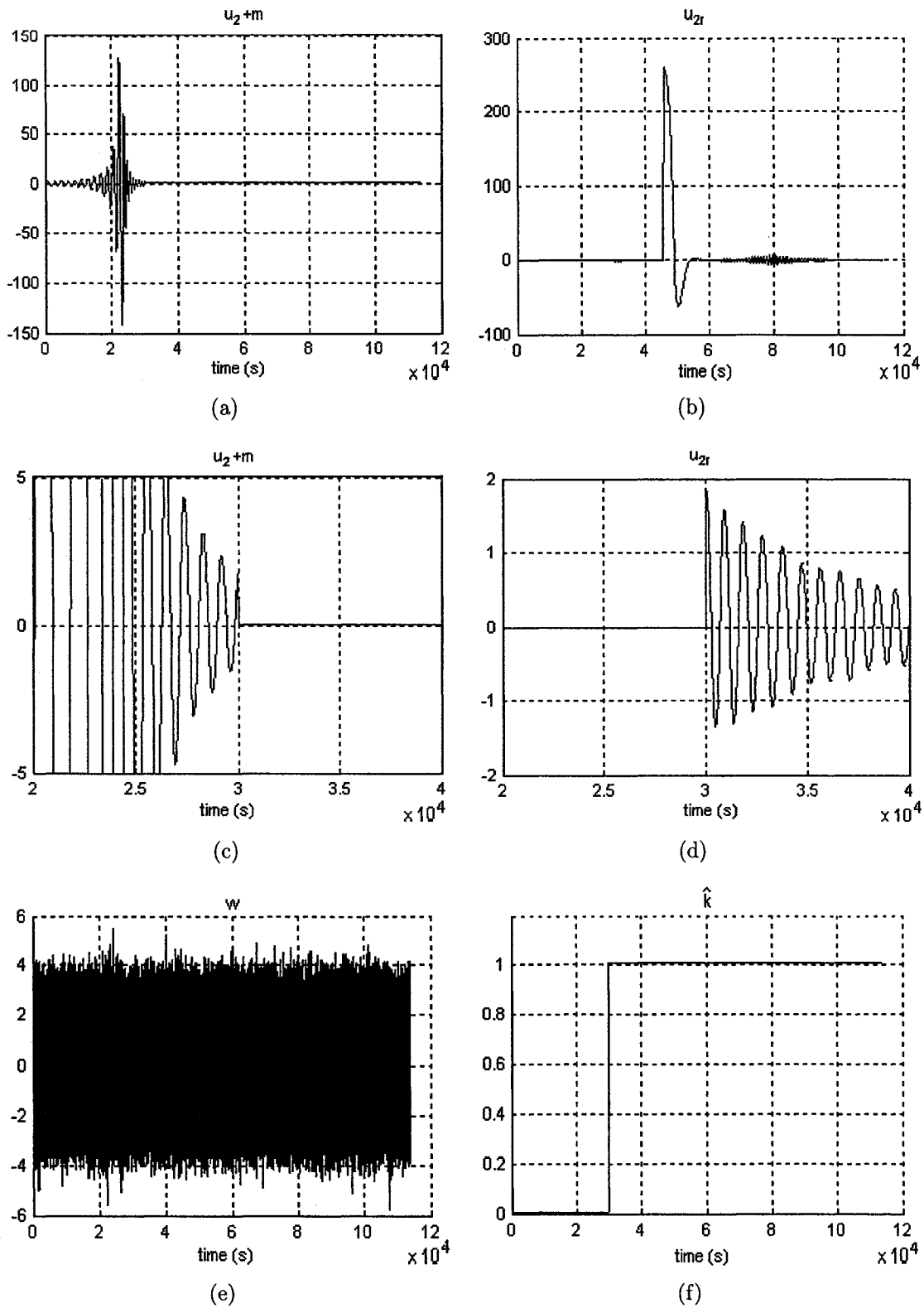

Figure 3.4: (Continued)The behavior of the FDIR on the satellite orbital model

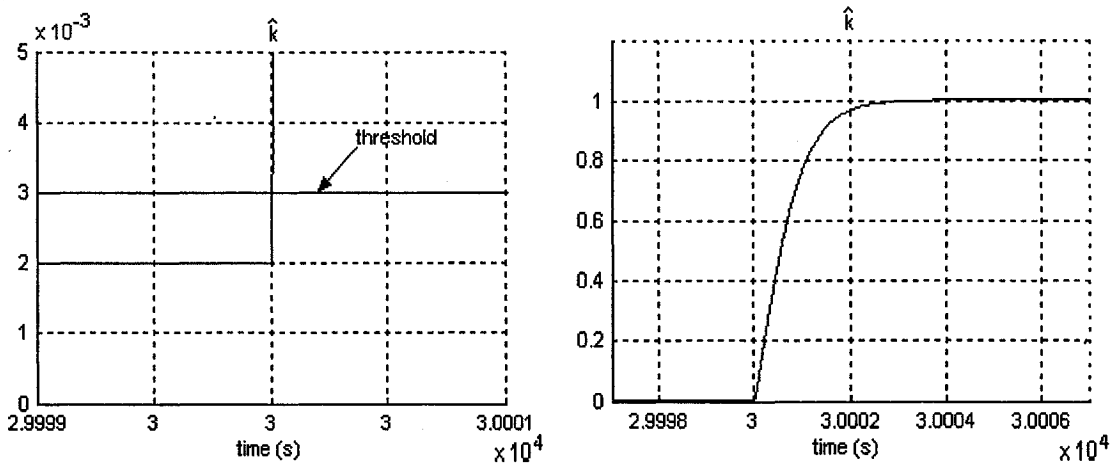

(a) (b)

Figure 3.5: (Continued)The behavior of the FDIR on the satellite orbital model

Chapter 4

FDIR Scheme for the Satellite Attitude Model

In this chapter, the proposed new residual generator is applied to the satellite attitude model and as in Chapter 3 the robustness of this residual generator is investigated. The algorithm is very similar to the one we developed for the orbital model. The main difference is that the residual generator consists of three estimators for three parameters since our goal is to detect and isolate three concurrent faults.

4.1 The Variable Structure Control

As discussed earlier, the necessary condition for designing a residual generator for the satellite system is that the states must be bounded. That implies that we have to first design a controller for the satellite attitude model. In our simulations, we will use a variable structure control for the system. Boškovi [8] proposes a variable structure

control for the satellite attitude model in some detail. The variable structure control proposed in [8] has several advantages, namely (i) it can tolerate bounded external disturbances and uncertainties in the parameters; (ii) it takes control input saturation into account explicitly; and (iii) the computation of this algorithm is very simple. In this section, we will first review the variable structure control proposed in [8].

For the satellite attitude model (2.92), (2.93) and (2.94), A represents the inertial reference frame and B represents the body-fixed reference frame. Thus, the direction cosine matrix $C^{B/A}$ relating B to A is given by

$$C^{B/A} = \left(\varepsilon_0^2 - \varepsilon^T\varepsilon\right) I_{3\times 3} + 2\varepsilon\varepsilon^T - 2\varepsilon_0\varepsilon^\times \tag{4.1}$$

Let the desired rotational motion of the satellite be described by the attitude motion of a frame D whose orientation with respect to A is specified by the Euler parameter (ξ, ξ_0) satisfying $\xi^T\xi + \xi_0^2 = 1$. Let $C^{D/A}$ be the direction cosine matrix

$$C^{D/A} = \left(\xi_0^2 - \xi^T\xi\right) I_{3\times 3} + 2\xi\xi^T - 2\xi_0\xi^\times \tag{4.2}$$

Furthermore, let v represents the angular velocity of D with respect to A, where we have

$$v = 2\left(\xi_0\dot{\xi} - \dot{\xi}_0\xi\right) - 2\xi^\times\dot{\xi} \tag{4.3}$$

Also, let (η, η_0) be the Euler parameter representing the orientation of frame B

with respect to frame D. Then, we obtain

$$\eta = \xi_0 \varepsilon - \varepsilon_0 \xi + \varepsilon^{\times} \xi \tag{4.4}$$

$$\eta_0 = \xi_0 \varepsilon_0 + \xi^T \varepsilon \tag{4.5}$$

The direction cosine matrix relating B to D is given by

$$C^{B/D} = C^{B/A} \left(C^{D/A} \right)^T \tag{4.6}$$

Therefore, the angular velocity $\omega \in R^3$ of B with respect to D is

$$\omega = \Omega - C^{B/D} v \tag{4.7}$$

Following the above one we can obtain the seven-dimensional dynamic model of the system in terms of the states ω, η and η_0 as follows

$$\begin{aligned} J\dot{\omega} = & - \left(\omega + C^{B/D} v \right)^{\times} J \left(\omega + C^{B/D} v \right) \\ & + J \left(\omega^{\times} C^{B/D} v - C^{B/D} \dot{v} \right) + u + m + u_r \end{aligned} \tag{4.8}$$

$$\dot{\eta} = \frac{1}{2} \left(\eta^{\times} \omega + \eta_0 \omega \right) \tag{4.9}$$

$$\dot{\eta}_0 = - \frac{1}{2} \eta^T \omega \tag{4.10}$$

Our control objective is to design a control input signal u so that the following

specifications are satisfied:

$$\lim_{t\to\infty} \eta(t) = \lim_{t\to\infty} \omega(t) = 0$$

Towards this end we introduce the sliding surface s characterized as

$$s = \omega + p\eta$$

The control law is selected as

$$u = -\sum(s)\, u_m \tag{4.11}$$

where $\sum(s) = diag\begin{bmatrix} sgn(s_1) & sgn(s_2) & sgn(s_3) \end{bmatrix}$

To reduce the chattering effects of the control law, the control is modified as following:

$$u = -\sum\nolimits_m (s) u_m \tag{4.12}$$

where $\sum_m(s) = diag\begin{bmatrix} \frac{s_1}{|s_1|+\delta} & \frac{s_2}{|s_2|+\delta} & \frac{s_3}{|s_3|+\delta} \end{bmatrix}$ and δ is a small positive constant.

4.2 Development of the New Residual Generator

As assumed in (2.95), the fault vector is represented by $m = -k \odot u$ where $\odot$ denotes the Hadamard product. Our goal is to generate a bank of estimators to identify the vector k and treat the estimators as the residual generators. Following the same structure as developed in Chapter 3, we will design two procedure residual

generators one for the case before one initiate the recovery procedure and the other one after one triggers the recovery procedure.

Furthermore, in this section, it is assumed that there are no external disturbances in the system and w in (2.92) is a zero vector. The impact and effects of the disturbances on the residual generator is discussed in section 4.3.

4.2.1 The fault detection and isolation before triggering the recovery procedure

Before triggering the recovery procedure, the redundant control input u_r is set to be zero, and by ignoring the disturbances for now system (2.92) becomes:

$$J\dot{\Omega} = -\Omega^{\times} J\Omega + u - k \odot u \tag{4.13}$$

Let us set $K = \begin{bmatrix} K_1 & K_2 & K_3 \end{bmatrix}^T = \begin{bmatrix} 1 & 1 & 1 \end{bmatrix}^T - k$, hence

$$J\dot{\Omega} = -\Omega^{\times} J\Omega + K \odot u \tag{4.14}$$

For the above system, it is assumed that $\hat{K} = \begin{bmatrix} \hat{K}_1 & \hat{K}_2 & \hat{K}_3 \end{bmatrix}^T$ is the estimate of K and $\hat{k} = \begin{bmatrix} \hat{k}_1 & \hat{k}_2 & \hat{k}_3 \end{bmatrix}^T$ is the estimate of k.

The proposed fault estimator candidate subsystem is now represented by (4.15)–(4.21) which used for estimating k as follows:

$$\bar{u} = \frac{1}{s+a} u \tag{4.15}$$

$$\bar{\Omega} = -\frac{1}{s+a}(\Omega^{\times} J\Omega) + \frac{a}{s+a} J\Omega \tag{4.16}$$

$$J\hat{\Omega} = \bar{\Omega} + \hat{K} \odot \bar{u} \tag{4.17}$$

$$\varepsilon = \begin{bmatrix} \varepsilon_1 & \varepsilon_2 & \varepsilon_3 \end{bmatrix}^T = (J\Omega - J\hat{\Omega}) \odot \begin{bmatrix} \frac{1}{n_1^2} & \frac{1}{n_2^2} & \frac{1}{n_3^2} \end{bmatrix}^T \tag{4.18}$$

$$\dot{P}_i = \beta P_i - \frac{1}{n_i^2} P_i^2 \bar{u}_i^2, \qquad i = 1,2,3 \tag{4.19}$$

$$\dot{\hat{K}}_i = P_i \varepsilon_i \bar{u}_i, \qquad i = 1,2,3 \tag{4.20}$$

$$\hat{k} = \begin{bmatrix} 1 & 1 & 1 \end{bmatrix}^T - \hat{K} \tag{4.21}$$

where a is a positive constant, $n = \begin{bmatrix} n_1 & n_2 & n_3 \end{bmatrix}^T$ is the normalizing signal, $\beta \geq 0$ is the forgetting factor, and $\bar{u} = \begin{bmatrix} \bar{u}_1 & \bar{u}_2 & \bar{u}_3 \end{bmatrix}^T$. In addition, we set $n_i^2 = 1 + \bar{u}_i^2$. The behavior of the above system is given by the following lemma.

Lemma 3 Under the conditions of the satellite's attitude model (2.92)–(2.94), the residual generator given before invoking the recovery procedure given by (4.15)–(4.21) guarantees the convergence of the parameter estimator, that is $\lim_{t\to\infty} \hat{k}(t) = k$.

According to the results presented for Lemma 1, we can easily observe that

$$\frac{s}{s+a} J\Omega + \frac{a}{s+a} J\Omega \to J\Omega \quad as \quad t \to \infty$$

Therefore, after the transients for the convergence of the above equation, we obtain

$$\begin{aligned}
&\frac{1}{s+a}(-\Omega^{\times} J\Omega + K \odot u) + \frac{a}{s+a} J\Omega \\
&= \frac{1}{s+a}(-\Omega^{\times} J\Omega) + \frac{a}{s+a} J\Omega + \frac{1}{s+a} K \odot u \\
&= \bar{\Omega} + K \odot \bar{u} = J\Omega
\end{aligned}$$

Consequently,

$$\begin{aligned}
\varepsilon &= \begin{bmatrix} \varepsilon_1 & \varepsilon_2 & \varepsilon_3 \end{bmatrix}^T \\
&= (J\Omega - J\hat{\Omega}) \odot \begin{bmatrix} \frac{1}{n_1^2} & \frac{1}{n_2^2} & \frac{1}{n_3^2} \end{bmatrix}^T \\
&= \left[(K - \hat{K}) \odot \bar{u} \right] \odot \begin{bmatrix} \frac{1}{n_1^2} & \frac{1}{n_2^2} & \frac{1}{n_3^2} \end{bmatrix}^T
\end{aligned}$$

That is,

$$\varepsilon_i = \frac{(K_i - \hat{K}_i)\bar{u}_i}{n_i^2}$$

We now propose the following Lyapunov functions candidates

$$V_i = \frac{\left(\hat{K}_i - K_i\right)^2}{2}$$

where at $\hat{K}_i = K_i$, it satisfies $V_i = 0$ and $V_i > 0, \forall \hat{K}_i \neq K_i$. Taking the time derivative

of V_i along the trajectories of the system (4.20) yields

$$\begin{aligned}\dot{V}_i &= \left(\hat{K}_i - K_i\right)\dot{\hat{K}}_i \\ &= \left(\hat{K}_i - K_i\right) P_i \varepsilon_i \bar{u}_i = -\frac{\left(\hat{K}_i - K_i\right)^2 P_i \bar{u}_i^2}{n_i^2}\end{aligned}$$

According to the results for Lemma 1, we know that $P_i(t) > 0$ when $P_i(0) > 0$. Thus, $-\frac{\left(\hat{K}_i - K_i\right)^2 P_i \bar{u}_i^2}{n_i^2} < 0$, $\forall \hat{K}_i \in R - \{K_i\}$, and $\dot{V}_i$ will be less than zero in a finite time. Therefore, $\hat{K}_i$ tends to K_i, according to Barbashin-Krasovskii theorem, and $\hat{k}_i$ tends to k_i as $t \rightarrow \infty$.

4.2.2 The fault detection and isolation after triggering the recovery procedure

When there exists one or more faults in the system, we could invoke the recovery procedure by assigning u_{ri} $(i = 1, 2, 3)$ to $\hat{k}_i u_i$ for compensating the faults. As in the previous subsection again we are neglecting the disturbances for now. System (2.92) becomes:

$$J\dot{\Omega} = -\Omega^{\times} J\Omega + (u + \hat{k} \odot u) - k \odot u \tag{4.22}$$

Our proposed candidate fault residual generator subsystem is governed by (4.23)–(4.29), for estimating the parameter k as follows:

$$\bar{u}_i = \frac{1}{s+a}\left(u_i + \hat{k}_i u_i\right) \tag{4.23}$$

$$\bar{\Omega} = -\frac{1}{s+a}(\Omega^{\times} J\Omega) + \frac{a}{s+a} J\Omega \tag{4.24}$$

$$J\hat{\Omega} = \bar{\Omega} + \hat{K} \odot \bar{u} \tag{4.25}$$

$$\varepsilon = \begin{bmatrix} \varepsilon_1 & \varepsilon_2 & \varepsilon_3 \end{bmatrix}^T = (J\Omega - J\hat{\Omega}) \odot \begin{bmatrix} \frac{1}{n_1^2} & \frac{1}{n_2^2} & \frac{1}{n_3^2} \end{bmatrix}^T \tag{4.26}$$

$$\dot{P}_i = \beta P_i - \frac{1}{n_i^2} P_i^2 \bar{u}_i^2, \qquad i = 1, 2, 3 \tag{4.27}$$

$$\dot{\hat{K}}_i = P_i \varepsilon_i \bar{u}_i, \qquad i = 1, 2, 3 \tag{4.28}$$

$$\hat{k}_i = \frac{1 - \hat{K}_i}{\hat{K}_i}, \qquad i = 1, 2, 3 \tag{4.29}$$

Lemma 4 Under the conditions of the satellite's attitude model (2.92)–(2.94), the residual generator given after invoking the recovery procedure given by (4.23)–(4.29) guarantees the convergence of the parameter estimator, that is $\lim_{t \to \infty} \hat{k}(t) = k$.

Towards this end from (4.29), we have

$$\hat{K}_i = 1 - \frac{\hat{k}_i}{1 + \hat{k}_i} \tag{4.30}$$

We also known that

$$\frac{s}{s+a} J\Omega + \frac{a}{s+a} J\Omega \to J\Omega \quad as \quad t \to \infty$$

Therefore, after the transients for the convergence of the above equation, we obtain

$$\frac{-\Omega^{\times} J\Omega + ([\ 1 \quad 1 \quad 1\ ]^T + \hat{k} - k) \odot u}{s+a} + \frac{a}{s+a} J\Omega = J\Omega \tag{4.31}$$

and thus

$$\bar{\Omega} + \left(\begin{bmatrix} 1 & 1 & 1 \end{bmatrix}^T - k \odot \begin{bmatrix} 1+\hat{k}_1 & 1+\hat{k}_2 & 1+\hat{k}_3 \end{bmatrix}^T \right) \odot \bar{u} = J\Omega$$

and $J\hat{\Omega} = \bar{\Omega} + \hat{K} \odot \bar{u} = \bar{\Omega} + \begin{bmatrix} 1 & 1 & 1 \end{bmatrix}^T - k \odot \begin{bmatrix} 1+\hat{k}_1 & 1+\hat{k}_2 & 1+\hat{k}_3 \end{bmatrix}^T$, hence

$$\varepsilon_i = \frac{\hat{k}_i - k_i}{1+\hat{k}_i} \frac{\bar{u}_i^2}{n_i^2}$$

so that

$$\dot{\hat{K}}_i = P_i \varepsilon_i \bar{u}_i = P_i \frac{\hat{k}_i - k_i}{1+\hat{k}_i} \frac{\bar{u}_i^2}{n_i^2} \tag{4.32}$$

From (4.30), we have

$$\dot{\hat{K}}_i = -\frac{\dot{\hat{k}}_i}{\left(1+\hat{k}_i\right)^2} \tag{4.33}$$

Combining equations (4.31) and (4.32), we get

$$\dot{\hat{k}}_i = \frac{-P_i(\hat{k}_i - k_i)(1+\hat{k}_i)\bar{u}_i^2}{n_i^2}$$

By utilizing the Lyapunov function candidates

$$V_i = \frac{1}{2}\left(\hat{k}_i - k_i\right)^2$$

then, it can be shown that

$$\dot{V}_i = \left(\hat{k}_i - k_i\right)\dot{\hat{k}}_i = \frac{-P_i\left(1+\hat{k}_i\right)\bar{u}_i^2\left(\hat{k}_i - k_i\right)^2}{n_i^2}$$

Since when the system is in the recovery mode, $\hat{k}_i$ is larger than a threshold (this will be discussed later), which is larger than zero, then $(1+\hat{k}_i)$ must be larger than zero. Also, $P_i(t) > 0$ when $P_i(0) > 0$. Thus, $\frac{-P_i\left(1+\hat{k}_i\right)\bar{u}_i^2\left(\hat{k}_i-k_i\right)^2}{n_i^2} < 0$, $\forall \hat{k}_i \in R - \{k_i\}$, and $\dot{V}_i$ will be less than zero in a finite time. Therefore, according to Barbashin-Krasovskii theorem, $\hat{k}_i = k_i$ is a stable equilibrium point, and $\hat{k}_i$ tends to k_i as $t \rightarrow \infty$.

4.3 Impacts of Uncertainties and Disturbances on the Residual Generator

Note that our residual generator is a bank of estimators for identifying the parameters. Our design is based on the assumptions that the other satellite model parameters are exactly known a priori, that sensors are noise free and there are no disturbances to the system. Consequently, when these assumptions do not hold, the residual generator will be affected and the estimates might not be accurate and unbiased. In this section, we will investigate the impact and effect of uncertainties and disturbances on the residual generator.

4.3.1 Parametric uncertainties

In [8] the author has shown that the variable structure controller proposed was capable of handling the parametric uncertainties. In this subsection we assume that the actual inertia matrix of the satellite is now presented as $J_r = \delta_1 J$. according to the results obtained in Lemma 3, after certain transients we have

$$\frac{1}{s+a}(-\Omega^{\times} J_r \Omega + K \odot u) + \frac{a}{s+a} J_r \Omega = J_r \Omega$$

therefore,

$$\frac{1}{\delta_1}\left(\frac{1}{s+a}(-\Omega^{\times} J_r \Omega + K \odot u) + \frac{a}{s+a} J_r \Omega\right) = J\Omega$$

and

$$\begin{aligned}
&J\Omega - J\hat{\Omega} \\
&= \frac{1}{\delta_1}\left(\frac{1}{s+a}(-\Omega^{\times} J_r \Omega + K \odot u) + \frac{a}{s+a} J_r \Omega\right) \\
&\quad - \left(\frac{1}{s+a}(-\Omega^{\times} J\Omega + \hat{K} \odot u) + \frac{a}{s+a} J\Omega\right) \\
&= \frac{1}{\delta_1}\left(\frac{1}{s+a}(-\Omega^{\times} \delta_1 J\Omega + K \odot u) + \frac{a}{s+a} \delta_1 J\Omega\right) \\
&\quad - \left(\frac{1}{s+a}(-\Omega^{\times} J\Omega + \hat{K} \odot u) + \frac{a}{s+a} J\Omega\right) \\
&= \left(\frac{1}{s+a}(-\Omega^{\times} J\Omega) + \frac{a}{s+a} J\Omega\right) - \left(\frac{1}{s+a}(-\Omega^{\times} J\Omega) + \frac{a}{s+a} J\Omega\right) \\
&\quad + \frac{1}{\delta_1}\frac{1}{s+a} K \odot u - \frac{1}{s+a}\hat{K} \odot u \\
&= \left(\frac{1}{\delta_1} K - \hat{K}\right) \odot \bar{u}
\end{aligned}$$

Therefore,

$$\varepsilon_i = \left(\frac{1}{\delta_1}K - \hat{K}\right)\frac{\bar{u}_i}{n_i^2}$$

which shows that $\hat{K}_i$ will approach $\frac{1}{\delta_1}K_i$, and thus

$$\hat{k}_i \to 1 - \frac{1}{\delta_1} + k_i, \qquad i = 1, 2, 3, \quad as \quad t \to \infty \tag{4.34}$$

From the above analysis, one can observe that the uncertainties of the inertia matrix affect the convergence properties of the residual generator. Even when there are no faults, the error between the estimate of k and the actual value of k is not going to be zero.

4.3.2 Uncertainties of outputs

In the satellite attitude model, we assumed that the inertial angular velocity and quaternions are measured. However, due to the errors in the sensors, the measured outputs may not be accurate, and as a result, the residual generator will be very sensitive to the measured outputs of the system. In this section, we will investigate the impacts and effects of the uncertainties in the outputs on the residual generator performance.

Assume that the actual angular velocity Ω is rewritten as $\Omega_r = \delta_2\Omega$, for some δ_2 representing uncertainty. We have

$$\bar{\Omega}_r + K \odot \bar{u} = J\Omega_r$$

and

$$\frac{1}{\delta_2}\bar{\Omega}_r + \frac{1}{\delta_2}K \odot \bar{u} = J\Omega$$

Therefore

$$J\Omega - J\hat{\Omega} = \left(\frac{1}{\delta_2}\bar{\Omega}_r - \bar{\Omega}\right) + \left(\frac{1}{\delta_2}K - \hat{K}\right) \odot \bar{u}$$

Let us define $\tilde{K} = \hat{K} - K$, hence

$$\dot{\tilde{K}} = \dot{\hat{K}} = \left(P \odot \left(\left(\frac{1}{\delta_2}\bar{\Omega}_r - \bar{\Omega}\right) + \left(\frac{1}{\delta_2}K - \hat{K}\right) \odot \bar{u}\right) \odot \bar{u}\right) \odot \begin{bmatrix} \frac{1}{n_1^2} & \frac{1}{n_2^2} & \frac{1}{n_3^2} \end{bmatrix}^T$$

or

$$\dot{\tilde{K}} = \left(P \odot \left(\frac{1}{\delta_2}\bar{\Omega}_r - \bar{\Omega}\right) \odot \bar{u} + P \odot \begin{bmatrix} \frac{1}{\delta_2} - 1 & \frac{1}{\delta_2} - 1 & \frac{1}{\delta_2} - 1 \end{bmatrix}^T \odot K \odot \bar{u} \odot \bar{u}\right)$$
$$\odot \begin{bmatrix} \frac{1}{n_1^2} & \frac{1}{n_2^2} & \frac{1}{n_3^2} \end{bmatrix}^T - \left(P \odot \tilde{K} \odot \bar{u} \odot \bar{u}\right) \odot \begin{bmatrix} \frac{1}{n_1^2} & \frac{1}{n_2^2} & \frac{1}{n_3^2} \end{bmatrix}^T$$

If we now set $k = 0$, we get

$$\dot{\hat{k}} = \left(-P \odot \left(\frac{1}{\delta_2}\bar{\Omega}_r - \bar{\Omega}\right) \odot \bar{u} - P \odot \left[\begin{bmatrix} \frac{1}{\delta_2} - 1 & \frac{1}{\delta_2} - 1 & \frac{1}{\delta_2} - 1 \end{bmatrix}^T + \hat{k}\right] \odot \bar{u}\right)$$
$$\odot \begin{bmatrix} \frac{1}{n_1^2} & \frac{1}{n_2^2} & \frac{1}{n_3^2} \end{bmatrix}^T \tag{4.35}$$

From the above analysis, one can observe that, similar to the parametric uncertainties, the uncertainties in the outputs affect the convergence properties of the residual generator. Furthermore, this impact cannot be presented by a simple convergence property as the case of the parametric uncertainties.

4.3.3 Impacts of disturbances

The satellites generally suffer from small but persistent disturbances. In equation (2.92), we use w to represent these disturbance torques. These torques are very small, and are typically around $10^{-4}N \cdot m$. There are mainly four sources of external torque disturbances that may affect the satellite, namely gravity-gradient effects, magnetic-field torques on the vehicle, impingement by solar-radiation, and aerodynamic torques for low-altitude orbits. They can be affected by the satellite orientation, mass properties, and design symmetry. Readers may refer to [9] for details regarding quantifying these disturbances.

In this chapter, we will only investigate the impact of disturbances on the residual generator qualitatively and consider the disturbances as noise of normal distribution. Figure 4.1 illustrates the impact of disturbances in our numerical simulations. In this figure, we have assumed that there is no fault and no uncertainties in the outputs and the parameters. Under the presence of the above disturbances the impact and effects on the residuals are below 2×10^{-5}. Consequently, when thresholds are to be selected, these errors will be taken into account explicitly.

4.4 Selection of the Threshold Logic

Similar to the satellite orbital model, one needs to consider the transient time of convergence of $\hat{k}$ as well as selection of the threshold logic in order to avoid initiating false alarms. The approach for estimating the transient time convergence of $\hat{k}$ is investigated qualitatively. We will show that the selection of threshold is different from

the results obtained for the orbital model in the previous chapter. Parametric uncertainties, disturbances and uncertainties on the outputs will all affect the convergence properties of residual generators. For parametric uncertainties, due their simple convergence properties, we still use the same technique as the one that was utilized in the orbital model, that is we will calculate the largest possible errors resulting from the parametric uncertainties based on (4.34). For disturbances, we quantitatively analyze the impact through numerical simulations and estimate the magnitude of these factors. For uncertainties in the outputs, the analysis is much more complicated. Towards this end, we will use a dynamic estimate of the impact of uncertainties of the outputs. Specifically, consider the following equation that is based on (4.35):

$$\begin{aligned}\dot{\kappa} = &- P \odot \left(\frac{1}{\delta_2} \bar{\Omega}_r - \bar{\Omega} \right) \odot \bar{u} \\ &- P \odot \left[\left[\begin{array}{ccc} \frac{1}{\delta_2} - 1 & \frac{1}{\delta_2} - 1 & \frac{1}{\delta_2} - 1 \end{array} \right]^T + \kappa \right] \odot \bar{u} \end{aligned} \tag{4.36}$$

It can be observed that using (4.36) provides us with an envelope about which the impact of the uncertainties in the outputs on the residuals may be evaluated.

Therefore, at each instant, we calculate the sum of the errors resulting from the parametric uncertainties, the estimate of impact of disturbances (approximately 2×10^{-5}, as discussed earlier), and κ. This sum will be considered as the threshold for the residual generator.

4.5 Simulation Results

In practice, the attitude control for a satellite is a very critical requirement as the satellite normally needs to change its attitude from time to time throughout its whole lifetime. Consider the Earth Observing-1 (EO-1) satellite as an example [35, 36]. After separation from the launch vehicle, Boeing Delta 2, the satellite spun with a specific rate. The attitude control system decreased the spin so that the EO-1 can enter into Sun Acquire mode. During normal operations, EO-1 has to maintain a fixed attitude with respect to the orbital frame in order to allow the fixed body science instruments and payload point toward the earth. However, on an approximately weekly basis, solar calibration requires a slew maneuver to point the instruments toward the sun, and a raster scan of the moon for instrument calibration is also performed every month.

In the simulations we performed below, a simple attitude adjustment for the satellite is required. Specifically, the satellite rotates 180° about the Euler axis, which is represented by a unit vector $\vec{e}$. As discussed earlier, B is the fixed body frame and A is the inertial frame. Suppose that unit vectors $\vec{a}_i$ and $\vec{b}_i$ $(i = 1, 2, 3)$ are fixed to the reference frames A and B, respectively. Then,

$$\begin{aligned}\vec{e} &= e_1\vec{a}_1 + e_2\vec{a}_2 + e_3\vec{a}_3 \\ &= e_1\vec{b}_1 + e_2\vec{b}_2 + e_3\vec{b}_3\end{aligned}$$

where e_i are the direction cosines of the Euler axis with respect to both A and B and $e_1^2 + e_2^2 + e_3^2 = 1$. The parameters we use in the simulations are as follows:

1. $e_1 = 0.5, \quad e_2 = 0.5$, and $e_3 = 0.5 \times \sqrt{2}$;

2. The inertia matrix of the satellite is selected as:

$$J = \begin{bmatrix} 20 & 0 & 0.9 \\ 0 & 17 & 0 \\ 0.9 & 0 & 15 \end{bmatrix};$$

3. The range of the parameters δ_1 and δ_2 are selected as $1 - 10^{-3} \leq \delta_i \leq 1 + 10^{-3}$, $i = 1, 2$.

Figures 4.1 and 4.2 illustrates the effect of the disturbances on the residuals. In these figures, it is assumed that no fault exists and no uncertainties on the outputs and the parameters of the model are considered. These results are now used quantitatively in selection of the thresholds.

Figures 4.3, 4.4 and 4.5 illustrate the effect of the bank of residual generators that are introduced in this chapter. It is assumed that a complete failure occurs for the actuator u_1 and the actuator u_3 at time of 1 second as shown in the figures of performances of $u + m$. From the figures of performances of $\hat{k}$, one may observe that the estimators for k_1 and k_3 identify the complete failures very quickly, but $\hat{k}_2$ stays zero since no fault exists at the actuator 2. Also, the redundant actuators u_{r1} and u_{r3} are initiated right after the occurrence of the faults to recover them. Moreover, the performance of the angular velocity Ω and quaternions have not been affected explicitly by the occurrence of the faults. The residual generators designed can detect and identify the complete actuator failures and initiate the redundant actuators

effectively. Furthermore, the isolation of the concurrent faults is also successfully achieved.

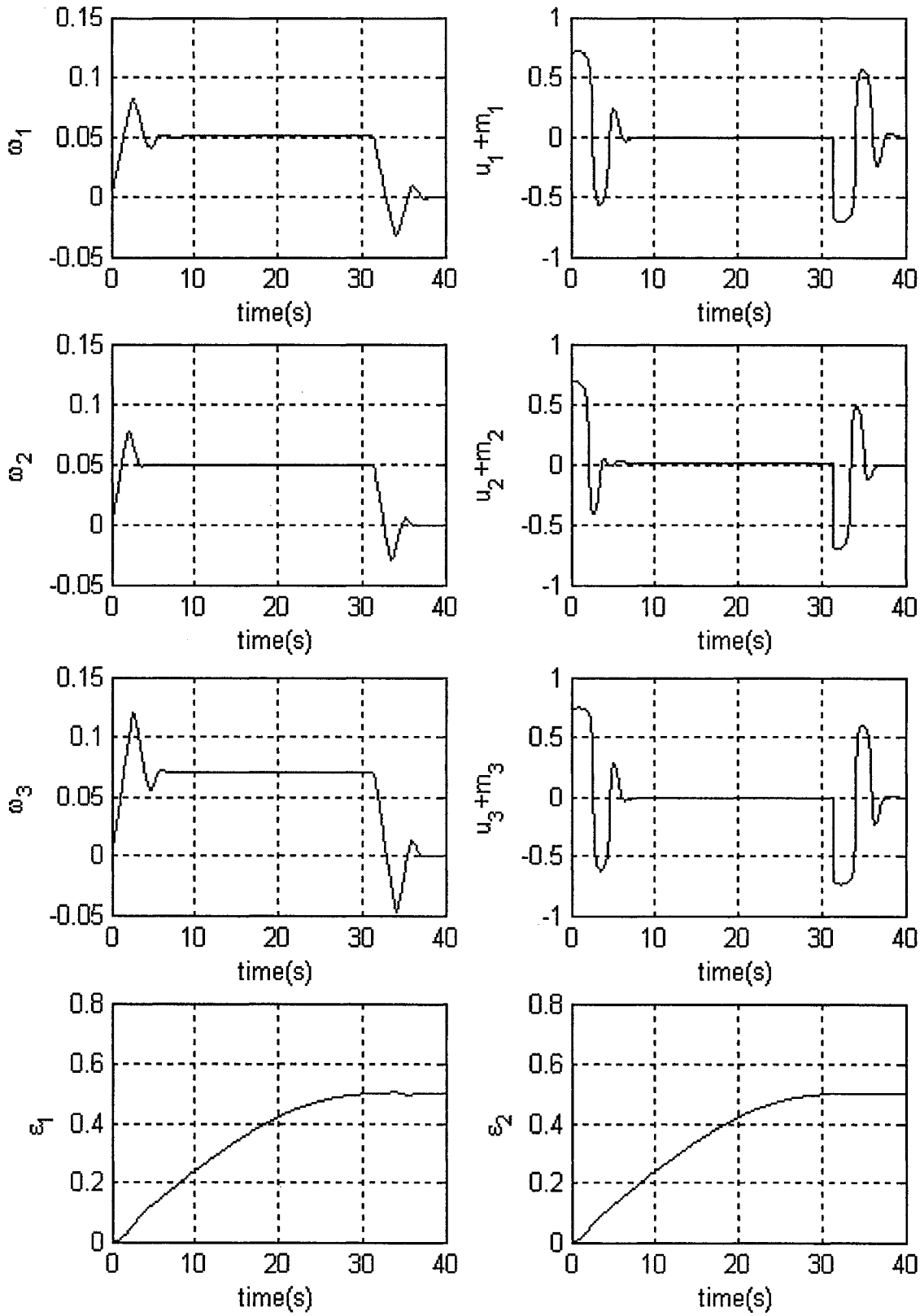

Figure 4.1: Impacts of the disturbances on the attitude control subsystem of a satellite

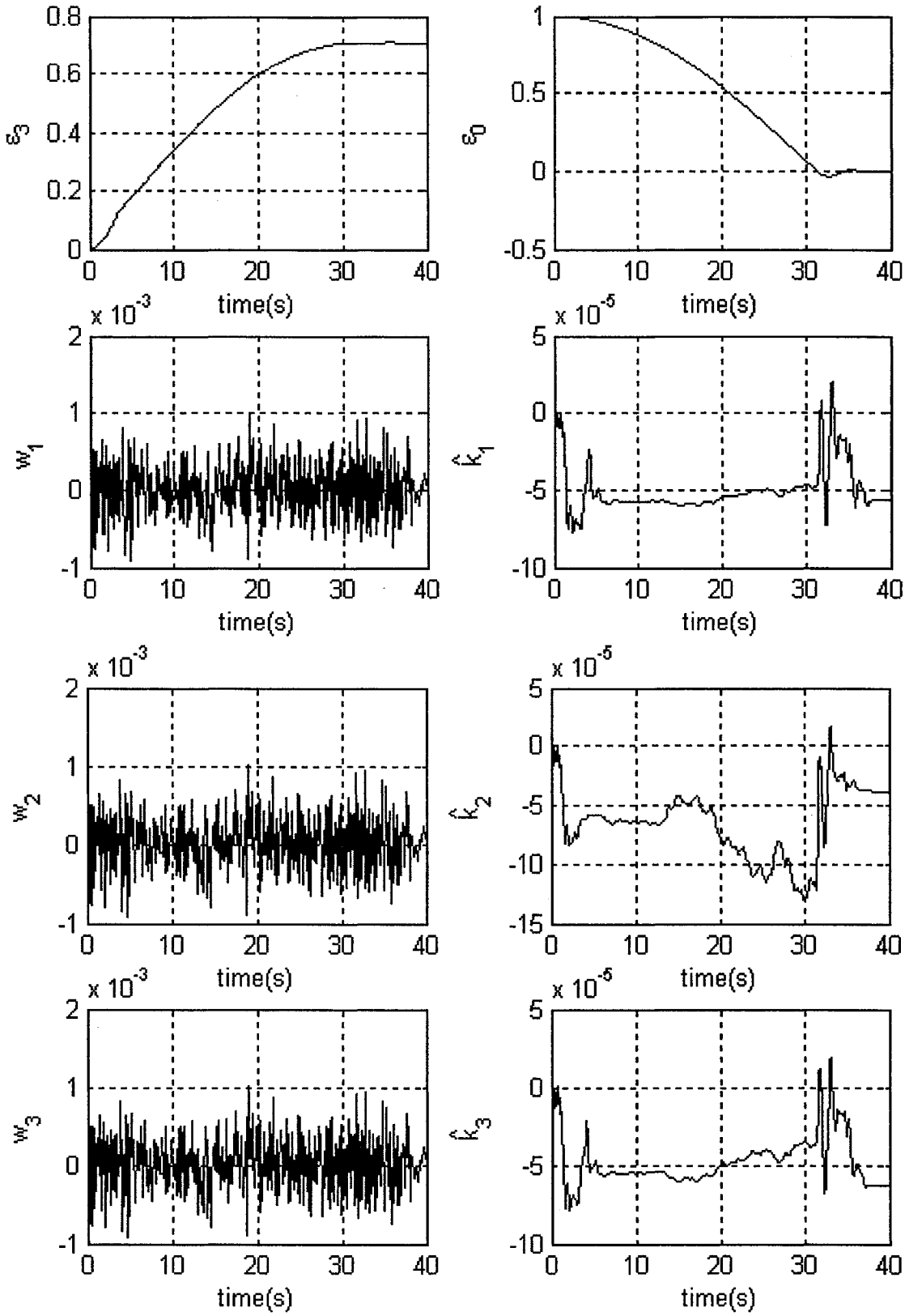

Figure 4.2: (Continued)Impacts of the disturbances on the attitude control subsystem of a satellite

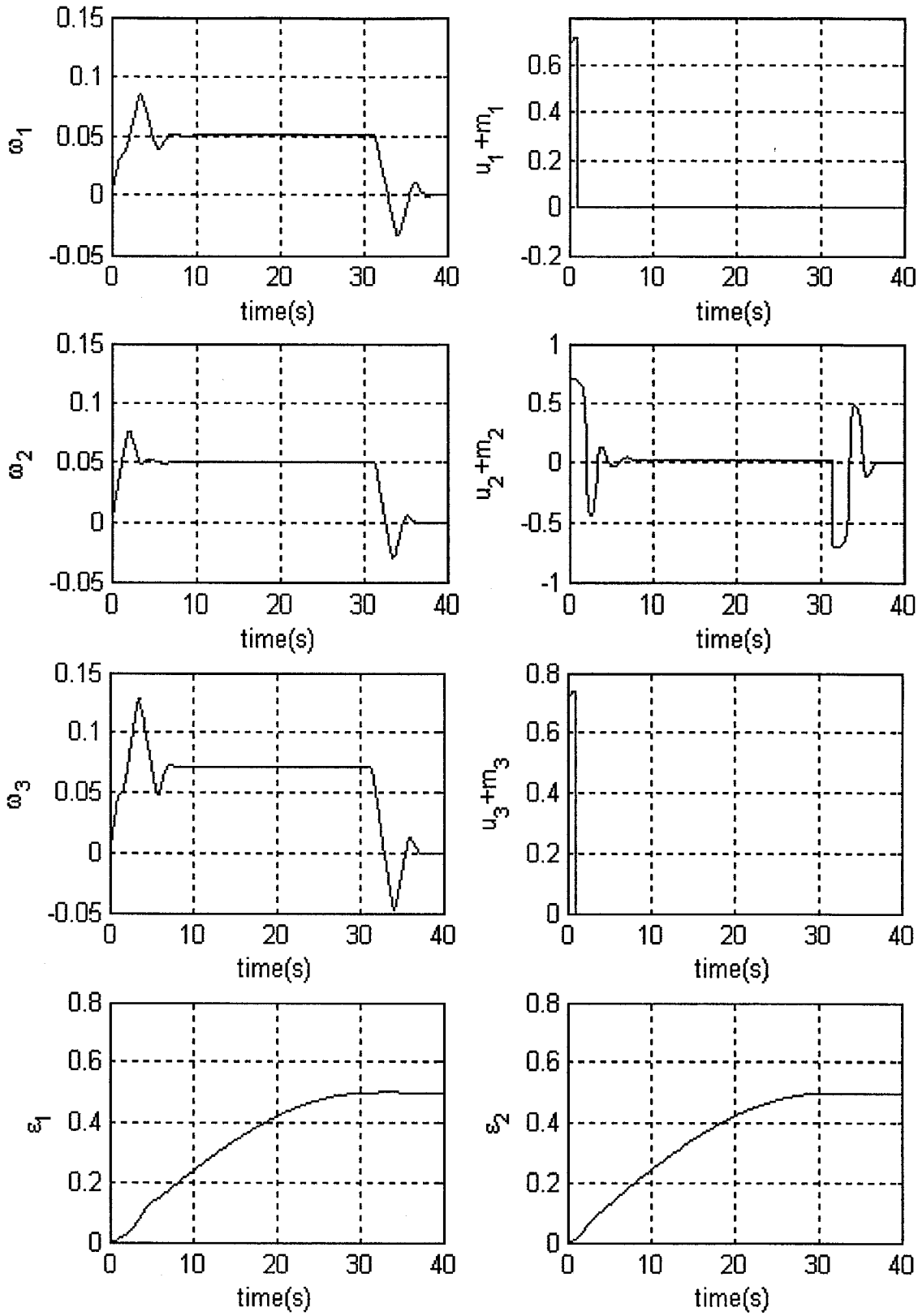

Figure 4.3: The behavior of the FDIR residual generator on the satellite attitude model subject to failures in actuators 1 and 3

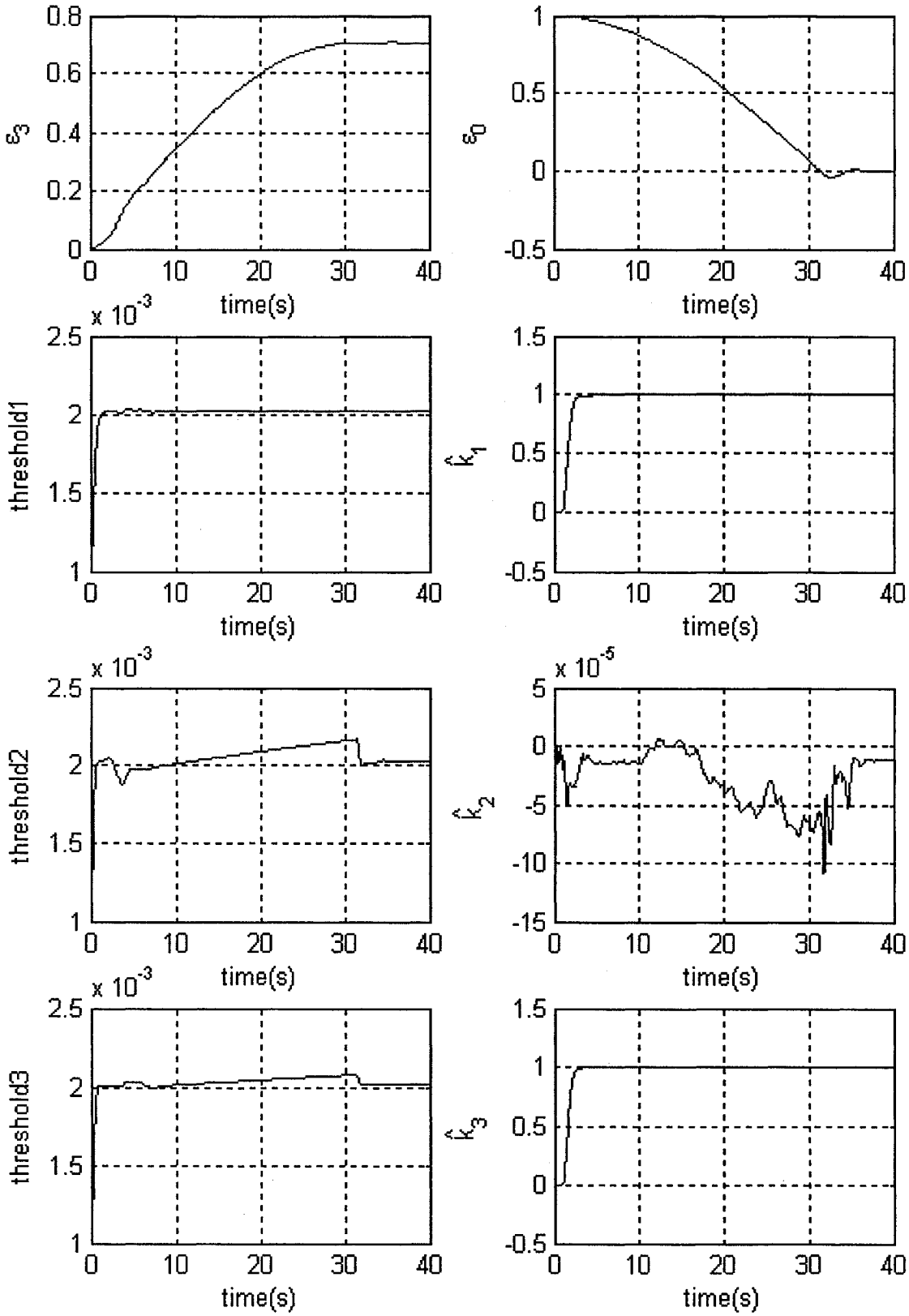

Figure 4.4: (Continued)The behavior of the FDIR residual generator on the satellite attitude model subject to failures in actuators 1 and 3

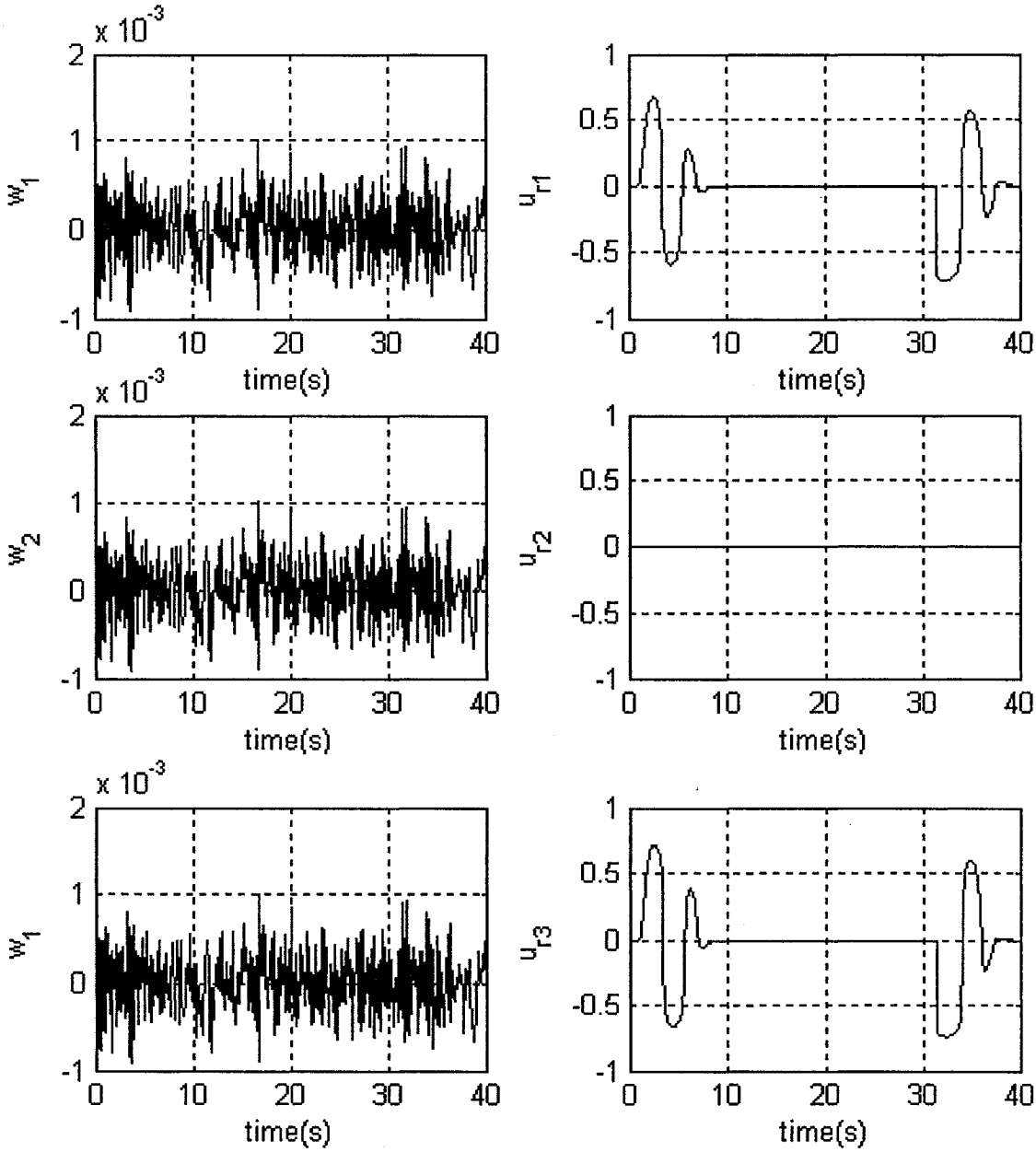

Figure 4.5: (Continued)The behavior of the FDIR residual generator on the satellite attitude model subject to failures in actuators 1 and 3

Chapter 5

Generalization of the FDIR Scheme to General Nonlinear Systems

In chapters 3 and 4, our proposed new residual generator was applied to a satellite orbital model as well as the satellite attitude model, respectively. Essentially, the new residual generator belongs to a class of parameter estimators. In this chapter, we will investigate whether this new residual generator can also be applied to a more general class of nonlinear systems.

Consider the nonlinear system governed by (2.1). Provided that the system satisfies the condition (2.7), one can then apply coordinate transformations to render it

equivalent into equation (2.12). Since the inputs $u \in R^m$, u can be rewritten as

$$u = \begin{bmatrix} u_1 & u_2 & \cdots & u_m \end{bmatrix}^T$$

and $g_1(x_1, x_2)$ can be written as

$$g_1(x_1, x_2) = \begin{bmatrix} g_{11}(x_1, x_2) & g_{12}(x_1, x_2) & \cdots & g_{1m}(x_1, x_2) \end{bmatrix}$$

Let us assume that the fault m in (2.12) corresponds to an actuator or input fault, and the corresponding input is u_i, therefore we obtain

$$g_{1i}(x_1, x_2) = l_1(x_1, x_2) \tag{5.1}$$

Let

$$\tilde{g}_1(x_1, x_2) = \begin{bmatrix} g_{11}(x_1, x_2) & g_{12}(x_1, x_2) & \cdots & g_{1(i-1)}(x_1, x_2) & g_{1(i+1)}(x_1, x_2) & \cdots g_{1m}(x_1, x_2) \end{bmatrix}$$

$$\tilde{u} = \begin{bmatrix} u_1 & u_2 & \cdots & u_{i-1} & u_{i-1} & \cdots & u_m \end{bmatrix}^T$$

Consequently, equation (2.12) can be rewritten as

$$\begin{aligned}
\dot{x}_1 &= f_1(x_1, x_2) + \tilde{g}_1(x_1, x_2)\tilde{u} + l_1(x_1, x_2)u_i + l_1(x_1, x_2)m \\
\dot{x}_2 &= f_2(x_1, x_2, x_3) + g_2(x_1, x_2, x_3)u + p_1(x_1, x_2, x_3)w \\
\dot{x}_3 &= f_3(x_1, x_2, x_3) + g_3(x_1, x_2, x_3)u + p_2(x_1, x_2, x_3)w \\
y_1 &= h_1(x_1) \\
y_2 &= x_2
\end{aligned} \tag{5.2}$$

Let us also assume that $m = -ku_i$ and consider y_2 as an input for the x_1-subsystem, so that the x_1-subsystem can be rewritten as

$$\begin{aligned}
\dot{x}_1 &= f_1(x_1, y_2) + \tilde{g}_1(x_1, y_2)\tilde{u} + l_1(x_1, y_2)(1-k)u_i \\
y_1 &= h_1(x_1)
\end{aligned} \tag{5.3}$$

Furthermore, it is assumed that the mapping $h_1 : x_1 \rightarrow y_1$ is bijective (one to one) and an inverse function $h_1^{-1} : y_1 \rightarrow x_1$ exists. Thus, we can obtain the state x_1 through the measured output y_1.

Our goal here is to design an estimator for the fault parameter k in equation (5.3). Let

$$U_i = l_1(x_1, y_2)u_i \tag{5.4}$$

and $K = 1 - k$, then (5.3) becomes

$$\dot{x}_1 = f_1(x_1, y_2) + \tilde{g}_1(x_1, y_2)\tilde{u} + KU_i \tag{5.5}$$

The proposed candidate for the residual generator subsystem may be characterized by (5.6)–(5.12), for estimating k, namely

$$\bar{U}_i = \frac{1}{s+a}U_i \tag{5.6}$$

$$\bar{x}_1 = \frac{1}{s+a}f_1(x_1, y_2) + \frac{1}{s+a}\tilde{g}_1(x_1, y_2)\tilde{u} + \frac{a}{s+a}x_1 \tag{5.7}$$

$$\hat{x}_1 = \hat{K}\bar{U}_i + \bar{x}_1 \tag{5.8}$$

$$\varepsilon = \frac{x_1 - \hat{x}_1}{n^2} \tag{5.9}$$

$$\dot{P} = \beta P - \frac{1}{n^2}P^2\bar{U}_i^2 \tag{5.10}$$

$$\dot{\hat{K}} = P\varepsilon\bar{U}_i \tag{5.11}$$

$$\hat{k} = 1 - \hat{K} \tag{5.12}$$

where a is a positive constant, $n > 0$ is the normalizing signal set to $n^2 = 1 + \bar{U}^2$, $\beta \geq 0$ is the forgetting factor. $\hat{K}$ is the estimate of K, and $\hat{k}$ is the estimate of k. The convergence of the estimator is now investigated below.

As have mentioned in previous chapters, we can easily show that the dynamical

system enjoys the property

$$\frac{s}{s+a}x_1 + \frac{a}{s+a}x_1 \to x_1 \quad as \quad t \to \infty$$

Thus, after the transients for the convergence of the above equation, we obtain

$$\begin{aligned}
&\frac{s}{s+a}x_1 + \frac{a}{s+a}x_1 \\
&= \frac{1}{s+a}\left[f_1(x_1, y_2) + \tilde{g}_1(x_1, y_2)\tilde{u} + KU_i\right] + \frac{a}{s+a}x_1 \\
&= \frac{1}{s+a}\left[f_1(x_1, y_2) + \tilde{g}_1(x_1, y_2)\tilde{u}\right] + \frac{a}{s+a}x_1 + \frac{1}{s+a}KU_i \\
&= \bar{x}_1 + K\bar{U}_i = x_1
\end{aligned}$$

Hence,

$$\varepsilon = \frac{x_1 - \hat{x}_1}{n^2} = \frac{\left(K - \hat{K}\right)\bar{U}_i}{n^2}$$

Consider as before the following Lyapunov function candidate

$$V = \frac{\left(\hat{K} - K\right)^2}{2}$$

where at $\hat{K} = K$, we have $V = 0$ and $V > 0$, $\forall \hat{K} \neq K$. Taking the time derivative of V along the trajectory of the system yields

$$\dot{V} = \left(\hat{K} - K\right)\dot{\hat{K}} = \left(\hat{K} - K\right)P\varepsilon\bar{U} = -\frac{\left(\hat{K} - K\right)^2 P\bar{U}^2}{n^2}$$

Consequently as in proof of Lemma 1 we know that $P(t) > 0$ when $P(0) > 0$. Thus, $-\frac{\left(\hat{K}-K\right)^2 P\bar{U}^2}{n^2} < 0$, $\forall \hat{K} \in R - \{K\}$, and $\dot{V}$ will be less than zero in a finite time. Therefore, $\hat{K}$ tends to K, according to Barbashin-Krasovskii theorem, so that $\hat{k}$ tends to k as $t \to \infty$. Consequently, one may consider the estimator for k as the residual generator, although the threshold should be selected in order to reduce the occurrence of the "false alarm" caused by the uncertainties in the system. As before, once the estimate of k exceeds this threshold, one may conclude that a fault has occurred.

Chapter 6

Conclusions and Future Work

In this thesis, a new residual generator was developed and applied to the observable subsystem of the satellite's nonlinear orbital model as well as the attitude model. A fault is treated as the change of certain parameters in the satellite's model. An estimator for this parameter is designed and considered as the residual generator. In order to reduce the impact of disturbances, the least-squares algorithm is used in the design of the estimator. Furthermore, the robustness of the residual generators for the satellite orbital model and the satellite attitude model was investigated. Finally, the possibility of applying the proposed residual generator to a more general class of nonlinear systems was investigated.

In Chapter 2, we discussed the necessity of designing a nonlinear FDIR scheme for nonlinear systems. We used an example to demonstrate that a linear FDIR based algorithm when applied to a nonlinear system will result in significant modelling errors that may result in false alarms and consequently will diminish the possibility of solving the fault detection problem.

Also, in Chapter 2, we reviewed the geometric method of [4] that provides the sufficient and necessary conditions for solving the nonlinear fault detection and isolation problems. When the nonlinear system satisfies these conditions, we can apply coordinate transformations to formally characterize a special observable subsystem. Following the application of the coordinate transformations, the FDIR problem is then reduced to that of designing a residual generator for the observable subsystem. Our approach for designing the residual generator is to treat the system anomaly caused by the fault as manifested by the change of certain parameters. We subsequently consider the estimators for these parameters as residual generators.

In Chapter 3, a sliding mode controller for the satellite orbital model is first designed. The advantages of the sliding mode controller are that it takes the input saturations into account explicitly and the computation of this controller is very simple. Secondly, we applied a new residual generator based on the least-squares parameter estimation to the satellite orbital model. We considered two cases, where the first case deals with FDI before the recovery procedure is initiated and the second case deals with FDI after the recovery procedure. It was shown that the residual generator is convergent and that different controllers affect the performance of the residual generator but does not affect its convergence property. Thirdly, we investigated the impact of the uncertainties of the system on the residual generator. For the satellite orbital model (2.35), uncertainties in the parameter θ_1 and the measurable output for the state ϕ do not affect the convergence of the residual generator, however the uncertainties in the parameter θ_2 and the measurable outputs for the states ρ and ω will affect the convergence characteristics of the residual generator. Due to the

application of the nonlinear geometric method [4], the disturbance defined in equation (2.35) is decoupled from the fault, and does not affect the convergence. Given that we assumed the knowledge on the ranges of the possible uncertainties, one can evaluate the impact of the uncertainties through (3.53), (3.54), and (3.55). Unfortunately, these effects may result in false alarms if not treated properly. Therefore, in section 3.5, we presented the selection criteria for the threshold logic in order to avoid a false alarm, although this addition may reduce the sensitivity of the fault detection scheme. We then used the sum of the errors calculated from the uncertainties investigated to determine the threshold. Simulation results are presented in section 3.6. We simulated a satellite in which a geosynchronous orbital change from transfer orbit to phasing orbit is taking place. We assumed that a complete fault occurs in the actuator during the changing in the orbit. It was found that the parameter estimator (residual generator) only required about 4 seconds to identify this complete failure and the recovery procedure was successfully recovering the fault.

In Chapter 4, we developed and applied a bank of residual generators based on the least-squares parameter estimation to the satellite's attitude model. Since there are three actuators that provide torques about three mutually perpendicular axes about the fixed body frame B, we constructed three residual generators. Each residual generator is responsible for a possible faulty actuator. As in Chapter 3, we investigated the robustness of the residual generators. We discussed the uncertainties in the inertia matrix of the satellite and its outputs for measuring the inertial angular velocity and provided the quantitative results as given in (4.34) and (4.35). Since the disturbances defined in equation (2.92) and the actuator inputs cannot be decoupled,

we investigated the effects of the disturbances qualitatively. Since the system (4.35) is not convergent, we designed a dynamic threshold according to (4.35). In section 4.5, the numerical simulation results are provided. We simulated the case in which a satellite rotates 180° about the Euler axis, and we found the residual generators proposed can detect and isolate the presence of two concurrent faults.

Since the proposed residual generators are applied to the specific models of the satellite orbital and attitude models, in Chapter 5, we investigated whether the proposed FDIR strategy based on our parameter estimation algorithm can be extended and applied to a more general class of nonlinear systems. We showed the convergence of the residual generator on this more general class of nonlinear systems. We also showed that if the mapping $h_1 : x_1 \rightarrow y_1$ in equation (5.3) is bijective (one to one) and the inverse function $h_1^{-1} : y_1 \rightarrow x_1$ exists, then the residual generator we proposed for the model (2.12) is convergent. Note that, we only proved the convergence of the residual generator when applied on the nonlinear system (2.12), and robustness of the residual generator still remains to be investigated in future work.

6.1 Future Direction of Research

An interesting topic for investigation in future is that of parameter estimation for general nonlinear systems. Considerable attention has been given to parameter estimation for linear systems in the literature. However, most real-life systems demonstrate nonlinear dynamic behaviors. Thus, parameter estimation techniques for nonlinear systems are necessary when linear models are not sufficiently accurate.

In this thesis, we only applied a nonlinear parameter estimator as a residual generator to two specific class of nonlinear models, namely the satellite orbital model and the satellite attitude model. Investigations on the parameter estimation for more general class of nonlinear systems will be a very interesting topic of research.

Furthermore, the satellite orbital model considered in this thesis is a "two dimensional model". That is, the orbit of the satellite is assumed to be always in a plane, but the practical satellite orbital models are "three dimensional". We therefore need to construct this "three dimensional model" and extend our residual generator to it before one can apply the proposed FDIR system to a real world satellite. Furthermore, the effects of the disturbances on the satellite orbital model need to be studied in more detail. We know that the main disturbances are caused by the gravitational forces of the sun and the moon, the nonspherical geometry of earth, atmospheric drag, and solar radiation. Therefore we may need to investigate these impacts on the residual generator of satellite orbital models in more depth in future.

Finally, the residual generators we proposed for the satellite orbital model and the satellite attitude model are nonlinear continuous time systems. In order to apply these residual generators to real satellites that are controlled by computers, we have to modify these algorithms to the discrete-time domain. Discrete-time systems are also well understood for linear time-invariant models, but a lot less works have been reported in the literature for nonlinear models. Thus, the investigation of FDIR scheme for nonlinear discrete-time systems is also a very challenging research work.

6.2 Contributions of the Thesis

In this thesis, the problems of nonlinear fault diagnosis and recovery of a satellite's orbital model as well as the satellite's attitude control model are investigated using parameter estimation techniques for design of fault residual generators. Given that a necessary condition for solving the fault diagnosis and recovery problem is that the states of the system must be bounded, a sliding mode controller is designed and applied to the satellite's orbital model. Furthermore, the robustness properties of the proposed residual generators to parametric uncertainty, disturbance and measurement signals for both the satellite's orbital model and the satellite's attitude control model are investigated. Finally, the generalization of the proposed residual generator to a general class of nonlinear systems is presented and promising preliminary results are reported.

Bibliography

[1] R. V. Beard, "Failure accommodation in linear systems through self-reorganization," Ph.D. dissertation, Massachusetts Inst. Tech., Cambridge, MA, 1971.

[2] H. L. Jones, "Failure detection in linear systems," Ph.D. dissertation, Massachusetts Inst. Tech., Cambridge, MA, 1973.

[3] M. –A. Massoumnia, "A geometric approach to the synthesis of failure detection filter," IEEE Trans. Automat. Contr., vol. AC-31, pp. 839-846, 1986.

[4] C. D. Persis and A. Isidori, "A geometric approach to nonlinear fault detection an isolation," IEEE Trans. Automat. Contr., vol. 46, NO. 6, pp. 853-865, 2001.

[5] J. D. Boškovi, Sai-Ming Li and R. K. Mehra, "Intelligent spacecraft control using multiple models, switching, and tuning," Proceedings of the 1999 IEEE, International Symposium on Intelligence Control/Intelligent Systems and Semiotics, Cambridge, MA, pp. 84-89, 1999.

[6] W. T. Kolk and R. A. Lerman, "Nonlinear system dynamics," Van Nostrand Reinhold, 1992.

[7] P. A. Ioannou and J. Sun, "Robust Adaptive Control," Upper Saddle River, NJ: PTR Prentice Hall, 1996.

[8] J. D. Boškovi, Sai-Ming Li and R. K. Mehra, "Robust adaptive variable structure control of spacecraft under control input saturation," Journal of Guidance, Control, and Dynamics, vol. 24, No. 1, pp. 14-22, 2001.

[9] J. R. Wertz and W. J. Larson, "Space mission analysis and design," 3rd ed., Dordrecht, Netherlands, Boston: Kluwer, 1999.

[10] R. N. Clark, "A simplified instrument failure detection scheme," IEEE Trans. Aerospace Electron. Syst., 14, pp. 558-563, 1978

[11] R. N. Clark, "Instrument fault detection," IEEE Trans. Aerospace Electron. Syst., 14, pp. 456-465, 1978

[12] P. M. Frank, "Fault diagnosis in dynamic systems using analytical and knowledge-based redundancy—a survey and some new results," Automatica, Vol. 26, No. 3, pp. 459-474, 1990.

[13] R. Isermann, "Process fault detection based on modeling and estimation methods—A survey," Automatica, 20, pp. 387-404, 1984.

[14] K. F. Fong and A. P. Loh, "A Frequency Domain Approach for Fault Detection," Preceedings of the 40^{th} IEEE, Conference on Decision and Control, pp. 1023-1028, 2001.

[15] B. Wie, "Space vehicle dynamics and control," Reston, VA: American Institute of Aeronautics and Astronautics, 1998.

[16] A. Isidori, "Nonlinear control systems," 3^{rd} ed., New York: Springer Verlag, 1995.

[17] J. Ahmed, V. T. Coppola, and D. S. Bernstein, "Adaptive asymptotic tracking of spacecraft attitude motion with inertia matrix identification," Journal of Guidance, Control and Dynamics, vol. 21, No. 5, pp. 684-691, 1998.

[18] H. K. Khalil, "Nonlinear systems," 3^{rd} ed., Upper Saddle River, N.J.: Prentice Hall, 2002.

[19] L. Alkalaj, "Advanced flight computing program" in proceedings of 1^{st} Workshop on Advanced Flight Computing and Industry, (Pasadena CA), pp. 104-166, 1993.

[20] G. B. Folland, "Real analysis: modern techniques and their applications," 2^{nd}ed, John Wiley & Sons, Inc., 1999.

[21] D. M. Himmelblau, "Fault diagnosis in chemical and petrochemical processes," Elsevier Press, Amsterdam, 1978.

[22] D. Mylaraswamy and V. Venkatasubramanian, "A hybrid Framework for Large Scale Process Fault Diagnosis," Comput. Chem. Eng, 21, S935-S940, 1997.

[23] S. A. Lapp and G. A. Powers, "Computer-aided synthesis of fault-trees," IEEE Trans. Reliability, 37, pp. 2-13, 1977.

[24] I. E. Potter and M. C. Sunman, "Thresholdless redundancy management with arrays of skewed instruments," Integrity in Electronic Flight Control Systems, AGARDOGRAPH-224, 15-11 to 15-25, 1977.

[25] M. Desai and A. Ray, "A fault detection and isolation methodology," Proc. 20^{th} Conf. on Desision and Control, pp. 1363-1369, 1981.

[26] E. Y. Chow and A. S. Willsky, "Analytical redunancy and the design of robust failure detection systems," IEEE Trans. Aut. Control, AC-29, pp. 603-614, 1984.

[27] X. C. Low, A. S. Willsky and G. L. Verghese, "Optimally robust redundancy relations for failure detection in uncertain systems," Automatica, 22, pp. 333-344, 1986.

[28] X. Ding, L. Guo and P. M. Frank, "A frequency domain approach to fault detection of uncertain dynamic systems," Proc. 32^{th} Conf. on Desision and Control, pp. 1722-1727, 1993.

[29] P. C. Hughes, "Spacecraft attitude dynamics," John Wiley & Sons, 1986.

[30] M. H. Kaplan, "Modern spacecraft dynamics and control," John Wiley & Sons, 1976.

[31] T. R. Kane, P. W. Likins and D. A. Levinson, "Spacecraft dynamics," McGraw-Hill, 1983.

[32] J. R. Wertz (editor), "Spacecraft attitude determination and control," Kluwer Academics Publishers, 1995.

[33] V. Utkin, "Sliding modes control in electromechanical systems," Taylor & Francis, 1999.

[34] National Aeronautics and Space Administration, Goddard Space Flight Center, "GOES I-M DataBook," Maryland, 1996.

[35] M. E. Perry, P. Alea, M. J. Cully, M. McCullough, P. Sanneman, N. Teti and B. Zink, "Earth Observing-1 Spacecraft Bus," 15^{th} Annual/USU Conference on Small Satellites, 2001.

[36] D. Speer and P. Sanneman, "Attitude determination and control for the new millennium EO-1 spacecraft," 1998.

[37] J. D. Boškovi, Sai-Ming Li and R. K. Mehra, "Intelligent control of spacecraft in the presence of actuator failures," Preceedings of the 38^{th} IEEE, Conference on Decision and Control, pp. 4472-4477, Phoenix, Arizona, 1999.

[38] J. D. Boškovi, Sai-Ming Li and R. K. Mehra, "On-line failure detection and identification (FDI) and adaptive reconfigurable control (ARC) in aerospace applications," Proceedings of the American Control Conference, pp. 2625-2626, Arlington, VA, 2001.

[39] R. Isermann, "Supervision, fault-detection and fault-diagnosis methods - an introduction," Control engineering practice, vol. 5, No. 5, pp. 639-652, 1997.